



universität  
wien

# DISSERTATION

Titel der Dissertation

Potential of a geoscientific multi-analytical approach to  
investigate technology and provenance of ceramic materials

Verfasserin / Verfasser

Cornelius Tschegg, Mag.

angestrebter akademischer Grad

Doktor der Naturwissenschaften (Dr. rer. nat.)

Wien, im September 2008

Studienkennzahl lt. Studienblatt:

A 091 431

Dissertationsgebiet lt. Studienblatt:

Geologie

Betreuerin / Betreuer:

Ao. Prof. Dr. Theodoros Ntaflou

---

# TABLE OF CONTENTS

|   |    |
|---|----|
| <b>Summary</b>  | 3  |
| <b>Zusammenfassung</b>  | 4  |
| <b>Acknowledgements</b>   | 5  |
| <b>Introduction</b>   | 6  |
| Archaeological science  | 6  |
| Ceramics - a general perspective  | 8  |
| The raw material choice and its preparation   | 9  |
| The ceramic firing  | 10 |
| Archaeological science of ceramic material  | 11 |
| The quest for provenance of ceramics  | 12 |
| Insights into ceramic technology  | 12 |
| Aims of the project   | 13 |
| Material specific research questions  | 14 |
| Methods   | 14 |
| <b>Synthesis</b>  | 16 |
| <b>References</b>   | 18 |
| <b>Appendices</b>   | 20 |
| (A)   | 20 |
| Tscheegg, C., Hein, I., Ntaflos, Th., 2008a. State of the art multi-analytical geoscientific approach to identify Cypriot Bichrome Wheelmade Ware reproduction in the Eastern Nile delta (Egypt). <i>Journal of Archaeological Science</i> 35, 1134-1147.   |    |
| (B)   | 35 |
| Tscheegg, C., 2008b. A geoscientific, methodologically integrated realisation to reconsider Egyptian pottery of the 18 <sup>th</sup> Dynasty in Hein, I. (Ed.): <i>The Manual of Bichrome Wheelmade Ware of the Eastern Mediterranean</i> . Verlag der Österreichischen Akademie der Wissenschaften, Wien (accepted). |    |
| (C)   | 49 |
| Tscheegg, C., Ntaflos, Th., Hein, I., 2008c. Thermally triggered two-stage reaction of carbonates and clay during ceramic firing - a case study on Bronze Age Cypriot ceramics. <i>Applied Clay Science</i> (in press).   |    |
| (D)   | 60 |
| Tscheegg, C., Ntaflos, Th., Hein, I., 2008d. Combined geological, petrological and geochemical method to reveal source material and technology of Late Cypriot Bronze Age Plain White ware ceramics. <i>Journal of Archaeological Science</i> (under review).   |    |
| <b>Curriculum Vitae</b>   | 80 |

## SUMMARY

The present PhD thesis concerns material-related archaeological interests that were approached using combined, state of the art, geoscientific analytical methods like XRF, ICP-MS, XRD, EPMA, SEM and Raman Spectroscopy. Ancient ceramics from different cultural backgrounds were investigated in order to reveal their origin as well as their specific manufacturing techniques. This provides necessary base information for further archaeological contemplations and allows getting new insights into ancient societies, their development, their habits and their interaction with other cultures.

The main issue was the detailed analysis of Bronze Age ceramics excavated in Cyprus as well as Egypt and other Mediterranean countries. With the use of an integrated methodological approach, it was possible to gain sufficient evidence for revealing the provenance of the study materials and additionally to examine physical and chemical characteristics of the ceramics, their manufacturing procedures, changes during ceramic firing and alterations during the post-depositional stage. Evidence from bulk- and mineral chemistry as well as from microstructural, micromorphological, petrological, geological and palaeozoological observations provided the required information to identify the used source materials and the way these were prepared and conditioned for pottery production. Besides these assignments of ceramic products to distinct source materials and certain production centres respectively, it was possible to get new insights into the knowledge and skills of Bronze Age potters by elucidating ceramic manufacturing technologies. Moreover, new aspects of mineralogical, geochemical and microtextural processes and transformations that take place during the ceramic manufacturing procedure (mainly during the firing) and their effects to the ceramic fabric are presented in the thesis.

## ZUSAMMENFASSUNG

Die vorliegende Arbeit beschäftigt sich mit materialbezogenen archäologischen Fragestellungen, die mit Hilfe von modernen geowissenschaftlichen analytischen Methoden wie etwa XRF, ICP-MS, XRD, EPMA, SEM und Raman Spektroskopie bearbeitet wurden. Antike Keramiken verschiedener kulturhistorischer Gegebenheiten wurden hinsichtlich ihrer Herkunft sowie ihrer spezifischen Herstellungsverfahren untersucht. Die auf naturwissenschaftlicher Basis gewonnenen Informationen sind erforderlich für weitere archäologische Forschungen und ermöglichen überhaupt erst einen fundierten Einblick in die Entwicklung von frühen Gesellschaftssystemen, deren Gewohnheiten sowie deren Interaktion mit anderen Kulturen.

Im Mittelpunkt dieser Arbeit stehen bronzezeitliche Artefakte, die sowohl aus Ausgrabungen in Zypern als auch Ägypten und anderen Ländern des Mittelmeerraumes stammen. Die „multi-analytische“ Herangehensweise ermöglichte es nicht nur, die Herkunftsorte der einzelnen Keramiken zu bestimmen, sondern darüber hinaus auch viele wichtige Aussagen über die physiko-chemischen Eigenschaften von Keramiken, ihre Herstellungstechnik, über Phasen-Transformationen während des keramischen Brandes und Veränderungen durch jahrtausendelange Bodenlagerung zu treffen. Gesamt- und Mineral-Chemismus sowie mikrotexturelle, mikromorphologische, petrologische, geologische und paläozoologische Informationen wurden herangezogen, um die verwendeten Ausgangsmaterialien sowie die Art der Aufbereitung dieser, naturwissenschaftlich einordnen zu können. Neben dieser Zuordnung von Keramiken zu bestimmten Rohmaterialien, aus denen sie gefertigt wurden sowie deren regionale Einschränkung, war es durch Spezifizierung der Herstellungstechnologien möglich, reichlich neue Erkenntnisse über die Fertigkeiten von Töpfern der späten Bronzezeit zu erfahren. Auch wenig untersuchte mineralogische, geochemische und mikrotexturelle Veränderung, die vor allem während des keramischen Brandes stattfinden und deren Auswirkungen entscheidend das keramische Gefüge prägen, werden in dieser Arbeit aufgezeigt.

## ACKNOWLEDGEMENTS

For the financial support, the Austrian Science Fund (FWF grant P18908-N19) has to be gratefully acknowledged.

I particularly want to thank my supervisor and promoter Theodoros Ntaflou. Besides he introduced me to the science of drinking the world's most precious coffees, I owe the largest part of my university career to him. He was always available for extensive encouraging discussions, was supportive of all new ideas and understood to spread his unlimited enthusiasm for scientific issues. Furthermore he was conducive to all professional and personal matters that arose during the study.

Special thanks go to Irmgard Hein (Institute of Egyptology – University of Vienna) who was the archaeological expert of the project. She provided the research questions, initiated all necessary collaborations, contributed significantly to all project- as well as research-related issues and beyond cared about all administrative belongings.

I am pleased about the agreement of Wolfram Richter and Max Bichler (Vienna University of Technology) to review and evaluate this thesis.

Manfred Bietak (Institute of Egyptology, Interdisciplinary Platform for Archaeological Studies – University of Vienna), Lindy Crewe (University of Manchester), Paul Åström (University of Gothenburg) and Michal Artzy (University of Haifa) have to be thanked for providing the project with study-material and related essential information. I'm especially grateful to Ragna Stidsing and Yossi Salmon (University of Haifa) who helped me to approach the world of archaeology by offering me numerous important conversations.

For technical support in the laboratories and inevitable help during data acquisition and data preparation, I really want to show appreciation to Petra and Wilfried Körner, Franz Kiraly, Christian Nachtnebel (†), Sigrid Hrabec, Monika Horschinegg, Michael Götzinger, Robert Krickl and Norbert „Oide Haut“ Irnberger.

I also have to express thanks to Erich Draganits, Susanne Gier, Hajnalka Herold, Hans Kurzweil and Hugh Rice, who always were open for helping and useful contributions.

For the nice time during my studies and the continuing friendship, I want to say “Thank you!” to the young earth-scientists at the Vienna University Anna Berger, Magda Bottig, Marcus Ebner, Ulli Exner, Monika Hölzel, Poldi Horkel, Wolfi Hujer, Christoph Iglseder, Johannes Loidl, Markus Meissl, Stephanie Neuhuber, Lukas Plan, Christian Rambousek, Berni Salcher, Andrea Schicker, Flo Wieselthaler and Andras Zamolyi.

My parents, who supported me financially but also in countless other aspects, are deeply grateful acknowledged.

At last, I want to thank my girlfriend Olga, also for helping me out in many respects, but mainly for having a lot of understanding for everything I did. She provided me an invaluable emotional support that significantly contributed to the outcome of this thesis.

# INTRODUCTION

## Archaeological science

---

In 1720, E. J. Halley commented on the provenance and age of the rocks of Stonehenge by means of petrologic evidences, in 1776 M. H. Klaproth determined and published chemical analyses of Greek and Roman coins as well as of Roman glass (Goffer, 1983). These studies formed the beginning of the present-day *archaeological science* or *archaeometry* – the use of natural sciences and their methodologies and techniques to handle archaeological issues. A work about paint pigments collected in Rome and Pompeii was already published in 1815 by H. Davy. The development of physical methods in the 19<sup>th</sup> century allowed application of those to archaeological matters. W. C. Röntgen for example, the discoverer of the X-rays described the absorption of X-rays by Pb-pigments of some Dürer paintings and introduced this technique to analyze pigments with the aim to detect art-forgery (Herz and Garrison, 1998). In the same year, G. Folgheraiter analyzed magnetic moments in Etruscan pottery, establishing geophysical methods for archaeometry. In 1837, L. Ross investigated ancient Greek marble quarries near Athens; G. R. Lepsius investigated numerous quarries trying to characterize them systematically by distinct criteria so that found rock-samples of archaeological backgrounds could be assigned. In the middle of the 19<sup>th</sup> century, J. E. Wocel realized that chemical compositions of artifacts occupy information of their source material and provenance and could even be used for relative dating. First chemical analyses of archaeological materials were published in 1853 by A. H. Layard on Assyrian Bronzes and glass. Between 1861 and 1875, J. Percy wrote divers publications about Mycenaean metal objects, revealing their metallurgical technologies. A first pioneer work of reconstructing palaeo-environments was done by R. Pumpelly in 1905 in Siberia, where he did detailed studies on prehistoric sites. Archaeological prospecting via aerial photography was born in 1919 in England, when J. D. Beazely located Roman structures from a balloon. With the establishment of instrumental measurement techniques like e. g. optical emission spectroscopy at the beginning of the 20<sup>th</sup> century, the main interests of the analysts changed to understand the level of technology represented by ancient metal artifacts (Pollard and Heron, 1996). In 1957, Sayre and Dodson applied NAA in their research on Mediterranean ceramics, in 1960 Emeleus and Simpson used NAA to test the ability of trace element compositions of Samian sherds to locate their provenance. Due to the increased emphasis on dating and physico-chemical analysis of archaeological materials, the term *archaeometry* was coined in the 1950's by C. Hawkes, the journal *Archaeometry* started to be printed in 1958. The second established journal dealing with scientific work on archaeological problems - *Journal of Archaeological Science* - was launched in 1974. Since this time, the number of researchers and research groups dealing with archaeological science rapidly increased. So did the quantity of scientific methods from various research-fields that were and are applied to the issue of enlightening archaeological problems. State of the art analytical chemical, physical, geographical and geological

techniques found application in archaeometry, increasing the possibility to gather sufficient information out of archaeological findings and environments to bring light into the “buried” world of archaeology.

As the collaborative work between archaeologists and natural scientists became not only intensified but also diversified, many fields of interest evolved. Some central aspects of this cooperation have been documented in the following section:

#### *Archaeological environment*

Geomorphologic and sedimentologic as well as geophysical techniques are applied to reconstruct ancient landscapes and historic anthropospheres.

#### *Site exploration and prospecting*

Investigation of archaeological sites via mainly geophysical and chemical methods in consideration of buried anthropogenic structures, remains or just evidence.

#### *Dating*

Relative and absolute age dating contribute to the appraisal of chronological questions in archaeology and help establishing international time systems. Site- as well as artifact-specific ages are of interest.

#### *Science of materials*

Artifacts are identified and investigated, mainly to ascertain their provenance and technology of fabrication.

Due to the rapid development of scientific research methods in the last years and decades, the archaeological science of materials, the analysis of artifacts respectively became very an important and reliable field of work in the archaeological sciences. Stone, metal, glass and ceramic artifacts are on grounds of their physical and chemical resistiveness abundant in many archaeological sites and therefore they represent crucial remains, bearing most of the archaeological evidence. Beside insights into development and habits of ancient cultures, these artifacts can obtain information of international importance as they e. g. disclose antique trade networks. Since primeval eras, humans used the naturally occurring materials from the surrounding to ease activities of their everyday life. Through time they began to modify the natural resources by shaping, refining, mixing, heating, combing, etc. them and by this means they were able to make them more suitable for their specific applications. This resulted in the initiation of synthetic materials (ceramics, glass, metals and alloys) with better performance, workability, endurance and appearance (Goffer, 1983). Before the human cultural development reached the point of superior metal-working in Bronze Age times, already in the Pottery Neolithic cultures, the production of ceramics appeared. Since then, ceramic materials evolved to essential components, not only in antiquity but till now and became key interests of archaeological research.

---

## Ceramics - a general perspective

---

One of the first major technological achievements of mankind was the use of shaped and fired clay to obtain specific objects for daily use and art (Goffer, 1983). The synthesis of ceramic material allowed for the first time to independently create and form objects which are needed for living and culture as well as to become uncoupled from naturally occurring materials. Already by the late Paleolithic, humans discovered that fire hardens objects made of clay and that adding different substances to the clay improves the physical properties of the object during the manufacturing process and afterwards. Defining ceramic as a substance that is formed out of a plastic raw material and reaches physical stability when fired, its incipencies can be dated back to 26,000 B.P. in the Czech Republic (Dolní Věstonice), the first real pottery vessels appear 21,000 B.P. (Herz and Garrison, 1998). At this time, firing temperatures typical for bonfires, not higher than 500-800°C were attained.

Theories about how pottery was discovered are various, one interesting hypothesis though was proposed by Goffer (1980). He explains that people recognized the phenomenon that evaporation of water from surface soils leads to the well-known mud cracks. Often, dish-like clay rich and concave soil crusts evolve which when fired in easy bonfires hardens to handy dishes. The physical properties (hardening, strengthening) which are achieved by this are comparable to those of primitive pottery. After Goffer, humans may have discovered these properties by accident what would naturally initiate the idea of forming, drying and firing clay to produce ceramics suitable for lots of uses.

Ceramic derives from the Greek word κεραμος (keramos - translated as "earthenware") and comprises beside fired clay products like bricks, tiles, plasters, mainly pottery. The term pottery itself comprises "wares" that are classified mainly on the basis of firing and surface treatment characteristics. Stoneware and porcelain summarize vitrified ceramics, fired at sufficient high temperatures (>1200°C) to fuse clay into a glassy matrix, whereas terra-cotta and earthenware include porous unvitrified material fired at lower temperatures (<<1000-1200°C).

As terra-cotta is fired usually below 900°C, it is the earliest appearing pottery in the world. Some primitive surface treatments (surface roughening or slip covering) are known from these vessels but in general they were made without special surface improving techniques.

Earthenware is fired at temperatures reaching 1100-1200°C, what leads to an enhancement of its physical properties and can enable fusing at the surface of the ceramic bodies, forming glaze. Coarse and plastic clays are generally used for manufacturing that oxidize to a red color when fired. The variety of products ranges from household, storage and container pottery to bricks roof- and wall tiles.

Stoneware is fired at temperatures of 1200-1350°C, sufficient to cause partial fusion and vitrification of the ceramic body. Iron-low medium grained clays are used resulting in an opaque, often light brown to grey appearing body.

Porcelains were first produced in China (206 B.C. – 220 A.D. after Herz and Garrison, 1998) reaching firing temperatures of 1280-1400°C and higher, a temperatures necessary to vitrify the fine-grained kaolinitic clay that is used for manufacturing. Quartz and K-feldspars are tempered to the



relatively pure clay firstly to reduce the vitrification temperatures as fluxes and secondly to give porcelain its translucency and hardness.

In this thesis, pottery, ceramics and ceramic material respectively will be used as general terms for artifacts that were made out very fine grained raw material with possibly either intentionally added or naturally included material of coarser size that was fired to sufficient temperatures to improve its physical properties. In the antiquity humans started to produce ceramic objects because of utilitarian reasons, only later when the first evolved civilizations appeared, ceramics partly became a noble, often nicely decorated eligible commodity. The techniques the ancient potters used to produce their products were manifold – in the following chapter the most important steps of pottery production are going to be briefly introduced.

### The raw material choice and its preparation

In general, the ceramic paste (ceramic body or fabric) consists of two main groups of constituents. Fine grained, clay sized plastic material (in many cases existing as a compound with naturally included detrital or organic material up to silt size) builds up the paste matrix. Silt and up to sand sized phases (non-plastics) that are naturally or intentionally embedded in the clayey paste matrix are called temper. Temper implies every (naturally or deliberately) added non-plastic (non-clay) material that changes the plasticity during the manufacturing procedure and finally increases the physical stability of the product (Velde and Druc, 1999). These components include inorganics like sand, crushed rock material, reworked and crushed ceramic material (grog), shell-fragments, etc. and organics like bone-fragments, straw, chaff, etc.

The fine grained paste matrix that makes up the major part of the ceramic body consists to a large degree of clay minerals. These make sure that the raw material when mixed with water reaches a sufficient plasticity and thus increases its work- and formability. Depending on the initial size sorting of the raw material which is going to be used for pottery production and keeping in mind that the main goal is the final product, one can take the available sediment as it is or can modify accordingly the substance towards his target specifications. Raw material conditioning techniques can include artificial refinements of the sediment achieved by hand-picking of large inclusions, sieving, decanting or levigating, or in contrast to that, intentional addition of coarser inclusions (tempering). The more technological conditioning methods the potter implements, the harder it is for the scientist to keep these modification steps apart and to fingerprint the used raw material(s). But then, unique and recognizable techniques can reveal certain pottery workshops and allow due to distinctive features to be differentiated from others.

Clays, in general, form due to alteration and physical/chemical/biological decomposition of rocks. Their composition is mainly controlled by the chemistry of their source rocks and processes of weathering and deposition. This leads to the fact that certain clays concerning their bulk chemistry and specific mineralogy can be unique and characteristic for particular areas, providing a material/location fingerprint. Problematic though is that clay minerals may structurally decompose and transform during ceramic firing (a topic studied in detail by Tschegg et al. 2008a and 2008c). The tempered material,

whether it's added intentionally or not, can give more perspective to locate the raw material of the ceramic as it is in most of the cases much more resistant to the firing than the clay. The whole assemblage of temper grains that can be found in a sherd occupies a lot of information about their source rocks and continuative about the regional geology where they are situated. Beside the bulk mineralogical "paragenesis" that reflects the hinterland geology, certain mineral chemistries can emphasize and confine assignments to specific rock types and certain areas.

## The ceramic firing

After the choice of the right base material and its possible modifications, the intended shape is formed out of this raw material and dried afterwards. Depending on the ware group and its requirements, in many cases surface treatments are carried out on the object after drying. To give the ceramic a smooth appearance, different surface treatments are known, one commonly applied method though is the dispersion of clay rich suspensions on the surface. The obtained slip can be colored with different oxides (Velde and Druc, 1999) and may provide the basis for further extraordinary surface decorations like glazes (vitrified shiny layer at surface) and all sorts of color beautifications and paintings.

The following and last step in the pottery creating procedure, the ceramic firing, is by far the most essential one. It is responsible for the transformation of a clayey material into a ceramic artificial substance that is durable, resistant and keeps its shape against external "hazards". The hardening of the synthetic material is a result of mineral breakdown reactions, -transformations and blasteses of new mineral phases that can only be achieved with a firing of the object at sufficient temperatures for a certain time. Mainly the clay components but also temper grains undergo thermal changes during firing. The exact temperatures though at which these reactions take place are hard to state precisely as several factors have influence on them (duration and atmosphere of firing, chemical and mineralogical composition of the ceramic paste, existence of calcareous inclusions, fluxes, etc.). Nevertheless a rough compilation of the most frequent reactions that can be observed with increasing temperatures can simplified be summarized after Rice (1987), Maggetti (1982), Noll (1991) as well as Herz and Garrison (1998) as following:

|             |   |
|-------------|---|
| 100-200°C:  | Loss of water of formation – dehydration;   |
| 200-400°C:  | Oxidation of organic material;  |
| 450-600°C:  | Lost of water in the clay structure – dehydroxylation of clay minerals starts;  |
| 550-750°C:  | $\beta$ -quartz is formed at 573°C; calcite and micas begin to break down;  |
| 750-850°C:  | Kaolinite and smectite lose their crystalline structure;  |
| 850-1100°C: | Calcite decomposes to lime (CaO) losing CO <sub>2</sub> , $\beta$ -quartz can transform to Tridymite; complete destruction of most clay mineral structures, some illite may persist; depending on the elements available, high temperature phases such as wollastonite, gehlenite, diopside and anorthite as well as mullite and spinel may start to form; incipient vitrification; |
| ▼ >1100°C:  | Dissolving silica initiates further vitrification;  |

Beside the mineralogical and chemical composition of the raw materials, temperature, duration of firing and firing atmosphere are determining base-parameters for the result. These latter frame-variables changed significantly over the time, as firing techniques and kiln-engineering improved. The first pottery was fired in open bonfires under  $\pm$  uncontrolled conditions whereas in the course of time potters started to use kilns for their firing procedure to achieve higher and stable temperatures under controlled atmospheric conditions. Other variables that can influence the firing outcome is in addition to the chemical and mineralogical composition of the paste also the size, morphology, sorting and crystallinity of the temper grains, the wall width of the body and the gradient of heating and cooling. The production requirements varied and were mainly depended on the specific ware group and its compassed use. E. g. for table ware that was often fabricated with calcareous temper, the temperature should not exceed the point of calcite-decomposition as the object then begins losing its strength. For fine ceramics with glazes however, the maximum reachable temperature was intended. The connection of the raw material choice with its associated conditioning and preparation techniques and the knowledge about all the firing variables and parameters directly controls the quality of the obtained ceramics.

## Archaeological science of ceramic material

---

Depending on the archaeological research question, the main aims of archaeological science of ceramic materials is to reconstruct the technology of pottery production with all given features and possible variations and to locate the pottery provenance. That way, distinct production centers and their organization, the extent of craft specialization, distribution and trade of objects away from these production centers and the consumption stage (use, maintenance) of pottery can be investigated and comprehended (Tite, 1999).

After Herz and Garrison (1998), main concerns of ceramic investigation are

- to study the nature and source of the used raw materials and the techniques applied for the pottery manufacturing (raw material conditioning, tempering, surface treatments, etc.) for reconstruction of ancient working methods;
- to learn about the physical properties and their changes during transformation of a sediment into a ceramic product;
- to understand the chemical and mineralogical reactions that occur during firing as an indicator for the potters skills; and
- to study use, provenance and trade of the wares.

## The quest for provenance of ceramics

Two general approaches for the determination of provenance of pottery shall be highlighted here. The first one is the mineralogical and geochemical analysis of the sherds of interest and the comparison of these to reference wares of known provenance. When pottery samples were found directly e. g. in a kiln of a certain site and a sufficient number of assuring analyses can determine their compositional uniqueness, they can be used as a reference of a distinct source. If compositional reference standards (“autochthonous pottery”) are established for a specific site or location, the comparison of sherds of unknown provenance to these references makes an appropriate assignment or a more or less definite non-accordance possible. Depending on the physical and chemical characteristics of these reference samples/groups (distinct mineralogical- and bulk chemical-, mineral chemical-, etc. features) an adequate analytical procedure can be established to compare these samples to other ones (early works done by e. g. Perlman and Asaro, 1969, Mommsen et al., 1988; recently by e. g. Vaughn et al., 2006, Monette et al., 2007, Tschegg et al., 2008a).

The second approach is to link the sherds of unknown origin with raw materials that are available in the area of the assumed provenance. After Goffer (1983), this determination of provenance of pottery is based on two assumptions; first that raw materials from different sources are chemically that different to be distinguished easily and second that chemical variations of raw materials of the same source are smaller than those of different sources. The direct linkage between ceramic materials and sediments requires much more analytical work, a combination of independent methods and a lot of understanding concerning pottery production techniques and regional geology (recent studies by e. g. Hein et al., 2004, Alden et al., 2006, Gliozzo et al., 2007, Tschegg et al., 2008d). The first issue that has to be tackled is the manufacturing procedure of the sherd to gain as much information as possible about raw material conditioning techniques. Refinement or tempering on the opposite can for example influence the bulk geochemistry of ceramics, either diluting or boosting the bulk chemical budget. For comparing bulk geochemical data of ceramics to assumed source sediments, it's therefore absolutely essential to know about these processes a priori. Precise conclusions and defined assignment make the application of integrated analytical techniques necessary. It's not sufficient hence, only to compare bulk chemical or -mineralogical data against each other to assign different ceramics and raw materials together, one has to take analogies concerning bulk chemistry, clay chemistry, mineral chemistries (mainly of heavy minerals), modal amounts of these minerals, phase morphologies, paste textures, fossil inclusions, etc. into account.

## The insight to ceramic technology

The reconstruction of pottery production techniques involves besides ascertaining what kind of raw material was used, also to study how this material was prepared, how the objects were formed, surface-treated and fired (Tite, 1999). The combination of optical investigation and chemical analysis can provide a lot of information about the preparation of the used sediment. The addition of non-plastic inclusions can be optically identified by grain-morphological (rounded or angular) aspects or bimodal

sorting for example, whereas levigation processes can be chemically figured out by obvious dilution of e. g. trace element contents at constant major and trace element ratios. The porosity of a sherd provides information about tempering of organic material, drying shrinkage, degassing during the firing and so on. Surface treatments can in most of the cases also be identified by optical analyses as the extremely fine surface layers but also glazes are easily identifiable.

The relationship and understanding of firing temperatures and their triggered transformations in mineralogy and/or microstructures of ceramics has been considerably improved in the last years (Maggetti, 1982, Jordán et al., 1999, Traoré et al., 2000, Cultrone et al., 2001, Tschegg et al., 2008c). For reasonable firing temperatures estimates without applying time-consuming experimental work, again only combined analytical techniques can bring clearness. Mineralogical analyses can be used to check if temperature indicating clay minerals are still detectable, to study decomposition reactions of mineral phases like calcite and to detect the blastesis of high temperature phases like Ca-silicates. Optical methods contribute to the estimation of the degree of paste matrix vitrification and of calcite decomposition or can provide other important microtextural information. The color of sherds may also give rough information about the firing temperature but mainly about the fact whether it was fired in an oxidizing or reducing atmosphere (Maggetti, 1984). Mineral chemical analyses can be useful concerning variations in the oxidation-states of Fe-bearing minerals that offer information about relative firing temperature differences (Tschegg et al., 2008a). Microtextural and –chemical changes concerning calcareous phases also occupy constructive complements to temperature estimates, although they were hardly understood in the past (Herz and Garrison, 1998, Tschegg et al., 2008c). The more integrative the analytical work is, the more accurate is the firing temperature estimation.

## Aims of the project

---

Dealing with ancient pottery technology and provenance is a key aspect of archaeological research, often resulting in new and basic information about antique cultures, their daily life and habits, their technologic and economic progresses as well as about relationships and interactions between ancient cultural societies.

The main target therefore was to develop an integrated method for pottery analyses, yielding in the possibility to answer concrete archaeological questions on certain ceramic ware groups. This included essential understanding of all technological aspects concerning pottery production on the one hand, and the localization of the pottery producing workshops on the other. Besides this, the understanding of the regional geomorphology and geology of the presumed provenance areas was of importance, in order to be able assigning the ceramic raw material to a distinct sediment source. Cyprus, with its unique geological framework and its nearly distinctive petrologic features, was an excellent candidate to prove this multi-analytical approach. Therefore the investigation of the Cypriot pottery group of Plain White Wares (PWW) was a main subject for this task. Bichrome Ware samples excavated in Egypt also showed a debatable relation to Cyprus and were therefore included to the

study. To gather all information of interest, we tried to use and combine as many geoscientific analytical methods as possible. That way, mistakes and falsities that turn out due to a lack of information could be avoided or at least minimized. The analytical techniques were applied to study the production practices as well as to locate the origin of these wares (firstly in the light of an international background - Egypt and Cyprus - then regionally on the island of Cyprus).

Another focus of the project was to establish a multidisciplinary cooperation between VIAS (Interdisciplinary Platform for Archaeological Studies – University of Vienna) and the Department of Lithospheric Research (University of Vienna).

## Material specific research questions

---

Ancient ceramics excavated in Cyprus, Egypt and the Canaanite coast were provided for the study to figure out their origin and optional trade as well as to learn about their specific manufacturing procedures.

During the Late Cypriot Bronze Age, Bichrome Wheelmade Ware was a widely distributed pottery in the Eastern Mediterranean. This spacious broadening makes this ware-group interesting and important for chronological purposes. The samples of Bichrome Wheelmade Ware investigated in this study were excavated in Tell el-Dab<sup>c</sup>a (Eastern Nile Delta, Egypt) and represent a noble, very well elaborated, characteristic decorated fine pottery. Doubts about origin as well as interests on technology, trade networks and potential “counterfeit-workshops” that are related to this commodity made it a worth and interest-sparking study material.

The Cypriot Plain White Wheelmade Ware (PWW) that was study-subject as well, reflects a Late Cypriot Bronze age utilitarian group of pottery. As this ware is quite simply made and served reportedly exclusive for everyday-life purposes (storage, consumption, etc.), it was thought to be locally produced and not traded intensively. Nevertheless, it appears very frequently (mainly on Cyprus but also over the Mediterranean region) and its distribution and technology was actually hardly understood. Sherds mainly excavated in Enkomi (Cyprus) but also in numerous other Cypriot locations together with comparison ceramics from Tell Abu Hawam (Israel) were therefore investigated to learn about the technological knowledge of PWW manufacturing workshops as well as to locate the exact origin. As no authentic reference ceramics were available that would make an assignment PWW samples to Enkomi possible, sediment samples of the area assumed of being potential raw materials were collected in Cyprus and added to the study.

## Methods

---

It was a serious ambition during this study not to focus on one specialized analytical method, neither optical nor chemical, in order to gain as much as comprehensive and self-contained information as possible. Integrating textural, microtextural and mineralogical observations with analyses of bulk and single component geochemistry turned out as an effective and highly representative approach for the investigation of ceramics and analogue materials.

Analytical methods that were used in the present study:

- *Optical microscopy (OM)* to get first rough information on the mineralogical composition as well as on textural characteristics of the paste and morphological features of included phases.
- *X-ray diffraction (XRD)* to gain an overview of the bulk mineral assemblage of studied ceramics and sediments. High temperature phases like e. g. gehlenite are effectively detectable, breakdown reactions of e. g. calcite or clay minerals can be reconstructed. Clay mineralogical analyses of investigated sediments were also performed using XRD.
- *Scanning electron microscopy (SEM)* to appraise the state of vitrification of certain ceramic samples and to study the decomposition, transformation and reaction of calcareous inclusions in high temperature fired ceramics.
- *Electron probe microanalysis (EPMA)* to study microtextural features of the paste as well as to gain chemical compositions of included mineral phases and paste matrices. Moreover, detailed investigations were carried out on medium-high temperature reactions as well as on the involved microstructural and chemical changes. Beside the characterization of inclusions and neoblasts of micron-scale, attention was also paid to microfossils.
- *Raman spectroscopy (RS)* to assess the state of crystallinity of calcite minerals in low, medium and high temperature regimes.
- *X-ray fluorescence analysis (XRF)* to gain bulk geochemical major and trace element compositions of investigated ceramics and sediments.
- *Inductively coupled plasma mass-spectrometry (ICP-MS)* to obtain bulk geochemical minor, trace and rare earth element compositions of ceramics and sediments.

## SYNTHESIS

In Appendices A-D, the scientific papers that arose out of investigation of the study-materials are presented.

Appendix (A) deals with Cypriot-style Bichrome Wheelmade Ware samples (excavated in Tell el-Dab<sup>a</sup> - eastern Nile Delta, Egypt) that were suspected of being faked in Egypt during the Late Bronze Age I. Combining mineralogical, petrologic, geological and geochemical information, it was possible to state that parts of these sherds really were produced in Cyprus and exported to Egypt whereas the other fraction was locally reproduced in Egypt. The provenance discrimination could be stated by analyzing and comparing the used raw materials (mainly their included mineral assemblage) from both groups to the regional geology of Egypt and Cyprus as well as to comparative material from both localities. The affiliation of one ceramic group to alluvia from the eastern Nile delta and the other group to Troodos (Cypriot ophiolite complex) derived sediments clearly turned out. With all applied methods, the distinction between the two wares and the analogies within them were without doubt comprehensible. For the assignments to Cyprus or Egypt, evidences obtained from bulk and mainly mineral geochemistry were essential.

Besides enlightening the provenance, a lot of information could be gained about the technological skills behind the differing ware groups. The original Cypriot Bichrome Wheelmade Ware reflects a highly developed pottery manufacturing that includes diligent pre-conditioning of the base material and firing temperatures of 950-1000°C. Phase transformations and neoblastesis of high temperature indicating minerals allowed the accurate firing temperature estimation. The imitational ware from Egypt reflects pottery manufacturing at a definitely lower technological level, as the ceramics seem to be made directly out of available Nile sediments and firing temperature estimates yielded only 600-800°C.

Appendix (B) concerns pottery samples of the 18<sup>th</sup> Dynasty with proved Egyptian origin and associates these ceramics with raw materials available in the Nile delta and alluvial sediments along the river Nile towards Upper Egypt. As there is a long tradition of studying Egyptian pottery, through time a classification system mainly based on textural observations evolved. The sole optical correlation of ceramics to this established scheme though is complex, imprecise, very subjective and therefore questionable.

In this paper, diverse sedimentary environments (with their specific petrographic, mineralogical, geochemical (bulk and paste-matrix) and sediment-petrologic features) along the river Nile and its delta region are presented, linked with an approach to assign Egyptian ceramics to these latter raw material sources. A direct correlation to raw materials and their typical areas where they crop out respectively was with the application of various analytical techniques possible. By this means



it was realizable to establish ceramic reference groups with clarified origin to those sherds of unknown provenance can be compared.

Appendix (C) discusses thermally triggered mineral reactions that take place in ceramic materials at increasing firing temperatures. Cypriot Bronze Age Plain White Wheelmade ware specimens were used as study material. Beside the general petrographical, mineralogical and geochemical characterization of these samples as well as the examination of their manufacturing procedure, temperature induced reactions and transformations concerning phyllosilicates and calcareous inclusions were key-issue of this paper. By microtextural, micromorphological and phase-geochemical analyses, two stages of carbonate breakdown and associated reactions could be reconstructed that are directly related to the reached temperatures during firing. The progress of carbonate decomposition, the growth of new minerals and the factors controlling these processes in ceramic materials were described and comprehended in detail. In a first stage, Ca diffuses from calcareous inclusions into the phyllosilicatic paste matrix, preparing all necessary conditions for the following reaction step – the growth of carbonate-enclosing Al-Si reaction domains through partial melting, the blastesis of Ca-silicates and the simultaneous complete dissociation of calcareous phases. The study for the first time shows how and where the often detected Ca-silicate phases grow, describes the microchemical processes that are involved and gives a further useful tool to estimate ceramic firing temperatures. Additionally it impressively demonstrates, how differently ceramic textures can develop due to varying firing temperatures although the raw material concerning both, bulk geochemistry and –mineralogy was identical.

Appendix (D) concerns Late Cypriot Bronze Age Plain White Wheelmade ware whose provenance, distribution and production technique are fairly unknown. The study material was excavated in several Cypriot archaeological sites and the northern Canaanite coast. Microtextural, geochemical, mineralogical and palaeozoological evidence allowed distinguishing four differing groups of pottery that were assigned to sediments that for comparative reasons were sampled in the eastern Mesaoria Plain (Cyprus).

Two groups were manufactured out of Pliocene sediments that are available in the area around Enkomi (eastern Cypriot coast) reflecting different raw material conditioning techniques though. Another group mirrors a very similar base material with the difference that it is considerably influenced by mafic-ultramafic rocks from the Troodos ophiolite complex indicating a sediment source that is still in the Mesaoria Plain but geographically closer to the Troodos mountains. The fourth group shows correlation to Holocene sediments that are also available in eastern Cyprus.

Due to the reliable assignment of these investigated Plain White ware samples from Cyprus and abroad to distinct raw material sources and their outcropping localities respectively, and moreover due to the understanding of their particular manufacturing procedures, it was possible to reveal the presence of diverse specialized pottery producing workshops that merchandized their goods on the island of Cyprus and beyond.

---

## REFERENCES

Alden, J.R., Minc, L., Lynch, T.F., 2006. Identifying the sources of Inka period ceramics from northern Chile: results of a neutron activation study. *Journal of Archaeological Science* 33, 4, 575-594.

Cultrone, G., Rodriguez-Navarro, C., Sebastian, E., Cazalla, O., De la Torre, M. J., 2001. Carbonate and silicate phase reactions during ceramic firing. *European Journal of Mineralogy* 13, 621-634.

Goffer, Z., 1980. *Archaeological Chemistry*. John Wiley, New York.

Goffer, Z., 1983. Physical studies of archaeological materials. *Rep. Prog. Phys.* 46, 1193-1234.

Giozzo, E., Vivacqua, P., Turbanti Memmi, I., 2008. Integrating archaeology, archaeometry and geology: local production technology and imports at Paola (Cosenza, Southern Italy). *Journal of Archaeological Science* 35, 4, 1074-1089.

Hein, A., Day, P.M, Cau Ontiveros, M.A, Kilikoglou, V., 2004. Red clays from Central and Eastern Crete: geochemical and mineralogical properties in view of provenance studies on ancient ceramics. *Applied Clay Science* 24, 3-4, 245-255.

Herz, N., Garrison, E.G., 1998. *Geological methods for archaeology*. Oxford University Press, New York.

Jordán, M.M., Boix, A., Sanfeliu, T., de la Fuente, C., 1999. Firing transformations of cretaceous clays used in the manufacturing of ceramic tiles. *Applied Clay Science* 14, 225-234.

Maggetti, M., 1982. Phase analysis and its significance for technology and origin, in: Olin, J.S., Franklin, A.D. (Eds.), *Archaeological Ceramics*. Smithsonian Institution Press, Washington, 121-133.

Maggetti, M., Westley, H., Olin, J.S., 1984. Provenance and Technical Studies of Mexican Majolica Using Elemental and Phase Analysis. *Archaeological Chemistry* 3, 151-191.

Monette, Y., Richer-LaFlèche, M., Moussette, M., Dufournier, D., 2007. Compositional analysis of local redwares: characterizing the pottery productions of 16 workshops located in Southern Québec dating from late 17<sup>th</sup> to late 19<sup>th</sup>-century. *Journal of Archaeological Science* 34, 123-140.

Mommsen, H., Lewandowski, E., Weber, J. and Podzuweit, Ch., 1988. Neutron Activation Analysis of Mycenaean Pottery from the Argolid: The Search for Reference Groups in Farquhar, R. M., Hancock, R. G. V., Pavlish, L. A. (Eds.), *Proc. Int. Symp. Archaeometry*, University of Toronto, 165-171.

- 
- Noll, W., 1991. *Alte Keramiken und ihre Pigmente*. E. Schweizerbart'sche Verlagsbuchhandlung, Stuttgart.
- Perlman, I., Asaro, F., 1969. Pottery analysis by neutron activation. *Archaeometry* 11, 21-52.
- Pollard, M., Heron, C., 1996. *Archaeological chemistry*. The Royal Society of Chemistry, Cambridge.
- Rice, P.M., 1987. *Pottery Analysis: A Sourcebook*. University of Chicago Press, Chicago.
- Tite, M.S., 1999: Pottery Production, Distribution, and Consumption – Contribution of the Physical Sciences. *Journal of Archaeological Method and Theory* 6, 3, 181-233.
- Traoré, K., Kabré, T.S., Blanchart, Ph., 2000. Low temperature sintering of a pottery from Burkina Faso. *Applied Clay Science* 17, 279-292.
- Tschegg, C., Hein, I., Ntaflos, Th., 2008a. State of the art multi-analytical geoscientific approach to identify Cypriot Bichrome Wheelmade Ware reproduction in the Eastern Nile delta (Egypt). *Journal of Archaeological Science* 35, 1134-1147.
- Tschegg, C., 2008b. A geoscientific, methodologically integrated realisation to reconsider Egyptian pottery of the 18<sup>th</sup> Dynasty in Hein, I. (Ed.): *The Manual of Bichrome Wheelmade Ware of the Eastern Mediterranean*. Verlag der Österreichischen Akademie der Wissenschaften, Wien (accepted).
- Tschegg, C., Ntaflos, Th., Hein, I., 2008c. Thermally triggered two-stage reaction of carbonates and clay during ceramic firing - a case study on Bronze Age Cypriot ceramics. *Applied Clay Science* (in press).
- Tschegg, C., Ntaflos, Th., Hein, I., 2008d. Combined geological, petrological and geochemical method to reveal source material and technology of Late Cypriot Bronze Age Plain White ware ceramics. *Journal of Archaeological Science* (under review).
- Vaughn, K.J., Conlee, C.A., Neff, H., Schreiber, K., 2006. Ceramic production in ancient Nasca: provenance analysis of pottery from the Early Nasca and Tiza cultures through INAA. *Journal of Archaeological Science* 33, 5, 681-689.
- Velde, B., Druc, I.C., 1999. *Archaeological Ceramic Materials: origin and utilization*, Springer-Verlag, Berlin Heidelberg.

## APPENDICES (MANUSCRIPTS)

### Appendix (A)

---

Tschegg, C., Hein, I., Ntaflos, Th., 2008a. State of the art multi-analytical geoscientific approach to identify Cypriot Bichrome Wheelmade Ware reproduction in the Eastern Nile delta (Egypt). *Journal of Archaeological Science* 35, 1134-1147.



## State of the art multi-analytical geoscientific approach to identify Cypriot Bichrome Wheelmade Ware reproduction in the Eastern Nile delta (Egypt)

C. Tschegg<sup>a,c,\*</sup>, I. Hein<sup>b,c</sup>, Th. Ntaflos<sup>a</sup>

<sup>a</sup> Department of Lithospheric Sciences, University of Vienna, Althanstr. 14, 1090 Vienna, Austria

<sup>b</sup> Institute of Egyptology, University of Vienna, Frankgasse 1, 1090 Vienna, Austria

<sup>c</sup> VIAS – Interdisciplinary Platform for Archaeological Studies, University of Vienna, Franz Klein-Gasse 1, 1190 Vienna, Austria

Received 16 May 2007; received in revised form 2 August 2007; accepted 21 August 2007

### Abstract

Bichrome Wheelmade Ware originally from Cyprus is under suspicion of being a local reproduction in the Eastern Nile Delta during the early 18th Dynasty (Late Bronze Age I). To elucidate this question, samples from Tell el-Dab<sup>a</sup> (Egypt) and from Cyprus were examined in detail. Petrologic and geochemical analytical techniques including optical microscopy, XRD, XRF, ICP-MS, EPMA were applied in order to emphasize the differences and similarities of the two products. Micro-textures and mineral-phase reactions provide information about conditioning procedures of raw materials as well as firing-temperatures reached during pottery fabrication. Bulk major and trace element abundances and the chemical compositions of pyroxenes, feldspars and oxide-minerals allows the distinctive discrimination of the wares and the correlation with provenance-indicating reference material.

The original Cypriot Bichrome Wheelmade Ware finds reflect high-level ceramic manufacturing technologies (including pre-conditioning of raw-materials and firing temperatures around 950–1000 °C); their decisive mineralogy and chemistry indicate East Cypriot sediments used for production. Phase reactions and the formation of secondary Ca-silicates like gehlenite and wollastonite make fine temperature estimates possible. The comparison of bulk-and mineral-chemistries to reference data from Cyprus reveals a good correlation with mafic and ultramafic sources together with the calcareous impact of the Kyrenia sediments. The imitational Bichrome Wheelmade Ware from Egypt reflects pottery made directly out of fine-grained Nile alluvia from the Eastern Nile Delta (probably near Tell el-Dab<sup>a</sup>). From textural investigations and firing-temperature estimates (600–800 °C) a less refined fabrication process is evident.

© 2007 Elsevier Ltd. All rights reserved.

**Keywords:** Bichrome Ware; Bronze Age; Cyprus; Egypt; Ceramic analysis; Provenance study; Multi-analytical approach; Mineral chemistry; Firing temperature

### 1. Introduction

The island of Cyprus in the centre of the Eastern Mediterranean Sea has great potential to illuminate the history of ancient trade routes and networks of the Eastern Levante, which became highly important in particular during the second half

of the 2nd Millennium B.C. with the fluctuation of the Copper trade.

Bichrome Wheelmade Ware is one of the most important mirrors for such Bronze Age Mediterranean networks at the beginning of the Late Cypriot Bronze Age (LC I). The ware was widely distributed in the entire Eastern Levante, from Turkey (Alalakh) over the Syrian, Lebanese and Canaanite coast, down to Egypt (Fig. 1a). In Cyprus, Bichrome Wheelmade Ware can be found at nearly 40 sites. This wide distribution makes it an important tool for associating the chronology of Cyprus with that of the Eastern Mediterranean civilizations.

\* Corresponding author at: Department of Lithospheric Sciences, University of Vienna, Althanstr. 14, 1090 Vienna, Austria. Tel.: +43 1 4277 53318.

E-mail addresses: [cornelius.tschegg@univie.ac.at](mailto:cornelius.tschegg@univie.ac.at) (C. Tschegg), [irmgard.hein@univie.ac.at](mailto:irmgard.hein@univie.ac.at) (I. Hein), [theodoros.ntaflos@univie.ac.at](mailto:theodoros.ntaflos@univie.ac.at) (Th. Ntaflos).

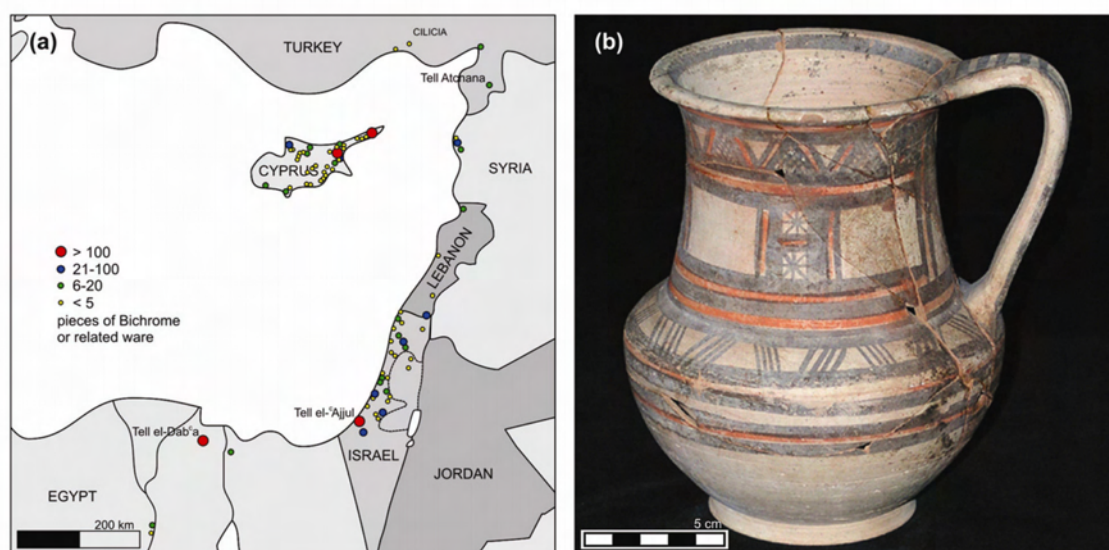


Fig. 1. (a) Distribution of Bichrome Wheelmade Ware in the eastern Mediterranean (taken from an unpublished internal report made by Ragna Stidsing, 2006; modified by author). (b) Typical appearance of Cypriot Bichrome Wheelmade Ware (photograph by Prof. Michal Artzy).

The often beautifully elaborated painting in red and black gives Bichrome Wheelmade Ware a very attractive appearance (Fig. 1b), which apparently made it requested in the Eastern Mediterranean. Because of its wide distribution and its easily recognizable characteristic decoration, Bichrome Wheelmade Ware can be used by archaeologists as a chronological marker for the LC I horizon, and consequently to correlate time-levels in the Late Bronze Age cultures from various regions in the Eastern Levant. For this reason, a large research-program (part of project SCIEM 2000) is currently being undertaken to solve chronological and distributive questions, with the origin-distinction of diverse types of the ware as one main target of the project. Furthermore, studies on typology and decoration are in progress. The large variety of vessel types and decoration motifs demonstrate that we have to consider the LC Bichrome story as a story of originals and imitations in different places in the region, as was already pointed out in Stockholm in 2001 (Hein, 2001a). In the past, several regions and suggestions for the origin of the Bichrome Ware were suggested. Under discussion were e.g.:

- Northern Syria (Petrie, 1931), Cappadocia (Petrie, 1932) or Cilicia (Petrie, 1934);
- Tell el-<sup>c</sup>Ajjul in the Gaza strip (Heurtley, 1939) with the idea, the Bichrome Ware was decorated by only one painter, he called the “Tell el-<sup>c</sup>Ajjul Painter” according to the large quantities found at this site;
- A Hurrian origin (inland Syria) was proposed by Epstein (1966), based on the motive, referring to material from Tell Atchana (Alalakh, levels VI and V);
- Cyprus was brought into the discussion by Hennessy (1963) and Trendall (1948);
- Cypriot origin was finally proved with the technical development of analytical methods, by Neutron Activation Analysis from Artzy et al. (1973, 1978). In these studies,

it was proved that samples from Megiddo could be of Cypriot origin, as well as locally produced in the Syro-Palestinian region.

The number of Egyptian sites with Bichrome Ware is rather small, and the largest amount so far is found in the Egyptian Eastern Nile delta, at <sup>c</sup>Ezbet Helmi (Tell el-Dab<sup>a</sup>), where a palatial area from the late Hyksos period and early 18th Dynasty was found (Bietak, 2005). Until today, a total number of 205 Bichrome Wheelmade Ware sherds/vessels from the site has been registered (excavation ongoing). Looking closely at this pottery, it becomes evident, that several types of fabrics exist. The ware shows different surface colours in the unpainted parts, as well as various types of texture characteristics – from unsorted and gritty to very homogenous.

A first attempt to separate fabric groups by visual analysis under a microscope (5 ware families were distinguished) was presented in 2001 (Hein, 2001b). This preliminary work clearly showed the necessity of more intensive analytical investigations, whereas in particular ware-group 3 from Tell el-Dab<sup>a</sup> was questionable in the debate of provenance. These finds show a macro- and microscopically resemblance to Egyptian Nile clay, although most of the sherds belong to vessel types (such as jugs or kraters) of non-Egyptian origin. The general appearance of ware group 3 (at present 34% of registered Bichrome Wheelmade Ware specimen from Tell el-Dab<sup>a</sup>) is mainly reddish-brown (Munsell: 2.5YR 6/4–6) and less varying to reddish-yellow (Munsell: 5YR 6/6). It has a macroscopically fine, quite homogenous but porous paste. In field observation, fine organic fibres are occasionally visible as well as few red grits and some fine black grits. The surface of the pieces is pebble-burnished and the fragments break hard. The interior surface is mostly more reddish brown, but this colour range depends on the sherds position. The

essential question for the archaeologist was, if a reproduction of Cypriot Bichrome Wheelmade Ware in the North Eastern Nile delta can be proved (as it is assumed from distinctive typological criteria and fabric similarities) or if the reproduction idea has to be dismissed.

For this reason, a multi-analytical approach has been developed and applied to scientific samples from Tell el-Dab<sup>c</sup>a and for comparison to sherds from Enkomi (Cyprus). The combination of the methods made it possible to investigate in detail ten samples found at Tell el-Dab<sup>c</sup>a, to compare these samples with reference material from Cyprus and the Nile delta, and to prove the origin of the selected ten Bichrome Wheelmade Ware sherds.

## 2. Analytical methods

Polished thin sections of the samples were investigated using an optical polarizing microscope to gain first information on texture and mineralogical composition. Photomicrographs in plane- and crossed-polarized transmitted light were taken to visualize paste and temper, making the samples easier to compare.

For the detailed investigation of microtextures, mineral- and matrix-chemistry as well as mineral-phase reactions, carbon-coated thin sections were analysed with a Cameca SX-100 electron-microprobe (University of Vienna, Department of Lithospheric Sciences). All mineral-analyses were made against natural standards, using four wavelength-dispersive spectrometers; acceleration voltage and beam current were 15 kV and 20 nA respectively, and standard correction procedures were applied. Pyroxenes and oxides were analysed with a focused 1  $\mu$ m beam, whereas all feldspar analyses were carried out with an expanded 5  $\mu$ m beam diameter, minimizing the loss of Na and K. Smallest mineral-inclusions were characterized using an energy-dispersive spectrometer (EDS). To obtain high-resolution backscattered-electron (BSE) images with a sample-dimension of 1.5–1.1 mm, a matrix of 5  $\times$  5 pictures was acquired and stitched together automatically, using the built-in function of the microprobe.

To get a comparable overview of the mineral assemblage present in the ceramics, powder diffraction (XRD) was conducted. The powder samples with preferred orientation were scanned over the interval of 2–70° 2  $\theta$  with a Phillips PW 1877 X-ray diffraction working with Cu-radiation at 45 kV and 35 mA (University of Vienna, Department for Geodynamics and Sedimentology). Surface alterations and coatings were removed from the sherds using a Proxxon Micromot grinder. Followed by washing samples with distilled water and drying. An electric achat-mill was used to grind each specimen into fine powder, guaranteeing homogeneity for all further investigations.

Major elements of the bulk material were analyzed with the sequential X-ray spectrometer Phillips PW 2400 equipped with a Rh-excitation source (University of Vienna, Department of Lithospheric Sciences). Fused beads were produced out of a mixture of specimen fired at 950 °C and flux (di-lithium tetraborate Li<sub>2</sub>B<sub>4</sub>O<sub>7</sub>), diluted 1:5 to gain accurate and precise results.

In order to measure trace and rare earth elements (REE) with ICP-MS, 100 mg of each sample were digested in an

acid mixture consisting of 2 ml HNO<sub>3</sub> and 2 ml HF (both Merck Suprapur reagents) in Teflon beakers. The procedure included a triple heating in closed beakers at 180 °C for more than 48 h each on a hot-plate with intermediate evaporation stages. After the last evaporation, the residuals were dissolved in 10 ml 2 N HNO<sub>3</sub> and diluted to 100 ml using high purity water to achieve a final dilution factor of 1:1000. The analyses were performed on a Perkin Elmer ELAN 6100 DRC fitted with an automatic sampler (University of Vienna, Department of Lithospheric Sciences). In order to minimize drift-effects, 0.1 ml Rh was added to each sample as internal standard. For external calibration, four solutions with Merck Multi-element ICP-MS calibration Standard 2, four with Merck Multi-element ICP-MS calibration Standard 3 and another four with Merck Multi-element ICP-MS calibration Standard 5 with differing dilutions were prepared. REEs together with U and Th were analysed in a first run, all other trace elements in a second run. To assess precision and accuracy of the acquired data and additionally to control the digestion procedure, three geological reference samples (G1, BCR1, BE-N) were analysed repeatedly during the measurements (reference values, measured values together with their standard deviation are presented in Table 1).

The loss of ignition (LOI) was quantified firing each dried and powdered sample for 3 h at 950 °C, the CO<sub>2</sub> content with a LECO RC-412 multiphase carbon determinator.

For statistical analysis, SPSS 13.0 was used. To reduce the dimensionality of the data and compare a batch of measurements with other reference-data, principal component analysis (PCA) was performed. P because of its high volatility, U, Pb and Li because of their low stability in soils and Pr, Nd, Gd, Tb, Dy, Ho, Er, Tm and Yb because of their strong correlation with La, were excluded for all PCAs (Zhu et al., 2004).

## 3. Results

### 3.1. Bulk chemistry – major elements

Characterizing the raw material used for pottery production, it seemed to be meaningful to assess and compare elemental ratios of elements with similar geochemical behaviour rather than absolute weight percent of distinct elements. Element ratios do not react as sensitively to some raw material conditioning-techniques (e.g. levigation or decantation, quartz- and carbonate-tempering) and therefore they can provide stronger arguments for a certain material source.

Table 1 presents the major element concentration of ten Bichrome Wheelmade Ware sherds excavated in Tell el-Dab<sup>c</sup>a. As the bulk composition, with respect to major elements, is strongly controlled by the modal proportions of present single phases – which themselves may vary over a large range – a broad scatter in element concentrations can be expected. Despite this fact, the Cypriot sherds have a very homogenous major element composition, which allows a clear division of the whole set into two chemically distinguishable groups, one of Cypriot and one of Egyptian origin (Fig. 2a). Larger variations can be observed in the Egyptian samples, concerning SiO<sub>2</sub> (up to 11.1 wt.%)





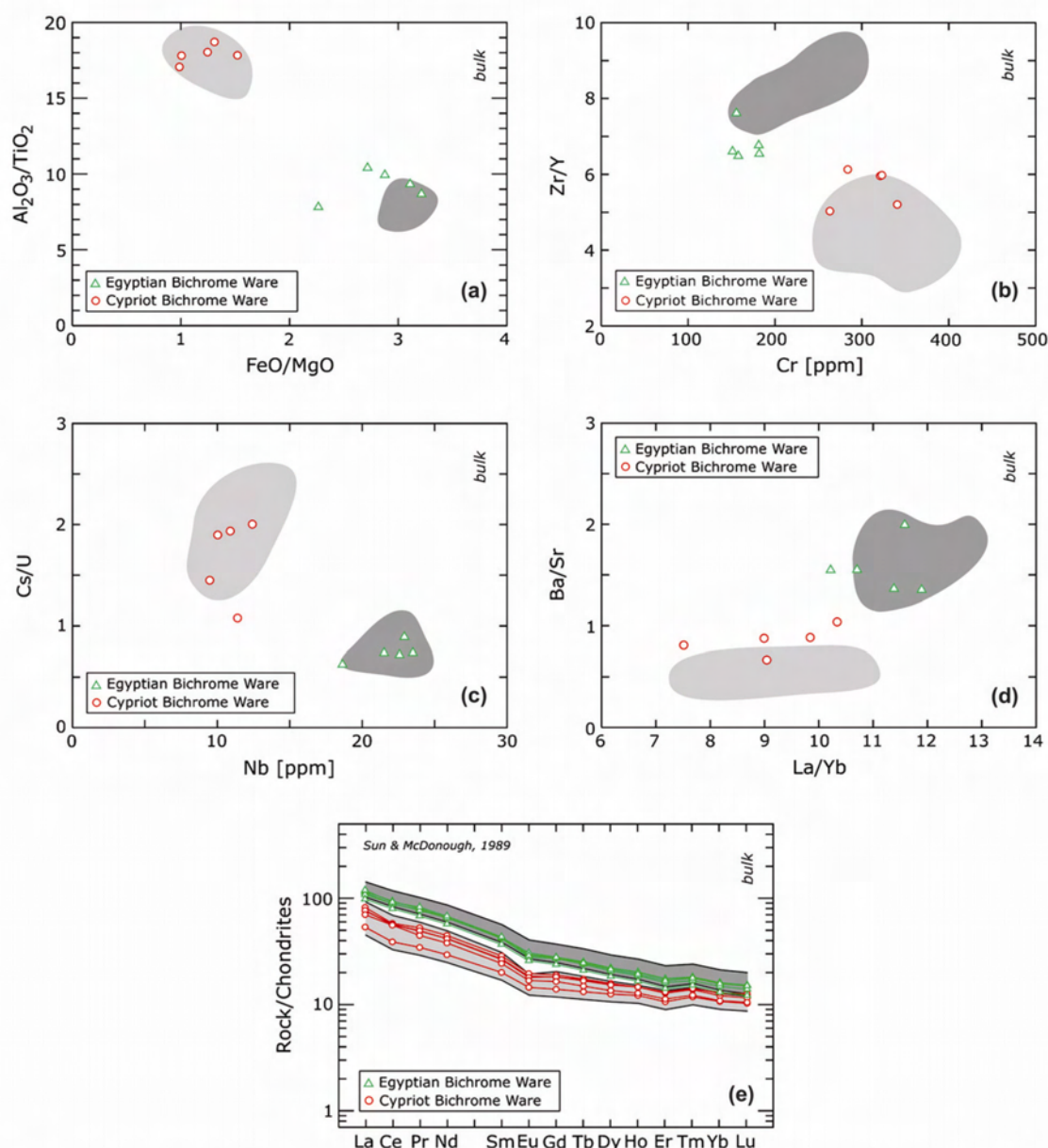


Fig. 2. (a–d) Characterizing bulk variation diagrams of imitated Egyptian and original Cypriot Bichrome Wheelmade Ware samples from Tell el-Dab<sup>a</sup>. Dark grey contoured fields comprise combined reference data from Egypt – Nile silts (11 analyses) from Redmount and Morgenstein (1996). Light grey fields comprise combined reference data from Cyprus – Plain White Ware (12 analyses) and in (d) mean of 38 pieces Corinthian-style roof tiles (Gomez et al., 2002) additionally. (e) Chondrite-normalized (Sun and McDonough, 1989) rare earth abundance patterns for Egyptian and Cypriot Bichrome Wheelmade Ware samples. Dark grey area comprises Egyptian reference data (11 analyses of Nile silt, mean of 27 analyses Nile river sediment composite and 5 analyses of Nile alluvium) from Redmount and Morgenstein (1996) and Hamroush (1992). Light grey area comprises 12 analyses of Plain White Ware, Corinthian-style roof tiles (mean of 38 analyses from Gomez et al., 2002) and pottery analyses from Kition, Hala Sultan Tekke and Enkomi (Bryan et al., 1997).

and CaO (up to 10.4 wt.%). This relationship emerges from slightly differing quartz proportions of the temper-fraction and chemical variations of the used raw material, which is sporadically more calcareous. Remarkable is the high amount of

secondary calcium ( $CaO_{sec}$ ) in the Cypriot samples, which varies from 1.3–6.7 wt.% and apparently is associated with recarbonation processes during burial. In contrast, the  $CaO_{sec}$  contents in the Egyptian samples are very low and ranges from 0.3 to 0.6 wt.%.

### 3.2. Bulk chemistry – trace elements

Trace element compositions of both, Egyptian and Cypriot origin Bichrome Wheelmade Ware specimen are given in Table 1. The measured abundances show relatively small variations within their groupings. The distinct differences in trace element chemistry between the groups are represented by noticeably higher concentrations of REE, Y, Ba, Zr and Nb in sherds of Egyptian origin, whereas the Cypriot sherds have higher amounts of Sc, Cr, Cs, Sr and Li. Some representative trace elements and element ratios together with reference-data from both localities are visible in Figs. 2b–d.

Because of their low variability in nature and their equivalent geochemical behaviour, REEs are very meaningful and suitable in discriminating and classifying natural rocks as well as ceramic samples. The Bichrome Ware sherds of Egyptian origin have a higher total amount of REE (141–167 ppm) than those from Cyprus (73–109 ppm), which separates them in two easily distinguishable groups (Fig. 2e). The La/Sm ratios show no significant difference between the groups (Egyptian: 4.1–4.5 and Cypriot: 4.3–4.7), whereas the La/Yb ratios indicate steeper REE patterns of the Egyptian ware (10.2–11.9) with respect to the Cypriot (7.5–10.3). Compared with reference-data from both localities, the measured REE reveal a good match, making a characterization and classification of the two wares possible.

### 3.3. Principal component analysis of major and trace elements

Fig. 3a shows the score plot of a reduced dataset, comparing a restricted number of measured element abundances of all investigated Bichrome Ware samples with reference information from Cyprus and Egypt. The chosen data were limited by the availability of elements in the cited publications. 14 elements (Ti, Fe, Mn, Ca, Na, Sc, Co, Rb, Cs, La, Lu, Hf, Ta and Th) of all ten specimens together with the reference

values were used to conduct the PCA in Fig. 3a. The two principal components subsume 67.46% of the total variance (PC 1: 41.37%, PC 2: 26.09%), showing a well separated clustering of the two different wares and a clear assignment to their origin. The PCA in Fig. 3b was conducted on 32 elements (Si, Ti, Al, Fe, Mn, Mg, Ca, Na, K, Be, Sc, V, Cr, Co, Cu, Zn, As, Rb, Sr, Zr, Nb, Ag, Cd, Cs, Ba, La, Sm, Eu, Yb, Hf, Ta and Th) of the ten samples of interest. PC 1 (69.94%) and PC 2 (14.70%) subsume 84.64% of the total variance. Thus, PC 1 is very significant and emphasises the good segregation of the dataset over the x-axis, whereas the less significant PC 2 is more scattered. The low Ba-content in sample 8477K is responsible for its outstanding position on the y-axis.

### 3.4. Petrography and mineralogy

Petrographic observations verify the existence of two different pottery groups. Paste texture, porosity and paste mineralogy, quantity, size, shape, sorting and mineralogy of inclusions were investigated. The main distinguishing petrographic features are given in Table 2 and Figs. 4a,b). Well preserved  $\pm$  rounded mineral phases (mainly quartz and K-feldspar) in the paste-matrix as well as mainly large rounded quartzes, K-feldspars, basaltic rock fragments and grog temper in the Egyptian ware strikingly contrast with thermally altered  $\pm$  angular paste-matrix minerals (quartz and plagioclase) and scarce tempered carbonate remnants intergrown with Ca-silicates in the Cypriot ware are remarkable.

Powder diffraction pattern analysis provides a quick-look overview of the present main minerals, the possibility to identify fine-grained Ca-silicates as well as to emphasise the classification of these wares. Fig. 5 illustrates the mineralogical key-differences of the investigated specimens observed by XRD. In both wares, no clay-mineral peaks were detectable. The major quartz peak is twice as high in the Egyptian ware as in the Cypriot, indicating higher modal composition and better crystallinity. Moreover, the Egyptian pattern is dominated by potassium-feldspar-, pyroxene-, hematite- and less plagioclase-peaks unlike the Cypriot pattern, in

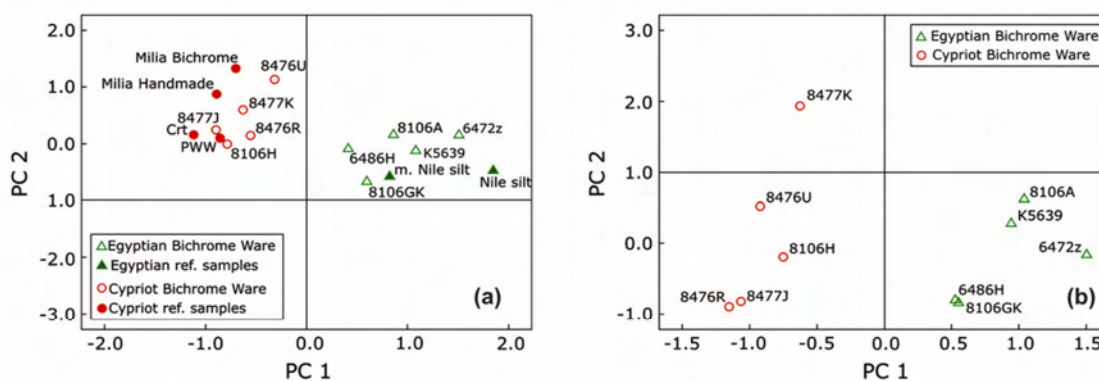


Fig. 3. Score plots of principal component analyses calculated (a) on the reduced dataset, showing the investigated Bichrome Wheelmade Ware specimen together with local reference materials (see text). Egyptian reference data (mean of: 11 analyses Nile silt and 6 analyses mixed Nile silts) from Redmount and Morgenstein (1996) are shown as full triangles, Cypriot reference data (mean of: 38 Corinthian-style roof tiles – Crt, 27 analyses of Milia Bichrome, 8 analyses of Milia Handmade and 12 analyses of Plain White Ware – PWW) from Gomez et al. (2002) and Artzy et al. (1973) as full circles. (b) Score plot conducted on 32 major and trace elements, clearly differentiating the Bichrome Wheelmade Ware samples from Tell el-Dab'a of assumed Egyptian and Cypriot origin.

Table 2  
Main petrographic features of Bichrome Wheelmade Ware samples from Tell el-Dab<sup>a</sup>

|                       | Egyptian origin samples   | Cypriot origin samples  |
|-----------------------|---|---|
| Paste-matrix          | Fine sandy silt   | Silty clay, calcareous, highly vitrified  |
| Paste-matrix minerals | ±rounded quartz-, K-feldspar- and accessory minerals  | ±angular quartz-, plagioclase- and accessory minerals   |
| Temper grains         | Moderately sorted, major fraction with 300–500 µm sub-rounded components  | Poorly sorted, few angular grains (100–200 µm) and 300–600 µm carbonatic fragments  |
| Porosity              | Mainly due to burned organic matter   | Surface subparallel degassing pores   |
| Common components     | Quartz, K-feldspar, anorthite, ilmenite, spinel, titanite, apatite  |   |
| Specific components   | Silicified foraminifera, organic matter, augite, grog, basaltic rock fragments, hematite, monazite, biotite, zircon | Albite, chromite, Cr-spinel, gehlenite, wollastonite, secondary calcite, Cr-endiopside  |
| Comment               | Mineral phases well preserved, no mineral reactions due to firing   | Primary calcite grains decomposed and reacted to Ca-silicates; oxides mostly segregated, rim reactions on feldspar and quartz |

which plagioclase-, secondary calcite-, gehlenite- and wollastonite-peaks are present. Due to lower firing temperatures, the mineral phases in the Egyptian samples, especially feldspars and iron oxides show narrow and well defined peaks indicating a good crystal state, whereas particularly oxides and plagioclases in the Cypriot ware indicate thermal alteration with wider and lower peaks.

### 3.5. Mineral chemistry

Representative compositions (electron-microprobe analyses) of pyroxenes, K-feldspars, plagioclases, ilmenites and spinels are given in Table 3. The chemistry of these minerals (especially feldspars and pyroxenes) may vary over a wide range (even within the same rock) what often makes them to a non-appropriate tool to group and identify the provenance of materials. Nevertheless, the mineral chemistries examined in these samples were thoroughly homogeneous so that it was possible to figure out mineral-compositions that are characteristic for the investigated sherds and their origin.

Pyroxenes appear in all Egyptian samples, but only in three Cypriot ones. Analysis results are given in Table 3 and Figs. 6a,b. The pyroxenes of Cypriot origin are Cr-rich endiopsides indicating a mafic-ultramafic origin, in contrast to the high titanium augites from Egypt indicating a basaltic and/or gabbroic source. The Mg# of pyroxenes in sherds from Egypt varies between 0.74 and 0.78, whereas in the Cypriot it varies between 0.86 and 0.88. The Al<sub>2</sub>O<sub>3</sub> contents that range from 2.01 to 2.57 wt.% and the TiO<sub>2</sub> contents ranging from 0.95 to

1.37 wt.% in the Egyptian pyroxenes are consistent with an igneous origin. The very low TiO<sub>2</sub> contents (0.15–0.16 wt.%) and the much higher Cr<sub>2</sub>O<sub>3</sub> concentrations (0.49–1.33 wt.%) in the Cypriot pyroxenes, suggest an ultramafic origin.

Potassium feldspars are scarce in Cypriot samples. Even so, they show significant features in their major and trace element chemistry, separating them clearly from the Egyptians (Table 3, Fig. 6c). K<sub>2</sub>O ranges from 15.4 to 16 wt.%, Na<sub>2</sub>O from 0.54 to 0.87 wt.% in the samples from Egypt, whereas from 12.6 to 13.3 wt.% and 2.52 to 3.01 wt.% in the Cypriot ones. Additionally measured BaO contents on K-feldspars range from 0.60 to 0.96 in the Egyptian and from 0.00 to 0.28 wt.% in the Cypriot samples, separating the groups distinctively. As potassium-feldspars of various acidic rocks (rhyolites, rhyolite tuffs, trachytes, phonolites, etc.) can have Ba-contents in the range of the ones analysed in this study (Smith and Brown, 1988), a discrimination of the two origins is possible, but not a distinct assignment to rocks of a defined region.

Plagioclases are anorthites and have a very limited range of compositions within the groups making a clear division into Egyptian and Cypriot origins possible (Table 3). SiO<sub>2</sub>-, Al<sub>2</sub>O<sub>3</sub>-, CaO- and Na<sub>2</sub>O-contents vary between 52.2 and 54.0, 28.7 and 30.1, 12.3 and 13.4 and 3.95 and 3.99 wt.% in the Egyptian sherds and between 56.8 and 58.3, 26.1 and 27.0, 9.8 and 10.8 and 5.43 and 5.81 wt.% in the Cypriots respectively. Fig. 6d characterizes the Na<sub>2</sub>O and CaO concentrations of plagioclases together with some reference data of Egyptian origin. Albites appear only in the samples from Cyprus.

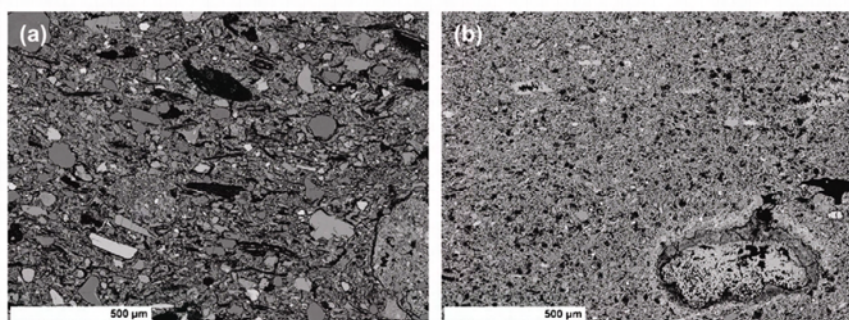


Fig. 4. Processed BSE images visualizing the fabric of (a) a representative Egyptian Bichrome Wheelmade Ware sample (8106A) and (b) a representative Cypriot Bichrome Wheelmade Ware sample (8476R); total width of both images is 1.5 mm.

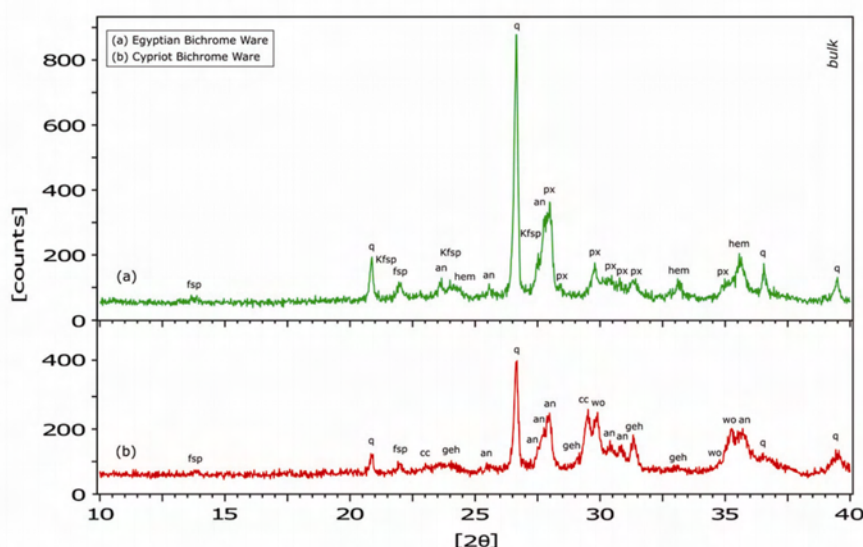


Fig. 5. XRD patterns of Bichrome Wheelmade Ware samples. (a) 8106A represents and characterizes sherds of Egyptian origin and (b) 8476R represents sherds of Cypriot origin. The indicated mineral phases are anorthite (an), calcite (cc), feldspar (fsp), gehlenite (geh), hematite (hem), potassium feldspar (Kfsp), pyroxene (px), quartz (q), and wollastonite (wo).

Ilmenite mineral-analyses are demonstrated in Table 3. The ilmenites in the Egyptian samples have generally lower  $\text{TiO}_2$ -contents (47.3–48.3 wt.%) than the ones in the Cypriot ware (53.0–55.0 wt.%). The opposite trend has been observed concerning FeO. FeO ranges from 41.9 to 47.0 wt.% in Egyptian and from 35.1 to 42.2 wt.% in Cypriot samples (Fig. 6e). Although the total sums of the measurements are lower than 100%, the stoichiometric mineral calculation shows that all analysed minerals are real ilmenites despite alteration processes. With exception of sample 8106GK, the ilmenites in Egyptian sherds show a Ti and Fe deficit, unlike those in Cypriot samples, which indicate a Fe-deficit but an excess of Ti. The beginning conversion of primary ilmenite to a mixture of rutile, pseudobrookite and hematite when thermally influenced (over 850 °C) in addition to the coval oxidation of greater  $\text{Fe}^{2+}$  to  $\text{Fe}^{3+}$  that, when recalculated, raises the sum (Deer et al., 1962), can account for these deviations. Atypical amounts of CaO were detected in ilmenites of both localities, rising from 0.08 to 0.46 wt.% in the samples from Egypt and from 0.49 to 0.85 wt.% in the samples from Cyprus. Deer et al. (1962) reported ilmenite compositions in e.g. gabbros with CaO amounts up to 0.71 wt.%. The free and highly reactive CaO during the firing could also be responsible for the slight enrichment of calcium, at least in the Cypriot sherds.

Spinel analyses are reproduced in Table 3. The  $\text{TiO}_2$  contents in Ti-magnetites of Egyptian samples range between 20.5 and 25.8 wt.%, in the Cypriot ware between 4.18 and 6.40 wt.%,  $\text{Al}_2\text{O}_3$  from 1.29 to 1.99 wt.% and 0.07 to 0.86 wt.% respectively. FeO and  $\text{Fe}_2\text{O}_3$  concentrations vary in the Egyptian ware from 47.4 to 53.3 wt.% and 12.8 to 22.4 wt.% respectively (Fig. 6f). In the Cypriot ware they indicate a much higher oxidation-state and vary from 33.4 to 34.8 wt.% and 52.2 to 58.6 wt.%. The low sum can be ascribed

to a beginning exsolution of small hematite lamellae and thus not accounted  $\text{Fe}^{3+}$  together with a slight deficit of oxygen, what was indicated from the mineral calculation.

Analysed chromites, only found in Cypriot specimens, show  $\text{Cr}_2\text{O}_3$  concentrations ranging from 50.9 to 57.3 wt.%, while  $\text{Al}_2\text{O}_3$  is 11.8–17.5 wt.%, FeO is 18.4–19.9 wt.% and MgO is 8.3–11.3 wt.%.

## 4. Discussion

### 4.1. Estimated thermometry

Depending on the composition of the used raw-clay material, the firing temperature and -duration as well as the kiln atmosphere during firing, new microcrystalline phases form due to the mineral reactions of the decomposed clays with the tempered material. Because thermodynamic equilibrium is not necessarily achieved through the firing process, mainly mineral-phase reactions observed by microprobe analyses were used in addition to petrography and XRD pattern analysis to estimate rough firing temperatures.

Primary  $\text{CaCO}_3$  begins to break down at 600 °C and is decomposed completely around 800–850 °C releasing all  $\text{CO}_2$ . The breakdown of clays begins around 700 °C, setting free a highly reactive mixture of fine grained silica and aluminium (Rathossi et al., 2004). If primary calcite grains are present, the free CaO reacts with the decomposition-products of the clay and partly with other temper material (quartz and plagioclase) to form calcium silicates (Rathossi et al., 2004).

Gehlenite is a metastable phase in Ca-low ceramics with a maximum concentration at 850–900 °C (Noll, 1991). In a higher CaO-concentrated environment and at temperatures of around 850–950 °C, it is however stable and forms as a first



| Cypriot | Representative spinel microprobe analyses (wt.%) |                  |                                |                                |                                |      |      |      |      |       |       |       |       |                  | Numbers of ions on the basis of 8 oxygens |       |                  |       |       |  |  |  |
|---------|--|------------------|--------------------------------|--------------------------------|--------------------------------|------|------|------|------|-------|-------|-------|-------|------------------|---|-------|------------------|-------|-------|--|--|--|
|         | SiO <sub>2</sub>                                 | TiO <sub>2</sub> | Al <sub>2</sub> O <sub>3</sub> | Cr <sub>2</sub> O <sub>3</sub> | Fe <sub>2</sub> O <sub>3</sub> | FeO  | MnO  | MgO  | CaO  | Total | Si    | Al    | Cr    | Fe <sup>3+</sup> | Ti  | Mg    | Fe <sup>2+</sup> | Mn    | Ca    |  |  |  |
| 8106H   | 0.08   | 20.5             | 1.63                           | 0.07                           | 22.4                           | 47.4 | 0.93 | 0.06 | 1.11 | 93.3  | 0.008 | 0.077 | 0.002 | 0.672            | 0.616                                     | 0.004 | 1.584            | 0.031 | 0.005 |  |  |  |
| 8476R   | 0.08   | 21.2             | 1.52                           | 0.11                           | 20.6                           | 47.8 | 0.66 | 0.45 | 1.03 | 94.2  | 0.003 | 0.070 | 0.004 | 0.609            | 0.626                                     | 0.026 | 1.567            | 0.022 | 0.043 |  |  |  |
| 8476U   | 0.03   | 21.5             | 1.99                           | 0.86                           | 18.4                           | 47.4 | 0.65 | 0.47 | 0.24 | 91.7  | 0.008 | 0.094 | 0.027 | 0.557            | 0.652                                     | 0.028 | 1.600            | 0.022 | 0.010 |  |  |  |
| 8477J   | 0.28   | 25.8             | 1.60                           | 0.11                           | 12.8                           | 53.3 | 0.58 | 0.15 | 0.29 | 95.1  | 0.020 | 0.073 | 0.003 | 0.375            | 0.755                                     | 0.009 | 1.735            | 0.019 | 0.012 |  |  |  |
| 8477K   | 0.59   | 24.4             | 1.29                           | 0.01                           | 14.8                           | 50.0 | 0.80 | 0.64 | 0.10 | 92.3  | 0.011 | 0.061 | 0.000 | 0.446            | 0.736                                     | 0.038 | 1.677            | 0.027 | 0.004 |  |  |  |
|         |  | 5.15             | 0.15                           | 0.05                           | 56.2                           | 34.8 | 0.38 | 0.30 | 0.13 | 97.7  | 0.020 | 0.007 | 0.002 | 1.650            | 0.151                                     | 0.017 | 1.136            | 0.012 | 0.005 |  |  |  |
|         |  | 4.18             | 0.07                           | 0.00                           | 58.6                           | 33.4 | 0.17 | 0.13 | 0.27 | 97.0  | 0.004 | 0.003 | 0.000 | 1.741            | 0.124                                     | 0.007 | 1.104            | 0.006 | 0.011 |  |  |  |
|         |  | 6.40             | 0.86                           | 0.00                           | 52.2                           | 34.4 | 0.17 | 0.65 | 0.28 | 95.1  | 0.008 | 0.040 | 0.000 | 1.560            | 0.191                                     | 0.038 | 1.144            | 0.006 | 0.012 |  |  |  |

\* Total iron is shown as FeO. Mg# = molar MgO/(MgO + FeO).

reaction product around larger calcite minerals (Veniale, 1990). When temperature exceeds 950 °C, gehlenite is still stable when coexisting with wollastonite, but if the present silica-content is sufficient, it starts to break down giving wollastonite and anorthite (Rathossi et al., 2004 and ref. therein).

In all original Cypriot Bichrome Wheelmade Ware samples, we were able to analyse gehlenite in reaction rims around decomposed large calcite grains together with small intergrown domains composed of wollastonite and anorthite. In addition considering the highly vitrified isotropic paste, the thermally altered rims of feldspar- and quartz-grains and the XRD patterns, we assume a firing temperature of approximately 950–1000 °C in an oxidizing kiln atmosphere. The exsolution of ilmenites and magnetites into secondary phases and their recorded high concentration of Fe<sup>3+</sup> confirm the temperature estimate. Secondary pores, oriented roughly parallel to the surface are temperature-triggered bubbles due to escaping gasses, which are released under the assumed temperature (Velde and Druc, 1999).

The imitated Bichrome Ware samples from Egypt are certainly fired at lower temperatures (<<950 °C). As there are no primary-calcite grain remnants in these samples and the initial clay composition is partly slight calcareous, though obviously too fine-grained, secondary Ca-silicates were not able to form (Maggetti, 1982). No mineral phases indicate rim- or other phase-reactions. The oxides show no exsolution and their mineral calculation indicate a much lesser state of oxidation. There is no evidence for vitrification or sintering processes (starting soonest at 700 °C, Velde and Druc, 1999) in these samples and completely oxidized organic matter suggests an oxidizing firing process. As firing of fine-grained and weak calcareous pastes do not show low-temperature-indicating intergranular mineralogical changes (Maggetti, 1982; Noll, 1991) and low firing in general just produces poorly crystallized, thermally decomposed clay-mineral phases (Noll, 1981), it is harder to estimate the range of the firing temperature. The light brown colour of the non-isotropic paste and the absence of clay-mineral peaks at last, together with the other information let us roughly approximate a firing temperature of around 600–800 °C (Maggetti et al., 1984).

#### 4.2. Provenance

With all applied methods, the Egyptian Bichrome Wheelmade Ware production can distinctively distinguished from the Cypriot one. Major and trace elements as well as the element-based principal component analyses indicate the clear clustering into two groups. Comparing the bulk chemistry of all investigated sherds with reference-data from both origin localities, a very good match is described (Figs. 2 and 3).

The Bichrome-samples of Egyptian origin correlate well with the geochemically characterized Nile silts and mixed Nile silts, which were used as raw material for pottery production in Egypt since prehistoric periods and still are in use (Redmunt and Morgenstern, 1996). Particularly in the Nile-delta area, alluvium was and is the most used source material for Egyptian potters. Rare earth and trace element analyses of

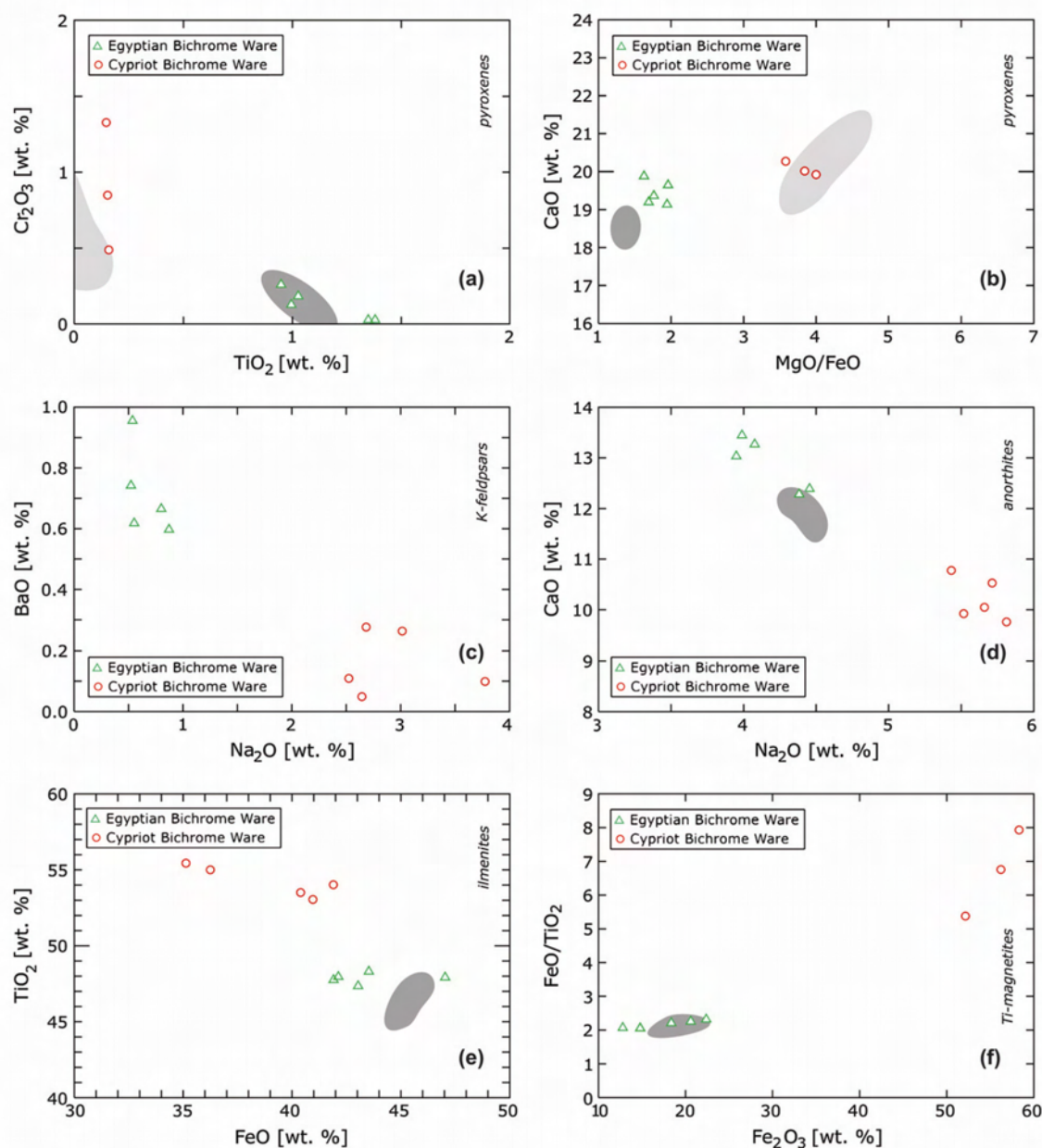


Fig. 6. (a–f) Co-variation diagrams for representative mineral analyses of assumed Egyptian and Cypriot origin Bichrome Wheelmade Ware samples. (a, b)  $\text{TiO}_2$  vs.  $\text{Cr}_2\text{O}_3$  and  $\text{MgO/FeO}$  vs.  $\text{CaO}$  of clinopyroxenes, (c)  $\text{Na}_2\text{O}$  vs.  $\text{BaO}$  of potassium feldspars, (d)  $\text{Na}_2\text{O}$  vs.  $\text{CaO}$  of anorthites, (e)  $\text{FeO}$  vs.  $\text{TiO}_2$  of ilmenites and (f)  $\text{Fe}_2\text{O}_3$  vs.  $\text{FeO/TiO}_2$  of Ti-magnetites. Dark grey contoured fields comprise combined reference data of Egyptian origin (Mallory-Greenough et al., 1998); light grey fields comprise combined reference data of Cypriot origin (Thy and Xenophontos, 1991; Cameron, 1985).

Nile alluvium and Nile river sediment composite (NRSC) are given by Hamroush (1992 and ref. therein), which also correspond in all elements with the Egyptian Bichrome Wheelmade Ware ceramics from Tell el-Dab<sup>a</sup> (Fig. 2e). As the investigated sherds reflect the characteristics of this raw material very well (what is shown by the very low compositionally variations of

Nile sediments and Bichrome pottery), it seems obvious that the raw material in the Nile delta area used for Bichrome pottery-manufacturing was not pre-processed much and in all probability no artificial tempering-methods were applied. This is also indicated by petrographical investigation, as there is no sign for artificially assembled grain-fractions.

Chemical bulk analyses of Cypriot Bichrome Wheelmade- as well as Handmade Ware from Milia (reported by Artzy et al., 1973) provide a strong and proven reference dataset for this unique pottery ware and its source-provenance. The element abundances gathered from the Tell el-Dab<sup>a</sup> samples conform to these references, giving intense evidence for the original source-area. Bryan et al. (1997) identified chemically characterized groups of Cypriot sherds from the Larnaca region (Kition and Hala Sultan Tekke) as well as from Enkomi, both of which show similar major and trace element composition compared to the specimens analysed in this study (Fig. 2). The characteristics of Corinthian-style roof tiles that are consistent with the features of calcareous sediments of the Mesaoria Plain, are meant to have their source provenance around Enkomi (Gomez et al., 2002). These referred roof tiles also show a strong chemical correlation with the investigated Bichrome Wheelmade Ware of Cypriot origin and provide a further restriction for its source area. At last, Plain White Ware samples excavated in Enkomi were chemically analysed during this study and compared with the Cypriot Bichrome Wheelmade Ware sherds found in Tell el-Dab<sup>a</sup>. As this ware is quite simply made, it is suitable as reference material and represents local source material from the Enkomi-region quite well. The bulk chemistry of all described east coast Cypriot reference materials point to a well-defined match with the investigated Bichrome Ware of assumed Cypriot origin, supporting the provenance-area estimation around Enkomi and Milia (with Mesaoria Plain sediments as raw material).

The mineralogical assemblage as well as the composition of different mineral phases are, in addition to the bulk chemistry, helpful and useful tools for characterizing and grouping ceramics and show in this case a distinct separation of sherds with two different origins. Much potassium feldspar, augite, basaltic rock fragments, monazite (occurring only in acidic plutonic rocks), organic matter (mainly chaff), silicified foraminifera and reworked ceramic material (grog) as well as the lack of Cr-rich and carbonatic phases in the Egyptian fabric make it mineralogically distinguishable from the Cypriot fabric, which is dominated by anorthite, chromite, Cr-spinels, endiopsides, secondary Ca-silicates and decomposed-primary as well as secondary calcite. The textural characteristics of paste-matrix and larger inclusions and their interaction respectively, investigated mainly via EPMA (Figs. 4a,b) indicate two different techniques of pottery production. The Egyptian ware seems to be directly made out of unconditioned local raw material (fine-grained Nile alluvium), as fabric and paste are also coherent with descriptions of Nile alluviums by Nordström and Bourriau (1993) and ancient Egyptian ceramics made out of Nile-silt by Noll (1981). The raw material for the Cypriot samples was in all probability decanted or levigated and artificially tempered before firing. The just slightly differing CaO contents in the Cypriot Bichrome Wheelmade Ware and the considered reference wares at the roughly equal trace element concentrations as well as the appearance of a temper fraction of 300–600 µm angular, smashed carbonatic material, indicates artificial tempering.

Mallory-Greenough et al. (1998) described basaltic temper in New Kingdom Egyptian pottery and gave analyses of

included pyroxenes, plagioclases, ilmenites and spinels, which correlate nicely with the same mineral-phases found in the Bichrome Ware from Tell el-Dab<sup>a</sup> with assumed Egyptian origin (Figs. 6a,b,d–f). As these fragments of late Cenozoic tholeiitic and slightly alkaline basalts from the Cairo area are fluvial transported downstream in the Nile, they can be found in the alluvial sediments around Tell el-Dab<sup>a</sup>. Augites from the lower pillow lavas of Cyprus (dacitic andesite suite) in comparison do not correlate with augites in sherds from Egyptian origin, having an average composition which is lower in TiO<sub>2</sub>, Al<sub>2</sub>O<sub>3</sub>, Na<sub>2</sub>O and CaO but much higher in FeO and higher in MnO (Thy and Xenophontos, 1991).

Looking at Cyprus, Thy and Xenophontos (1991) analysed lavas as well as their constituent mineral assemblage (pyroxenes, plagioclases and spinels) from the easternmost Troodos upper pillow lava sequence. The results show similar compositions to the minerals found in the Cypriot sourced ceramics. Pyroxenes from the basaltic andesite suite represent a comparable chemistry to the endiopsides from 8106H, 8476R and 8476U (Figs. 6a,b). Phenocryst clinopyroxenes from the Arkapas fault belt lavas, investigated by Cameron (1985) and pyroxenes from the Troodos plutonic rock series analysed by Hébert and Laurent (1990) also have similar and notable limited compositional variations, showing that pyroxenes are, in this case, also suitable for comparison and characterisation. Diopsides and Cr-spinels in the sediments of the Mesaoria Plain, deriving from the Lapithos pillow lavas (Kyrenia range) and other heavy minerals coming from the Kithrea flysch are reported by Garzanti et al. (2000).

Potassium feldspars are scarce in the Cypriot sherds, but do occur in all samples (as small inclusions in the paste matrix). Baroz (1980), Knippper and Sharas'kin (1995) as well as Garzanti et al. (2000) reported late Cretaceous rhyolite bodies, rhyodacitic tuffs (on the southern slope of the range) and felsites in the Kyrenia range, which are all K-feldspar bearing. Potassium feldspars from Palaeocene lamprophyric and trachytic volcanism in the Kyrenia range are described by Baroz (1980), but in all cases, no detailed mineral-compositions are given. In the Egyptian Bichrome Ware, K-feldspars are much more frequent and beside small grains in the paste matrix, they are represented also as large inclusions. Fig. 6c indicates how distinctively the two sources are distinguishable via mineral-chemical investigation of potassium feldspars.

Although plagioclases have a wide compositional range, comparable anorthite measurements are given from the Troodos ophiolite lower pillow lavas (Thy and Xenophontos, 1991), showing relatively good correlation with anorthites from Bichrome sherds of Cypriot origin. The composition of anorthites from basaltic rock fragments that occur in the Nile-delta area (Mallory-Greenough et al., 1998) match very well with the ones found in Bichrome Wheelmade Ware samples of Egyptian origin (Fig. 6d).

Fig. 6e illustrates the good match of Egyptian ilmenites found in the Egyptian Bichrome Ware sherds with the same minerals from basaltic rock fragments as well as their separation from ilmenites of Cypriot origin.

The mineralogy of chromites in Cyprus is described by Cameron (1985) and McElduff and Stumpfl (1991) shows



a wider range of compositions, in which the chromites analysed in the Cypriot Bichrome samples fit well.

Ti-magnetites in the Cypriot ware are too altered to be compared to fresh equivalents. In the Egyptian ware they are not exsolved and show a good correlation with Ti-magnetites from basalts of the Nile delta area (Fig. 6f).

Carbonate rock fragments (including mostly sparite), which are present only as dissolved remnants in the sherds, are supposed to derive from the Kyrenia range. Beach sediments of the Famagusta Gulf, mainly composed of oceanic sediments and lavas of the Lapithos Group, recycled turbidites of the Kithrea Flysch and Pliocene to Quaternary sediments of the Mesaoria Plain (Garzanti et al., 2000) seem to be a suitable raw material source for the Cypriot Bichrome Wheelmade Ware sherds found in Egypt.

## 5. Conclusion

This study shows that it is possible to affirm the archaeological idea of a Bichrome Wheelmade Ware production in the Eastern Nile delta. The use of comprehensive geochemical and petrological analytical methods unequivocally allows discrimination of local Egyptian Bichrome Ware from the imported original Cypriot Bichrome Ware. The main differences can be seen in their specific texture, mineralogy, bulk- and mineral chemistry and manufacturing procedure. The sherds of Cypriot origin show conspicuous large decomposed carbonate-fragments intergrown with their certain reaction products (Ca-silicates) in a homogenous, very fine-grained, levigated and vitrified paste-matrix. The mineralogical assemblage is thermally stressed and comprises among other distinct minerals, Mg- and Cr-rich phases indicating a mafic-ultramafic (ophiolitic) source. The estimated high firing temperature of Cypriot Bichrome sherds distinguishes them clearly from the reproduced Egypt ware, which were fired at much lower temperatures. A heterogeneous, coarser-grained paste, including minerals from a broad variety of rocks, characterizes the Egyptian fabric. Remarkable and discriminating phases are basaltic rock fragments, grog, organic and fossil materials and monazite minerals. Considering major and trace element compositions of the bulk, the two wares can be unequivocally distinguished by higher amounts of elements like Ca, Mg, Cr and Sr in the Cypriot in contrast to higher amounts of Al, Ti, REE, Ba and Zr in the Egyptian ware.

Comparing the overall physical and chemical characteristics of the two pottery-groups to reference material of both origins clearly reveals their affiliations. The imported Bichrome Wheelmade Ware from Cyprus was produced at a higher technological level using pre-processed raw material most likely from the area around Enkomi and Milia. The potters from Egypt used non- or insignificant conditioned alluvial Nile sediments, which are available everywhere in the lower Nile delta, and imitated the highly sought-after Bichrome Wheelmade Ware with a less developed manufacturing-technique. As the characteristics of raw material and fabrication are thoroughly homogeneous within the two pottery groups, a certain production place for both wares is more likely than several workshops. From the archaeological point of view, we can assume that the

studied pottery was a luxurious commodity and apparently a worth subject for imitation, not only in Canaan, but also in Egypt.

## Acknowledgements

We acknowledge the support from the Austrian Science Foundation (FWF Special Research Program F14 - SCIE M 2000 and FWF grant P18908). Manfred Bietak, the first speaker of SCIE M 2000 and director of VIAS (Interdisciplinary Platform for Archaeological Studies – University of Vienna), who kindly supported all pottery studies, has to be thanked in multiple functions, also as the director of the Austrian Archaeological Institute in Cairo and director of the Austrian excavations at Tell el-Dab<sup>a</sup>. We are grateful to Lindy Crewe (University of Manchester) for providing the project with samples from Cyprus, to Prof. Michal Artzy (University of Haifa) for basic support in Cypriot pottery studies and to Yossi Salmon and Ragna Stidsing (University of Haifa) for their helping benefit and detailed information on samples. The two reviewers are thanked for their assistance to improve this paper.

## References

- Artzy, M., Asaro, F., Perlman, I., 1973. The origin of the "Palestinian" Bichrome ware. *Journal of the American Oriental Society* 93 (4), 446–461.
- Artzy, M., Perlman, I., Asaro, F., 1978. Imported and local Bichrome Ware in Megiddo. *Levant* 10, 99–111.
- Baroz, F., 1980. Volcanism and continent-island collision in the Pentadaktylos range, Cyprus. In: Panayiotou, A.E. (Ed.), *Ophiolites, Proc. Int. Symp. Nicosia, Cyprus*.
- Bietak, M., 2005. Neue Paläste aus der 18. Dynastie. In: Jánosi, P. (Ed.), *Structure and Significance. Denkschriften der Österreichischen Akademie der Wissenschaften 33. Untersuchungen der Zweigstelle Kairo des Österreichischen Archäologischen Institutes* 25, Wien, pp. 131–168.
- Bryan, N.D., French, E.B., Hoffman, S.M.A., Robinson, V.J., 1997. Pottery sources in Bronze age Cyprus: a provenance study by neutron activation. *Report of the Department of Antiquities*, 31–64.
- Cameron, W.E., 1985. Petrology and origin of primitive lavas from the Troodos ophiolite, Cyprus. *Contributions to Mineralogy and Petrology* 89, 239–255.
- Deer, W.A., Howie, R.A., Zussman, J., 1962. *Rock-Forming Minerals*, Vol. 5. Longmans, London.
- Epstein, C., 1966. *Palestinian Bichrome Ware*. E.J. Brill, London.
- Garzanti, E., Andò, S., Scutellà, M., 2000. Actualistic Ophiolite Provenance: the Cyprus Case. *Journal of Geology* 108, 199–218.
- Gomez, B., Neff, H., Rautman, M.L., Vaughan, S.J., Glascock, M.D., 2002. The source provenance of Bronze age and Roman pottery from Cyprus. *Archaeometry* 44 (1), 23–36.
- Hamroush, H.A., 1992. Pottery analysis and problems in the identification of the geological origins of ancient ceramics. In: Ballet, P. (Ed.), *Cahiers de la céramique égyptienne. Institut français de l'archéologie orientale, Cairo*, pp. 39–54.
- Hébert, R., Laurent, R., 1990. Mineral chemistry of the plutonic section of the Troodos ophiolite: new constraints for genesis of arc-related ophiolites. In: Malpas, J., Moores, E.M., Panayiotou, A., Xenophontos, C. (Eds.), *Ophiolites, Oceanic Crustal Analogues. Geol. Surv. Dep., Nicosia*, pp. 149–163.
- Hein, I., 2001a. On Bichrome and Base Ring Ware from several excavation Areas at 'Ezbet Helmi. In: Aström, P. (Ed.), *The Chronology of Base-Ring and Bichrome Wheelmade Ware. Vitterhets historie och Antikvitets Akademien, Konferenser 54, Stockholm*, pp. 231–247.
- Hein, I., 2001b. Untersuchungen und vorläufige Bilanz zur Keramik aus 'Ezbet Helmi, speziell Areal H/V. *Egypt and the Levant* 11, 121–147.

- Hennessy, J.B., 1963. *Stephania. A Middle and Late Bronze-Age Cemetery in Cyprus*. Colt Archaeological Institute Publications, London.
- Heurtley, W.F., 1939. A Palestinian Vase Painter of the Sixteenth Century BC, A Palestinian Vase-Painter of the Sixteenth Century BC. *Quarterly of the Department of Antiquities, Palestine VIII*, 21–37.
- Knippper, A.L., Sharas'kin, A.Ya., 1995. Correlation of tectonic events in the Mesozoic history of the northeastern Mediterranean. *Geotectonics* 29 (1), 9–18.
- Maggetti, M., 1982. Phase analysis and its significance for technology and origin. In: Olin, J.S., Franklin, A.D. (Eds.), *Archaeological Ceramics*. Smithsonian Institution Press, pp. 121–133.
- Maggetti, M., Westley, H., Olin, J.S., 1984. Provenance and technical studies of Mexican majolica using elemental and phase analysis. *Archaeological Chemistry* 3, 151–191.
- Mallory-Greenough, L.M., Greenough, J.D., Owen, J.V., 1998. Provenance of temper in a New Kingdom Egyptian pottery sherd: evidence from the petrology and mineralogy of basalt fragments. *Geoarchaeology* 13 (4), 391–410.
- McElduff, B., Stumpfl, E.F., 1991. The chromite deposits of the Troodos Complex, Cyprus – evidence for the role of a fluid phase accompanying chromite formation. *Mineralium Deposita* 26, 307–318.
- Noll, W., 1981. *Bemalte Keramiken Altägyptens: Material, Rohstoffe und Herstellungstechnik*. In: Arnold, D. (Ed.), *Studien zur altägyptischen Keramik*, pp. 103–138. Ph. von Zabern, Mainz.
- Noll, W., 1991. *Alte Keramiken und ihre Pigmente*. E. Schweizerbart'sche Verlagsbuchhandlung, Stuttgart.
- Nordström, P.N., Bourriau, J., 1993. Ceramic technology: clays and fabrics. In: Arnold, D., Bourriau, J. (Eds.), *An Introduction to Ancient Egyptian Pottery*. Ph. von Zabern, Mainz.
- Petrie, W.M.F., 1931. *Ancient Gaza I*, London.
- Petrie, W.M.F., 1932. *Ancient Gaza II*, London.
- Petrie, W.M.F., 1934. *Ancient Gaza IV*, London.
- Rathossi, C., Tsolis-Katagas, P., Katagas, Ch., 2004. Technology and composition of Roman pottery in northwestern Peloponnese, Greece. *Applied Clay Science* 24, 313–326.
- Redmount, C.A., Morgenstein, M.E., 1996. Major and trace element analysis of modern Egyptian pottery. *Journal of Archaeological Science* 23, 741–762.
- Smith, J.S., Brown, W.L., 1988. *Feldspar Minerals, Vol. 1*. Springer-Verlag, Berlin, Heidelberg.
- Sun, S., McDonough, W.F., 1989. Chemical and isotopic systematics of oceanic basalts: implications for mantle composition and processes. In: Saunders, A.D., Norry, M.J. (Eds.), *Magmatism in the Ocean Basins*, 42. Geological Society of London Special Publication, pp. 313–345.
- Trendall, A.D., 2000. *Handbook to the Nicholson Museum*, second ed. University of Sydney, Sydney, New South Wales.
- Thy, P., Xenophontos, C., 1991. Crystallization orders and phase chemistry of glassy lavas from the pillow sequences, Troodos Ophiolite, Cyprus. *Journal of Petrology* 32 (2), 403–428.
- Velde, B., Druc, I.C., 1999. *Archaeological Ceramic Materials: Origin and Utilization*. Springer-Verlag, Berlin, Heidelberg.
- Veniale, F., 1990. Modern techniques of analysis applied to ancient ceramics. In: Veniale, F., Zerra, U. (Eds.), *Proc. ICOMOS-CE Workshop, Advanced Workshop: Analytical Methodologies for the Investigation of Damaged Stones*, pp. 1–45. Pavia, Italy.
- Zhu, J., Shan, J., Qiu, P., Wang, Ch, He, D., Sun, B., Tong, P., Wu, Sh., 2004. The multivariate statistical analysis and XRD analysis of pottery at Xigongqiao site. *Journal of Archaeological Science* 31, 1685–1691.

## Appendix (B)

---

Tschegg, C., 2008b. A geoscientific, methodologically integrated realisation to reconsider Egyptian pottery of the 18<sup>th</sup> Dynasty in Hein, I. (Ed.): The Manual of Bichrome Wheelmade Ware of the Eastern Mediterranean. Verlag der Österreichischen Akademie der Wissenschaften, Wien (accepted).

## A GEOSCIENTIFIC METHODOLOGICALLY INTEGRATED REALISATION TO RECONSIDER EGYPTIAN POTTERY OF THE 18<sup>TH</sup> DYNASTY

Cornelius Tschegg

Department of Lithospheric Research, University of Vienna, Althanstr. 14, 1090-Vienna, Austria  
*cornelius.tschegg@univie.ac.at*

### INTRODUCTION

Since over 25 years authors try to determine and categorize ceramics from ancient Egypt on the basis of the raw material that was used for pottery production (ARNOLD, 1980, ARNOLD, 1981, HOPE ET AL., 1981, NOLL, 1981, NORDSTRÖM, 1986, BOURRIAU AND NICHOLSON, 1992, HAMROUSH, 1992, NORDSTRÖM AND BOURRIAU, 1993, REDMOUNT AND MORGENSTERN, 1996, BOURRIAU ET AL., 2000, BOURRIAU ET AL., 2006). For this purpose, a descriptive framework-classification and nomenclature was developed in the 1980's, called "Vienna System" that as a visual approach tries to categorize ceramic fabrics by the variability of Egyptian sediments. Primary characteristics (clay/silt matrix and inclusions) and secondary features (colour, hardness, transverse strength and porosity) define the terminology for Egyptian pottery fabrics in the Vienna System in a time span from the late Predynastic to the end of the XIX<sup>th</sup> Dynasty (BOURRIAU ET AL., 2006).

During the present study it emerged that Nile delta pottery can be recognized quite easily and characterized well when studied with integrated and detailed analytical methods. Taking additional geochemical reference data of ancient and recent ceramics as well as local raw materials into account, determinations and affiliations of artefacts often turn out more reasonable and coherent. Matches to the Vienna System however, that are based only on conspicuous optical

features, can lead to premature argumentations and are sometimes confusing, so that consequently they have to be considered cautiously. Besides that, the problems of comprehending and publishing verbal descriptions of visually gathered fabric characteristics, remain (also stated by BOURRIAU AND NICHOLSON, 1992). The raw material that is available along the river Nile and the Nile delta region is heterogeneous, highly variable and its mineralogical features reflect an extremely wide geological hinterland. We intend to show that a detailed study not only focused on petrography but also on bulk geochemistry, phase-chemistry and mineralogy helps to understand the raw material choice as well as the methodological skill of ancient potters in Lower Egypt during the Early 18<sup>th</sup> Dynasty.

### SAMPLES AND ANALYTICAL TECHNIQUES

The investigated samples were found at <sup>c</sup>Ezbet Helmi/Tell el-Dab<sup>a</sup> in the Eastern Nile delta (see Fig. 1). Three pieces (8106A, 8106GK, K5639) are from an 18<sup>th</sup> Dynasty palatial area (BIETAK, 2005), two (6472z, 6486H) from a settlement area north-west of the Tell (area A/V, HEIN AND JÁNOSI, 2004) and one (KN5) from Upper Egypt. Questions of origin and production centres were already clarified by TSCHEGG ET AL. (2008) – all samples are considered to have Egyptian provenance. From archaeological/typological

---

In I. Hein (Ed.), 2008: The Manual of Bichrome Wheelmade Ware of the Eastern Mediterranean. Verlag der Österreichischen Akademie der Wissenschaften, Wien (accepted).

Cornelius Tschegg

criteria, K5639 represents typical Nile silt, a very common fabric in the Nile delta region. The Bichrome samples 6472z, 6486H, 8106A and 8106GK are after their typology and fracture criteria also recognisable as products made out of Nile sediments. The colours of these sherds are throughout reddish-brown varying sporadically to reddish-yellow. 8106GK is the only analysed specimen with a blackish colour. KN5 which from an archaeological viewpoint is a representative sample for Upper Egyptian marl clay fabrics was included in this study for comparative aspects.

Before analysing the specimens, surface alterations and coatings were removed using a Proxxon Micromot grinder. After that, the sherds were washed with distilled water and dried. An electric achat-mill was used to grind the samples, to refine and to homogenize them for all further analyses. Fused beads were produced out of a mixture of at 950° C fired specimen and flux, diluted 1: 5 to analyse bulk major chemistries with a sequential X-ray spectrometer (Phillips PW2400) equipped with a Rh- excitation source (University of Vienna, Department of Lithospheric Research). The loss on ignition (LOI) was quantified firing each dried and powdered sample for at 950° C. For measuring trace- and rare earth elements (REE) with inductively coupled plasma mass spectrometry (ICP-MS), 100 mg of each sample were digested in Teflon beakers. A Perkin Elmer ELAN 6100 DRC fitted with an automatic sampler (University of Vienna, Department of Lithospheric Research) was used to perform the analyses. To minimize instrumental drift-effects, Rh was added to each sample as internal standard; for external calibration, four solutions with differing dilutions (Merck multi-element ICP-MS calibration standards) were prepared. To assess the precision and accuracy of all measurements and additionally to control the digestion procedure, three international geological reference samples (G1, BCR1, BE-N) have been analysed. Polished thin sections were analysed with an optical

polarizing microscope, photomicrographs in plane- and crossed-polarized transmitted light were taken to visualize paste and temper. For the detailed investigation of microstructures, mineral chemistry and mineral-phase reactions, carbon-coated thin sections were analysed with a Cameca SX-100 electron-microprobe (University of Vienna, Department of Lithospheric Research). All mineral-analyses were made against natural standards, using four wavelength-dispersive spectrometers; acceleration voltage and beam current were 15 kV and 20 nA respectively, and standard correction procedures were applied. Microprobe analyses of clayish paste matrix chemistries were performed applying a defocused beam technique (3 µm beam diameter). The measurements were carried out multiple in order to control the reproducibility as well as to check the consistence of the analysed clay chemistry. To gain high-resolution backscattered-electron (BSE) images with a sample-dimension of 1.5 to 1.1 mm, a matrix of 5x5 pictures was acquired and stitched together automatically, using an instrumental integrated method. Scion Image for Windows (© Scion Corporation) was used to process backscattered-electron (BSE) images. Statistical calculations (principal component analysis - PCA and hierarchical cluster analysis – HCA) were performed with SPSS 13.0 for Windows (© SPSS Inc.).

#### **GEOLOGICAL OVERVIEW - NILE DELTA SEDIMENTS AND SOILS**

Generally, the alluvial sediments and soils of the Nile delta have been formed by deposition of Nile derived sedimentary products of igneous as well as metamorphic rocks from the Central African complexes and of volcanic rocks from the Ethiopian plateau as well as from the Red sea hills (SAID, 1990). The major fraction however consists of sediments coming from regional geological formations.

A geoscientific methodologically integrated realisation to reconsider Egyptian pottery of the 18<sup>th</sup> Dynasty

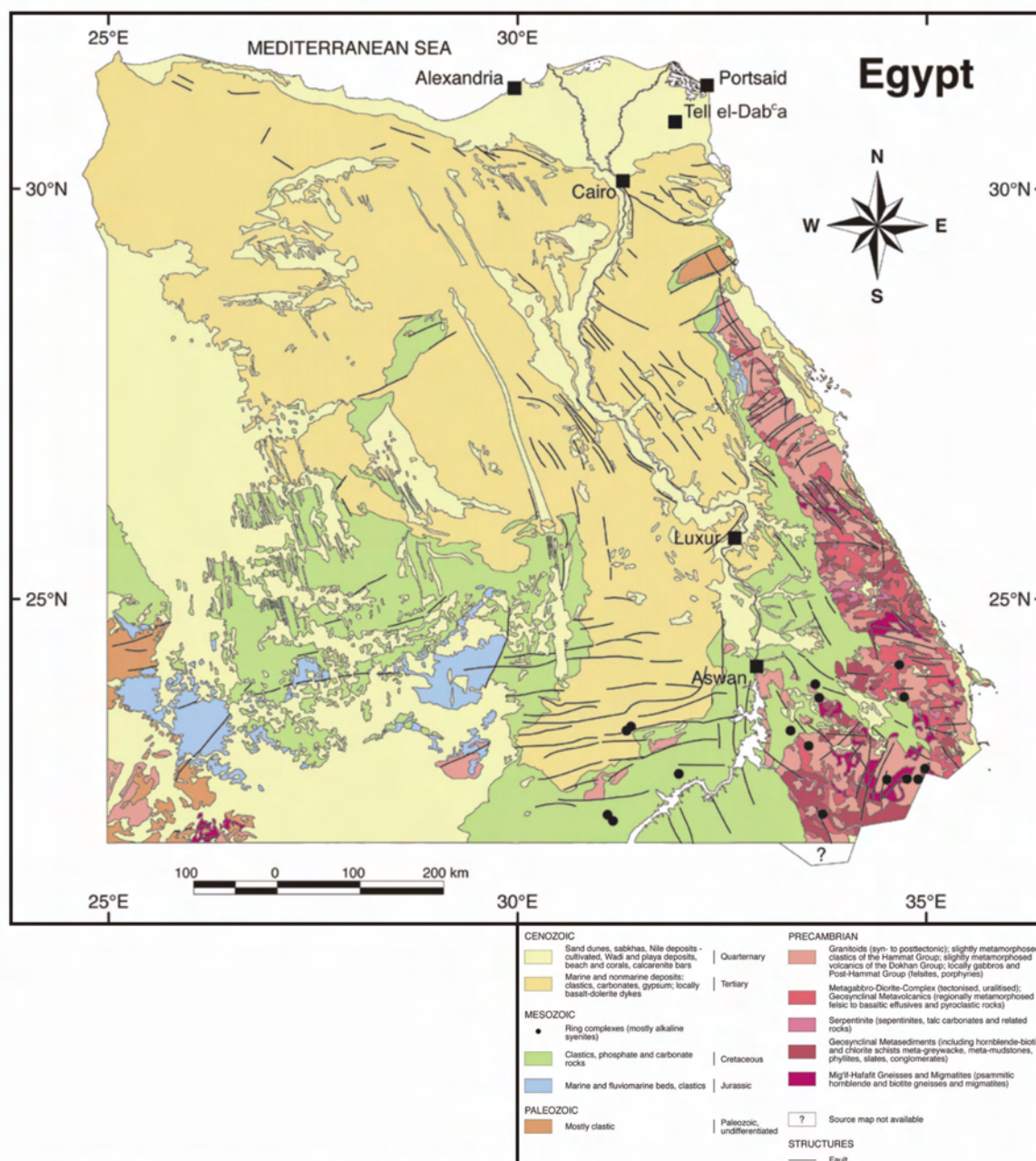


Fig. 1: Geological map of Egypt (modified from SCHLÜTER, 2006).

The regional Egyptian geology can very simply be divided as following (see Fig. 1):

- The Precambrian basement-complex is built up by mainly granitoids, gneisses and schists as well as younger basic igneous rocks (diorites) which intruded into the gneiss-schist complex. Calc-alkaline volcanics, pyroclastics, metasediments and clastic sediments are also related to the basement rocks.
- Palaeozoic rocks overlying the Precambrian basement can mainly be found in south-western Egypt and occur as sandstones and lesser marine shales and siltstones.
- The Mesozoic sedimentary formations comprise the late Jurassic to Cretaceous Nubian sandstones that extensively cover the basement rocks over most of North Africa. Northwards they interfinger with nearshore

Cornelius Tschegg

- marine sediments containing carbonates and phosphates.
- The Tertiary successions include Palaeocene shales and marls lying on top of the Mesozoic sandstones. Limestones with partly intercalated clays are deposited in Eocene to Oligocene times, whereas the Oligocene is again dominantly sedimented under continental conditions. After the opening of the Gulf of Suez and the Red Sea graben in the early Miocene, marine transgressions flooded over large areas in northern Egypt, where marine clays and fluvio-marine sediments were accumulated. In the late Miocene, arid climate conditions caused the deposition of evaporitic sequences and limestones which are located in Lower Egypt and build up the basement for the Pleistocene to recent sediments of the Nile delta.
  - The Quaternary sediments consist of a complex series of fluvial formations along the floodplain of the Nile (including the wadis) down to the delta. Mainly clays, silts and sands are deposited during this period.

Soils in the Nile delta are largely of silt-type. Along the river, sediments are often more sandy while further away they can have a more clayish character. Typical for river sediments, they show a positive (fine) skewness in their grain size distribution (TUCKER, 1985).

The clay minerals that are predominant in the north-eastern Nile delta are smectite- and kaolinite-group minerals. Illites and chlorites are of lesser importance and appear usually in very small proportions. In the sedimentary assemblages of the delta, kaolinites are more common than in the Nile river sediments (STANLEY AND LIYANAGE, 1986). Minerals belonging to the smectite group formed due to weathering and alteration of volcanic glasses with high silica content (MOORE AND REYNOLDS, 1997). As the smectite fraction in Nile delta sediments contain both beidellite and montmorillonite minerals, a

multiple provenance of smectite can be assumed (STANLEY ET AL., 1986). The local appearance of lower clay mineral contents (esp. smectites) is connected with physical changes of the fluvial system (e.g. transportation velocity) of the Nile. The very fine-grained clays are frequently recognized as mobile constituents in soils what leads to their depletion in surface layers and their accumulation below (PARKER AND RAE, 1998). The considerable amount of quartz and feldspars in the delta reflects their derivation from igneous or pre-existing immature sedimentary rock formations. In river sands like these, quartz is strongly enriched due to its high weathering resistance and can reach 95 % of the modal sediment proportions. Preserved plagioclases and potassium feldspars in the Nile delta sediments indicate limited chemical weathering conditions during the fluvial transportation and deposition. Iron- (hydro-) oxides appear controlled by the pH as hematites (arid conditions, neutral-high pH) as well as goethites (oxidizing conditions, low pH).

#### **NILE DELTA SEDIMENTS AS RAW MATERIALS FOR POTTERY PRODUCTION**

The sediments in the Nile delta region as well as along the Nile river valley are fluvially deposited material from a very spacious catchment area and therefore they mirror a broad variety of rocks. Because this high variability of raw material is also reflected in the ceramics that were produced in the area, several attempts were carried out, trying to categorize these fabrics. Most of the authors (for references see INTRODUCTION) tried to find distinctive petrographical features, whereas the more recent works also include chemical investigations on Egyptian pottery and its source material (BELLIDO, 1998, HAMROUSH, 1992, REDMOUNT AND MORGENSTERN, 1996, BOURRIAU ET AL., 2006, TSCHEGG ET AL., 2008). After REDMOUNT AND MORGENSTERN (1996) Nile silts and marl clays are the two main types of

A geoscientific methodologically integrated realisation to reconsider Egyptian pottery of the 18<sup>th</sup> Dynasty

sediments that were the most commonly used raw materials for pottery production in ancient Egypt:

- The Nile silts were deposited in the Quaternary and dominate the whole Nile delta area, have usually quite high contents of silicates (mainly quartz and feldspar) and finely disseminated hydroxides of iron. Grain-size distributions of these alluvial sediments vary from silt to silty clay, including micas and organic matter as significant constituents (NORDSTRÖM AND BOURRIAU, 1993).
- The Egyptian marls, marl clays or so called desert marls originate from late Cretaceous to Miocene silica-carbonatic sediments and can be found further upwards the Nile in Upper Egypt. Organic material is generally absent in marl-based material, the silica content of these sediments is throughout lower than in the Nile silts and high amounts of carbonates are obvious (NORDSTRÖM AND BOURRIAU, 1993).
- Due to depositional interferences, secondary accumulations of naturally mixed sediments exist in the Nile delta area as well as on the floodplains of the Nile river. These sediments are often termed mixed Nile silts. Also artificial mixtures of Nile silts together with marl clays, other local clays or carbonate materials are called mixed Nile silts.

That this simple distinction can not describe the whole variety of available raw materials is clear, nevertheless reasonable affiliations to distinct provenance areas via chemical analyses are possible. Discriminations taking the Vienna System into account are also possible but seem to be more problematic, as it was based only on macroscopical investigations and divided into a much bigger number of different groups and subgroups (Nile silt A-F, mixed Nile silts, marl clays A-G). For the marl group, BOURRIAU ET AL., 2006 showed the attempt of combining Vienna System discriminations with currently gathered petrographical and chemical data.

In the following text, a continuative and integrated approach for the differentiation of ancient Egyptian Nile delta pottery is presented.

## RESULTS

### Petrography

In general, the six investigated samples represent fine-sandy silts with smaller variations of their grain size distribution. The samples K5639 and 8106A represent typical Nile silt, they are moderately sorted and composed of well rounded, up to 500 µm large grog-inclusions that are the major visible elements. In the very-fine to fine sand fraction mainly subrounded to rounded quartz-, feldspar- and ironoxide-grains as well as rock fragments are present. The silt fraction consists of mainly subangular quartz- and feldspar minerals. A micaceous paste matrix with organic inclusions is observable.

6472z is fabricated out of a finer grained variation of Nile silt. Besides some single fine-sand sized subrounded quartz minerals, all inclusions are very fine-sand to silt sized and represent the same mineralogical assemblage as the other Nile silts.

The samples 6486H and 8106GK contain the same mineralogical assemblage as the other Nile silt samples, but with a different sorting and grain-size distribution. The major grain fraction predominantly contains subrounded fine-sand sized quartz minerals, mixed with slightly smaller feldspars. The absence of grog and organic inclusions together with less iron oxide amounts are characteristic for these samples.

KN5 represents a sherd, for that referring to the Vienna System, so called marl clay was used as raw material. Beside a high calcareous clayish paste matrix and some limestone fragments, the same mineralogical assemblage, grain-size distribution and sorting is present as in the Nile silt samples.



Cornelius Tschegg

Accessory minerals that can be found in all Egyptian ceramics are pyroxenes (augites), titanites, Ti-magnetites, ilmenites, monazites, zircons and apatite as well as micas. Chemical compositions of K-feldspars, plagioclases, Ti-magnetites and ilmenites were already presented in TSCHEGG ET AL. (2008). As the mentioned heavy minerals are detectable in all investigated sherds from Lower Egypt, they seem to be an indicative assemblage for the Nile delta and Nile river region. The processed BSE images (Fig. 2)

visually clearly separate Nile derived sediments (Nile silts and mixed Nile silts) from the calcareous marl clay sample. Most indicative for this separation, beside textural features, is the high Ca-content in the paste matrix and the therefore brighter appearance of the matrix. Furthermore the optical distinction between Nile silts, fine-grained Nile silts and mixed Nile silts is possible due to their different textures.

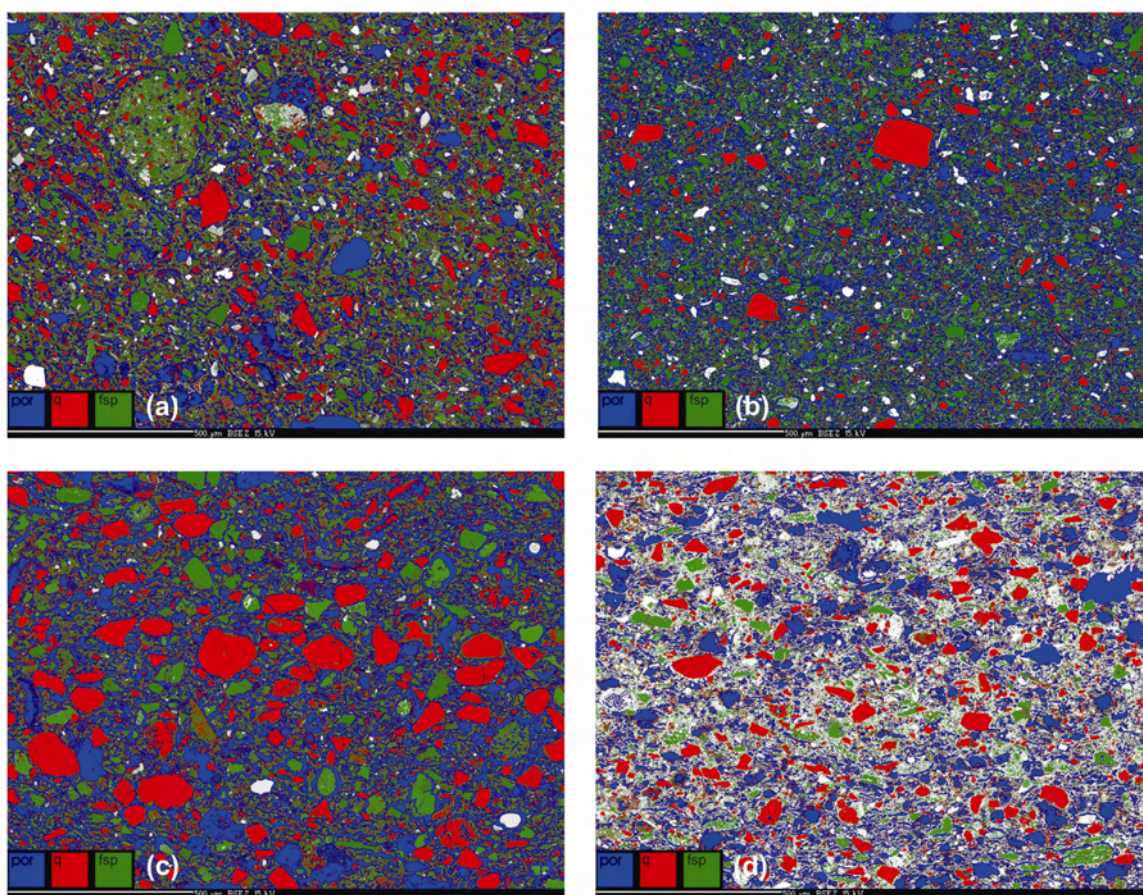


Fig.2: Processed BSE images of representative Bichrome Ware samples from <sup>6</sup>Ezbet Helmi/Tell el-Dab<sup>a</sup>. (a) Nile silt (K5639), (b) fine-grained Nile silt (6472z), (c) mixed Nile silt (8106GK) and (d) calcareous Nile silt (KN5). Colours indicate porosity (por), quartz (q) and feldspar (fsp).

### Bulk Chemistry

Bulk chemical compositions of major- and trace element abundances are presented in Table 1. General bulk chemical observations concerning major- and trace element compositions were already discussed in TSCHEGG ET AL. (2008). The

triangle in Fig. 3a gives a compositional overview of the analysed Bichrome Ware samples compared to reference material from Lower Egypt. The scattering of the samples is mainly due to strong variation of CaO (3.5-19.5 wt. %) and SiO<sub>2</sub> (50.9-62.0 wt. %).

A geoscientific methodologically integrated realisation to reconsider Egyptian pottery of the 18<sup>th</sup> DynastyTable1: Bulk major- and trace element compositions as well as paste-matrix chemistries of investigated Bichrome Ware samples from <sup>c</sup>Ezbet Helmi/Tell el-Dab<sup>a</sup>.

|                                | bulk chemistry |       |       |        |       |      | matrix chemistry       |       |       |        |       |       |
|--------------------------------|----------------|-------|-------|--------|-------|------|------------------------|-------|-------|--------|-------|-------|
|                                | 6472z          | 6486H | 8106A | 8106GK | K5639 | KN5  | 6472z                  | 6486H | 8106A | 8106GK | K5639 | KN5   |
| <i>XRF [in wt. %]</i>          |                |       |       |        |       |      | <i>EPMA [in wt. %]</i> |       |       |        |       |       |
| SiO <sub>2</sub>               | 55.9           | 55.0  | 59.1  | 50.9   | 62.0  | 52.9 | 53.9                   | 57.9  | 55.2  | 54.1   | 57.9  | 51.0  |
| TiO <sub>2</sub>               | 1.77           | 1.41  | 1.66  | 1.99   | 1.82  | 0.83 | 0.70                   | 0.57  | 0.78  | 0.67   | 1.42  | 1.06  |
| Al <sub>2</sub> O <sub>3</sub> | 17.7           | 14.8  | 15.6  | 15.5   | 15.8  | 15.4 | 23.3                   | 21.7  | 20.4  | 22.8   | 21.9  | 23.4  |
| FeO*                           | 8.57           | 7.80  | 8.49  | 8.36   | 9.24  | 4.08 | 4.66                   | 3.27  | 6.14  | 3.13   | 5.27  | 4.96  |
| MnO                            | 0.64           | 0.21  | 0.15  | 0.20   | 0.15  | 0.04 |                        |       |       |        |       |       |
| MgO                            | 3.00           | 2.90  | 2.74  | 3.77   | 2.88  | 2.68 | 3.25                   | 2.58  | 3.97  | 3.69   | 2.72  | 3.90  |
| CaO                            | 6.42           | 12.7  | 8.13  | 13.9   | 3.50  | 19.5 | 6.85                   | 10.92 | 7.59  | 11.3   | 4.53  | 13.6  |
| Na <sub>2</sub> O              | 1.70           | 1.70  | 1.91  | 1.78   | 2.34  | 1.20 | 2.74                   | 0.36  | 2.41  | 1.10   | 2.36  | 1.53  |
| K <sub>2</sub> O               | 2.86           | 2.60  | 1.84  | 1.83   | 2.55  | 2.08 | 4.54                   | 2.73  | 3.44  | 3.28   | 3.83  | 0.54  |
| P <sub>2</sub> O <sub>5</sub>  | 0.62           | 0.69  | 0.51  | 0.82   | 0.59  | 0.88 |                        |       |       |        |       |       |
| Total                          | 99.2           | 99.8  | 100.1 | 99.1   | 100.9 | 99.5 | 100.0                  | 100.0 | 100.0 | 100.0  | 100.0 | 100.0 |
| LOI                            | 1.93           | 1.82  | 1.40  | 1.20   | 1.65  | 9.37 |                        |       |       |        |       |       |
| <i>[ICP-MS [in ppm]</i>        |                |       |       |        |       |      |                        |       |       |        |       |       |
| Li                             | 20.5           | 23.9  | 19.1  | 15.4   | 14.8  | 26.7 |                        |       |       |        |       |       |
| Be                             | 1.91           | 1.88  | 1.68  | 1.38   | 1.67  | 2.3  |                        |       |       |        |       |       |
| Sc                             | 14.8           | 17.1  | 18.0  | 12.6   | 17.6  | 12.9 |                        |       |       |        |       |       |
| V                              | 179            | 141   | 196   | 142    | 200   | 142  |                        |       |       |        |       |       |
| Cr                             | 149            | 151   | 176   | 144    | 176   | 125  |                        |       |       |        |       |       |
| Co                             | 37.8           | 27.1  | 31.9  | 26.5   | 36.5  | 11   |                        |       |       |        |       |       |
| Cu                             | 53.1           | 50.2  | 65.2  | 52.0   | 77.0  | 64.3 |                        |       |       |        |       |       |
| Zn                             | 117            | 100   | 111   | 89.7   | 117   | 77.0 |                        |       |       |        |       |       |
| As                             | 3.61           | 3.48  | 3.22  | 3.34   | 2.37  | 10.8 |                        |       |       |        |       |       |
| Rb                             | 46.1           | 48.1  | 52.0  | 42.7   | 59.7  | 62.4 |                        |       |       |        |       |       |
| Sr                             | 281            | 366   | 300   | 349    | 292   | 734  |                        |       |       |        |       |       |
| Y                              | 33.2           | 31.4  | 33.4  | 28.5   | 34.1  | 32.5 |                        |       |       |        |       |       |
| Zr                             | 250            | 199   | 214   | 184    | 226   | 133  |                        |       |       |        |       |       |
| Nb                             | 21.5           | 22.9  | 23.5  | 18.5   | 22.6  | 14.7 |                        |       |       |        |       |       |
| Ag                             | 0.06           | 0.03  | 0.04  | 0.03   | 0.04  | 0.08 |                        |       |       |        |       |       |
| Cd                             | 0.26           | 0.20  | 0.18  | 0.18   | 0.14  | 0.11 |                        |       |       |        |       |       |
| Cs                             | 1.49           | 1.56  | 1.54  | 1.27   | 1.27  | 3.56 |                        |       |       |        |       |       |
| Ba                             | 569            | 497   | 470   | 478    | 456   | 433  |                        |       |       |        |       |       |
| La                             | 31.9           | 31.0  | 30.1  | 25.9   | 28.7  | 35.3 |                        |       |       |        |       |       |
| Ce                             | 62.6           | 64.1  | 60.2  | 54.1   | 60.6  | 64.0 |                        |       |       |        |       |       |
| Pr                             | 8.68           | 8.37  | 8.16  | 7.09   | 8.06  | 8.64 |                        |       |       |        |       |       |
| Nd                             | 34.8           | 33.9  | 33.3  | 29.1   | 33.5  | 33.4 |                        |       |       |        |       |       |
| Sm                             | 7.16           | 6.87  | 6.98  | 6.01   | 7.05  | 6.45 |                        |       |       |        |       |       |
| Eu                             | 1.76           | 1.70  | 1.82  | 1.58   | 1.89  | 1.42 |                        |       |       |        |       |       |
| Gd                             | 6.01           | 5.87  | 6.03  | 5.13   | 6.08  | 5.50 |                        |       |       |        |       |       |
| Tb                             | 0.96           | 0.94  | 0.98  | 0.82   | 1.00  | 0.85 |                        |       |       |        |       |       |
| Dy                             | 5.68           | 5.47  | 5.85  | 4.85   | 5.89  | 4.89 |                        |       |       |        |       |       |
| Ho                             | 1.13           | 1.10  | 1.18  | 0.97   | 1.19  | 0.99 |                        |       |       |        |       |       |
| Er                             | 2.86           | 2.74  | 2.98  | 2.40   | 3.00  | 2.56 |                        |       |       |        |       |       |
| Tm                             | 0.47           | 0.44  | 0.48  | 0.40   | 0.48  | 0.41 |                        |       |       |        |       |       |
| Yb                             | 2.74           | 2.59  | 2.81  | 2.27   | 2.82  | 2.34 |                        |       |       |        |       |       |
| Lu                             | 0.39           | 0.36  | 0.40  | 0.31   | 0.40  | 0.33 |                        |       |       |        |       |       |
| Hf                             | 5.08           | 3.67  | 4.40  | 3.72   | 4.53  | 2.58 |                        |       |       |        |       |       |
| Ta                             | 1.58           | 1.10  | 1.42  | 1.40   | 1.29  | 0.96 |                        |       |       |        |       |       |
| Pb                             | 17.3           | 12.5  | 15.6  | 10.9   | 10.6  | 7.68 |                        |       |       |        |       |       |
| Th                             | 8.66           | 7.96  | 7.67  | 6.14   | 6.37  | 9.28 |                        |       |       |        |       |       |
| U                              | 2.08           | 1.77  | 2.14  | 2.12   | 1.82  | 3.69 |                        |       |       |        |       |       |

\* Total iron is shown as FeO.

Cornelius Tschegg

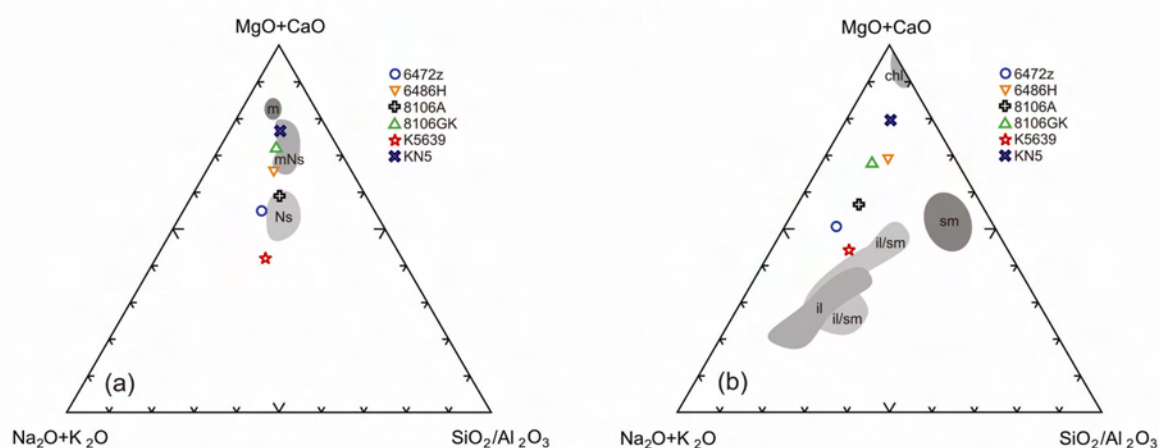


Fig. 3: Major element compositional triangles of investigated Bichrome Ware samples from <sup>6</sup>Ezbet Helmi/Tell el-Dab<sup>a</sup>. (a) Bulk chemistries; grey fields combine Nile delta and Nile river reference data from REDMOUNT AND MORGENSTERN (1996), Ns – Nile silts, mNs – mixed Nile silts, m – marls. (b) Paste-matrix chemistries; grey fields combine compositions of clay mineral groups from NEWMAN (1987), il – illite, il/sm – mixed layer illite/smectite, sm – smectite, chl – chlorite.

The rest of major- and trace elements show a quite similar composition, beside KN5 which can with aplenty of elements be separated from the other samples. 8106A and 6472z indicate a chemical correlation to Nile silts, K5639 plots close to them. 6486H, 8106GK correlate to the mixed Nile silt field, so does KN5, just because its low silica content though.

The principal component analysis (Fig. 4) is based on the abundance of 27 elements and illustrates the statistical comparison of the investigated sherds to local reference material from Lower Egypt. The score plot (Fig. 4a) explains 73.4 % of the total variance and clearly indicates the affiliation of K5639, 6472z and 8106A to Nile silt reference samples, whereas 6486H and 8106GK correlate with mixed Nile silt material. The loading plot (Fig. 4b) shows that mainly CaO with its associated Sr abundances are responsible for the clustering of Nile silts and mixed Nile silts. The isolated position of the marls is based on even higher amounts of Ca and Sr, but moreover on enriched Al<sub>2</sub>O<sub>3</sub>, La, Cs and Th abundances. The hierarchical cluster analysis (Fig. 5) was calculated with the same elements as the PCA, neglecting the outstanding marl clay reference samples and KN5. It combines all investigated samples together with Nile delta sediments at a

relatively high degree of similarity and separates them from samples that represent Nile river sediments from further south. A combination of the two statistical applications is worth in this case, as it clearly turns out that the PCA groups the analysed samples by their chemical variability and allows a distinct correlation and affiliation to local reference materials, whereas the HCA groups the samples geographically.

### Paste matrix chemistry

As via X-ray diffraction no clay mineral peaks were detectable (due to sufficient firing temperatures and the thermally triggered breakdown of phyllosilicates), an approach to investigate clay minerals by means of chemical analysis was undertaken on the paste matrix. Clay compositions are presented in Table 1. The determination of distinct clay minerals via chemical analysis is difficult due to the high chemical variability of these minerals in nature. As natural clay deposits, in particular alluvial ones, in general contain clay mineral mixtures, it's even worse. All measurements on the clayish matrix were carried out on selected points in order to avoid problems with inclusions or porosity.

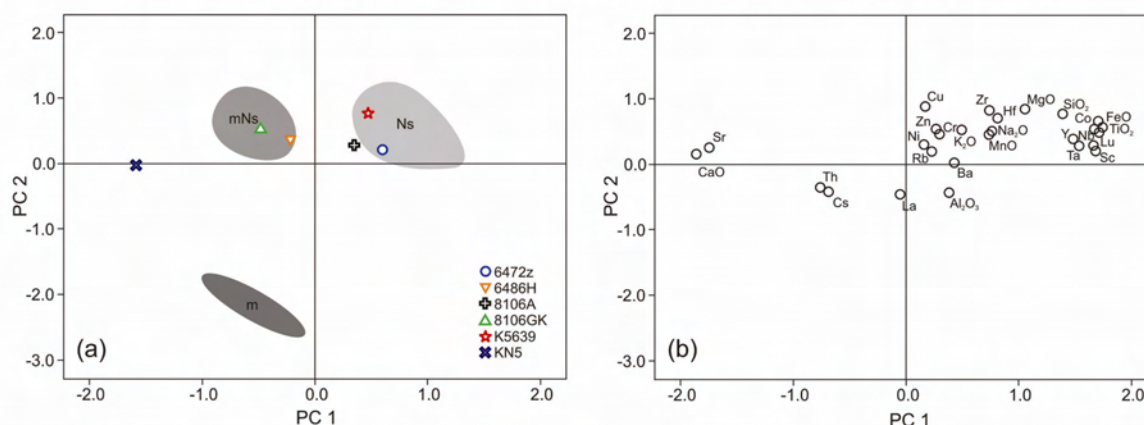
A geoscientific methodologically integrated realisation to reconsider Egyptian pottery of the 18<sup>th</sup> Dynasty

Fig. 4: Principal component analysis of investigated Bichrome Ware samples from <sup>o</sup>Ezbet Helmi/Tell el-Dab<sup>a</sup> with combined Lower Egypt reference data from REDMOUNT AND MORGENSTERN (1996). Ns – Nile silts, mNs – mixed Nile silts, m – marls. (a) Score plot, (b) loading plot. For conducting the PCA, 9 major element and 18 trace element abundances, restricted by the availability of elements in the cited publication, were used. Principal component 1 subsume 45.81 % and principal component 2 24.57 % of the total variance.

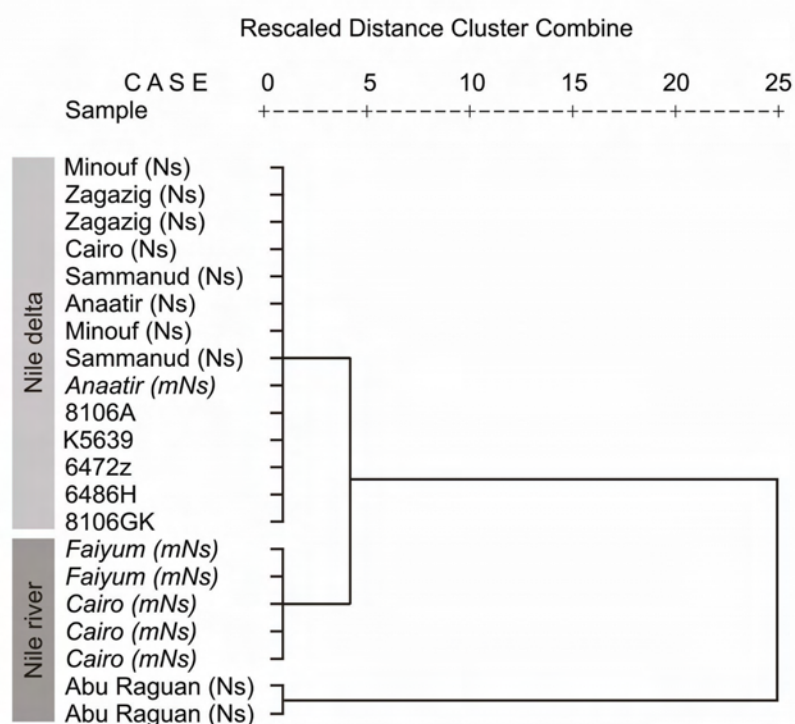


Fig. 5: Hierarchical cluster analysis of investigated Bichrome Ware samples from <sup>o</sup>Ezbet Helmi/Tell el-Dab<sup>a</sup>. Ns – Nile silts, mNs – mixed Nile silts. Calculation was conducted using the Ward method.

It turned out that again K5639, 6472z and 8106A that are assumed to be made out of Nile silt as well as 6486H and 8106GK – assumed mixed Nile silts - match together, indicating a common fine-material source. Due to natural mixing processes of such fine-grained sediments, no direct association with distinct clay minerals can

be made. It's obvious and important though that the bulk chemistry strongly correlates to the chemistry of the clay fraction, as bulk chemistry and clay chemistry follow the same trend (compare Fig. 3a and 3b).

Cornelius Tschegg

**DISCUSSION**

Taking the large variety of raw materials along the river Nile and its delta into account and thinking also on the human factor (potters choice) which controls the composition and fabric of the manufactured pottery, it seems to be obvious that a strict classification and affiliation of pottery produced in such a huge area from ancient times till now can hardly be done. Concerning the Vienna System, the determination of Nile silts and the distinction between Nile silt and marl fabrics appear to be comprehensible, whereas the further classification into subgroups can be precarious (also stated by BOURRIAU ET AL., 2000). Five types of Nile fabrics are distinguished in the Vienna System. The first three groups (Nile A, Nile B and Nile C) are differentiated by the size and amount of sand and straw inclusions, Nile D contains limestone inclusions and Nile E, which should be typical for the delta, is characterized by rounded grains of sand (NORDSTRÖM AND BOURRIAU, 1993).

The marls, included in the Vienna System have beside raw material characteristics, also a specific chronological range. Therefore also the production technology has influence on the differentiation, making affiliations to distinct raw material sources even more complex. After BOURRIAU ET AL. (2006), mixed fabrics (intentional/anthropogenic mixtures of Nile silt and marl) are chemically not reliably distinguishable from marl clays, so only the two major groupings of the Vienna System (marl and Nile clays) with several subgroups were differentiated in her studies.

Via petrological, geochemical and statistical observations we were able in this study to discriminate non-calcareous Nile and mixed-Nile silts from the calcareous sample KN5. The high calcareous paste matrix, the bulk chemistry and the petrographical features make it easy distinguishable from the samples made out of typical Nile silt. From archaeological

consideration KN5 has a typical marl fabric and taking the Vienna System and the description of Egyptian marl fabrics after NORDSTRÖM AND BOURRIAU (1993) into account, it fits to marls of group A (with the difference that the clay matrix is more calcareous, inclusions are mainly silt-very fine-sized quartz and less feldspar is observable). Looking at it more detailed, it becomes evident that KN5 would also match to the group of Nile D fabrics. Limestone fragments are scarce and completely unreacted, what indicates a low firing temperature. To avoid arguable assignments, it would be worth and less confusing to call samples, made out of such raw material, calcareous Nile sediment/silt instead of marl clay, as beside paste matrix and some included limestone fragments, the mineralogical assemblage is the same as in all other sherds made out of Nile alluvial sediments. All other investigated samples can with smaller variations be assigned to typical Nile sediments.

After the Vienna System (NORDSTRÖM AND BOURRIAU, 1993) K5639 and 8106A could be identified closest as a Nile C. 6472z is indeed finer grained but petrographically and mineralogically very similar and would correlate closest to Nile A fabrics, without temper. Chemically it resembles with 8106A. The rather thin red border zones in the fractures of all three samples show that they are fired quite short under oxidizing conditions at temperatures about 600 – 800 °C (temperature estimates after TSCHEGG ET AL., 2008). 8106GK and 6486H have a much higher amount of coarser inclusions (fine-medium sand size) and can be closest compared to Nile E fabrics. The black/dark-brown colour of the fracture and the greenish surface colour of 8106GK is in all probability associated to a second firing process or a deliberate smoking of the sherd in a kiln after the firing. Comparing the investigated Nile silts of this study to petrographical investigations on Egyptian ceramics of the 18<sup>th</sup> dynasty from HOPE ET AL. (1981), a very good correlation concerning fabric

A geoscientific methodologically integrated realisation to reconsider Egyptian pottery of the 18<sup>th</sup> Dynasty

and mineralogical assemblage turns out. The most obvious and common characteristics are the lack of calcareous inclusions (limestone fragments, calcite crystals or shells), the majority of silicate mineral phases (also pyroxenes) and plant remnants.

Comparing the gathered chemical data to neutron activation analyses from BOURRIAU ET AL. (2006), a compositional consistence of Nile delta pottery is comprehensible. More than this, a site-specific chemical fingerprint of Tell el-Dab<sup>a</sup> can be confirmed, as the investigated Bichrome Ware samples correlate well with the chemical group N35C and N41D, which by BOURRIAU ET AL. (2006) were also accounted as typical for Tell el-Dab<sup>a</sup>.

Concerning their mineralogical assemblage, the investigated Bichrome samples that are associated to Nile river and delta sediment show marginal differences. As the mineralogy strongly affects the bulk chemistry, it's unsurprising that deviations of the latter are also little. Comparing compositional variations of bulk major chemistries to paste matrix chemistries, it becomes evident that the bulk composition of ceramics is most intensively controlled by its clayish paste matrix chemistry. As none of the sherds beside KN5 contain limestone or other Ca-bearing fragments, the amount of CaO is almost exclusively dependent on the matrix (clay) chemistry. Minor differences concerning CaO contents can be explained by varying modal compositions of mainly anorthite and clinopyroxene.

## CONCLUSIONS

“Nile silt” with all its characterizing petrographical and mineralogical features is an adequate term to describe Nile alluvial sediments in the delta which were used for pottery production since antiquity. Taking also bulk chemical compositions into account, this group of

raw material can be stated and discriminated even more precisely. Thinking of the variability of sediments in the area, some irrelevant textural variations and chemical deviations have to be disregarded. Variations of Nile silt, which have a similar fabric but are slightly different in terms of petrographical characteristics (mainly a more sandy grain size distribution) and chemistry, can be called “mixed Nile silts”. This mixed Nile silts are naturally compounded river sediments and should not be confused with intentionally blended pottery fabrics. Their source and affiliation to Nile river sediments deduce from geological considerations and geographical accordance to reference material from Lower Egypt. Material with a small number of included limestone fragments or a higher calcareous paste matrix (like sample KN5) may for more clearness and consistence be called “calcareous Nile silt” instead of marl.

This way of classification goes together very well with the geographical appearance of ceramic fabrics but also with the availability of raw materials in the Nile valley (Lower Egypt). Assuming insignificant preconditioning of sediments that was applied for pottery production in the area at that time, the Nile silt fabrics are related to typical Nile delta sediments whereas the mixed Nile silts are related more to Nile river sediments respectively. The general appearance of material that is available along the river and its floodplains is reflected by the mixed Nile silt fabrics. Chemical investigations and their affiliation to reference data support the consistency.

The classification into “Nile delta sediments” or “Nile silts” that represent raw material from the delta and “mixed Nile sediments/silts” that represent material available along the river and its floodplains is precise, less confusing and geographically comprehensible. Detailed analyses, including petrography, mineralogy, mineral chemistry and bulk chemistry of excavated pottery together with in-depth

Cornelius Tschegg

information about the regional geology help to avoid puzzled affiliations to established classification schemes and beware of premature conclusions. Moreover it allows the determination of well characterized and well defined fabrics that consequently can function as “key samples” to which other specimens can be compared chemically and for field observations also visually. How effective chemical fingerprinting can be, shows the accordance of Bichrome Ware bulk compositions to Nile delta reference data from REDMOUNT AND MORGENSTERN (1996) and Tell el-Dab<sup>a</sup> site-specific data of BOURRIAU ET AL. (2006).

With an integrated approach, we were able in this study to assign the Egyptian Bichrome Wheelmade Ware samples 6472z, 8106A and K5639 to non-calcareous Nile silt that is and was the most common raw-material for pottery production in the Nile delta region. Samples

6486H and 8106GK reflect Bichrome pottery produced out of mixed Nile silt, a raw material that reflects alluviums available along the river Nile. KN5 is made of a calcareous variation of Nile silt, a raw material that obviously gets more abundant along the Nile valley towards Upper Egypt.

#### ACKNOWLEDGEMENTS

We are grateful to Manfred Bietak (Institute of Egyptology, Interdisciplinary Platform for Archaeological Studies, University of Vienna) for providing this study with pottery samples. Reviews of Irmgard Hein (Institute of Egyptology, University of Vienna) and Theodoros Ntaflou (Department of Lithospheric Sciences, University of Vienna) helped to improve the paper.

#### REFERENCES

- ARNOLD, D.  
1980 Keramik, in HELCK, W. AND WESTENDORF, W. (Eds.): *Lexikon der Ägyptologie*, Band III: 392-409. Wiesbaden.
- 1981 Studien zur altägyptischen Keramik. Deutsches Archäologisches Institut, Abteilung Kairo. Verlag Philipp von Zabern, Mainz.
- BELLIDO, B.A.  
1989 Neutron activation analysis of ancient Egyptian pottery. Ph.D. thesis, University of Manchester.
- BIETAK, M.  
2005 Neue Paläste aus der 18. Dynastie, in: JÁNOSI, P. (Ed.): *Structure and Significance*. Denkschriften der Österreichischen Akademie der Wissenschaften 33. Untersuchungen der Zweigstelle Kairo des Österreichischen Archäologischen Institutes 25, 131 – 168, Wien.
- BOURRIAU, J. D. AND NICHOLSON, P.T.  
1992 Marl Clay Pottery Fabrics of the New Kingdom from Memphis, Saqqara and Amarna. *Journal of Egyptian Archaeology*, No. 78, 29-91, London.
- BOURRIAU, J., SMITH, L. M.V. AND NICHOLSON, P.T.  
2000 New Kingdom pottery fabrics: Nile clay and mixed Nile/marl clay fabrics from Memphis and Amarna. *Occasional Publication 14*, Egypt Exploration Society, London.
- BOURRIAU, J., BELLIDO, A., BRYAN, N AND ROBINSON, V.  
2006 Egyptian pottery fabrics: a comparison between NAA groupings and the “Vienna System”, in: CZERNY, E. AND HEIN, I., HUNGER, H., MELMAN, D. AND SCHWAB, A. (Eds.): *Timelines: Studies in honour of Manfred Bietak*. Volume III. Peeters/Departement Oosterse Studies, Leuven.
- FITTON, L, HUGHES, M. AND QUIRKE, S.  
1998 Northerners at Lahun: Neutron Activation Analysis of the Minoan and related pottery in the British Museum, in QUIRKE, S. (Ed.): *Lahun Studies*. Reigate.

A geoscientific methodologically integrated realisation to reconsider Egyptian pottery of the 18<sup>th</sup> Dynasty

- HAMROUSH, H.A.  
1992 Pottery analysis and problems in the identification of the geological origins of ancient ceramics. *Cahiers de la céramique égyptienne*. 3, Cairo, IFAO, 39-54.
- HEIN, I. AND JÁNOSI, P.  
2004 Tell el-Dab<sup>a</sup> XI. Areal A/V, Siedlungsrelikte der Späten Hyksoszeit. Verlag der Österreichischen Akademie der Wissenschaften, UZK XXI, Wien 2004.
- HOPE, C.A., BLAUER, H.M. AND RIEDERER, J.  
1981 Recent Analyses of 18th Dynasty pottery, in ARNOLD, D. (Ed.): *Studien zur altägyptischen Keramik*, 139-166, Mainz.
- MOORE, D. AND REYNOLDS, R.C.  
1997 X-Ray Diffraction and the Identification and Analysis of Clay Minerals. Oxford Univ. Press.
- NEWMAN, A.C.D.  
1987 Chemistry of clays and clay minerals. Mineralogical Society Monograph No. 6, Longman, London.
- NOLL, W.  
1981 Bemalte Keramiken Altägyptens: Material, Rohstoffe und Herstellungstechnik, in ARNOLD, D. (Ed.): *Studien zur altägyptischen Keramik*, 103-138, Mainz.
- NORDSTRÖM, H.A.  
1986 Ton, in HELCK, W. AND WESTENDORF, W. (Eds.): *Lexikon der Ägyptologie*, Band VI: 629-634, Wiesbaden.
- NORDSTRÖM, H.A. AND BOURRIAU, J.  
1993 Ceramic Technology: Clays and Fabrics, in ARNOLD, D. AND BOURRIAU, J. (Eds.): *An Introduction to Ancient Egyptian Pottery*. Verlag Philipp von Zabern, 148-190, Mainz.
- PARKER, A. AND RAE, J. E.  
1998 Environmental Interaction of Clays, Clays and Environment. Springer.
- REDMOUNT, C.A. AND MORGENSTEIN, M.E.  
1996 Major and Trace Element Analysis of modern Egyptian Pottery. *Journal of Archaeological Science*, 23, 741-762.
- SAID, R.  
1990 The Geology of Egypt. Balkema, Rotterdam.
- SCHLÜTER, TH.  
2006 Geological Atlas of Africa. Springer, Berlin Heidelberg.
- STANLEY, D.J. AND LIYANAGE, A.N.  
1986 Clay-mineral variations in the northeastern Nile delta, as influenced by depositional processes. *Marine Geology* 73, 263-283.
- TSCHEGG, C., HEIN, I. AND NTAFLAS, TH.  
2008 State of the art multi-analytical geoscientific approach to identify Cypriot Bichrome Wheelmade Ware reproduction in the Eastern Nile delta (Egypt). *Journal of Archaeological Science* 35, 5, 1134-1147.
- TUCKER, M.  
1985 Einführung in die Sedimentpetrologie. Enke, Stuttgart.



## Appendix (C)

---

Tschegg, C., Ntaflos, Th., Hein, I., 2008c. Thermally triggered two-stage reaction of carbonates and clay during ceramic firing - a case study on Bronze Age Cypriot ceramics. Applied Clay Science (in press).



## Thermally triggered two-stage reaction of carbonates and clay during ceramic firing – A case study on Bronze Age Cypriot ceramics

Cornelius Tschegg<sup>a,\*</sup>, Theodoros Ntaflos<sup>a</sup>, Irmgard Hein<sup>b</sup>

<sup>a</sup> Department of Lithospheric Research, University of Vienna, Althanstr. 14, 1090 Vienna, Austria

<sup>b</sup> Institute of Egyptology, University of Vienna, Frankgasse 1, 1090 Vienna, Austria

### ARTICLE INFO

#### Article history:

Received 18 February 2008

Received in revised form 22 July 2008

Accepted 25 July 2008

Available online xxx

#### Keywords:

Ceramics

Firing temperature

Mineral reactions

Carbonates

Clay

Microtextures

### ABSTRACT

Cypriot Bronze-age Plain White Wheelmade ware samples were investigated in order to examine their chemical and mineralogical features, their manufacturing procedures and associated firing temperature controlled mineral reactions. Beside the geochemical characterisation of the ware group, the main focus of the study was to determine phase transformations (especially the reaction of calcareous inclusions in phyllosilicatic matrices) via petrographical, mineralogical, microtextural and phase-geochemical methods. Three groups of pottery, fired at increasing temperatures (group I: <600 °C, group II: 650–800 °C and group III: 850–1000 °C), could be distinguished taking their individual states of carbonate decomposition together with accompanying mineral reactions into account. In group I, no mineral transformations occur, whereas in group II and III, two conspicuous and temperature-indicative stages of carbonate reactions are observable. The first reaction stage takes place in group II samples and is characterized by the development of spherical reaction domains around paste matrix included calcareous grains by means of Ca-dispersion from the grains into the surrounding clayish matrix. This process provides the initial position for partial melting and blastesis of new mineral phases that follow. In the second-stage reaction, designative for group III, advanced carbonate decomposition takes place. Temperature triggered melts evolve from breakdown products of sufficiently heated clay minerals and build up glassy Al–Si rims at the interface of carbonates and the surrounding clay paste. At the same time, Ca-silicates grow in the domain of the Ca-affected matrix that indeed already evolved at lower temperatures (first-stage reaction) but only now reaches the sufficient heat for mineral blastesis. We assume that the carbonate-tempered ceramics were deliberately fired up to temperatures that are represented by group II but due to heterogeneous firing conditions parts of the vessels were unintentionally under- and overfired respectively.

© 2008 Elsevier B.V. All rights reserved.

### 1. Introduction

Firing is the most essential step in the pottery creating procedure. The modelled raw material hardens, strengthens, stabilizes and thus gets all necessary features for further treatment and use. This process is ascribed to the nature of the chosen raw material blend and mineral reactions/transformations therein, when heated to certain temperatures. As gradually firing temperatures increase, the microtextural relationships between paste matrix and their included minerals start to change. Endothermic followed by exothermic phase transformations (segregation, decomposition, replacement and blastesis) take place at the interface of included minerals and the clay matrix as well as in single mineral phases and the matrix itself (Riccardi et al., 1999). The high-T low-P transformations occur depending on the granulometry, mineralogy and chemistry of the clayish raw material, the chemical and mineralogical features of the optionally included temper

materials, the firing temperature and duration as well as the kiln atmosphere (Maggetti, 1982; Cultrone et al., 2001).

Dehydroxylation of clay minerals in general is reported to take place at temperatures between 450 and 900 °C causing collapse and transformation of crystal structures. This frequently leads to resemblance of an illite-like structure (Cultrone et al., 2001 and ref. therein). Depending on the clay mineral group though, the remaining structures of dehydroxylated smectite-, chlorite-, etc. group minerals can be detectable up to higher firing temperatures. Kaolinites break down between 500 and 600 °C (Shoval, 1988; Cultrone et al., 2001; Traoré et al., 2000), smectites between 600 and 800 °C (Shoval, 2003), chlorites around 850 °C (Rathossi et al., 2004) and illites up to 900 °C (Jordán et al., 1999). Drits et al. (1995) stated that dehydroxylation temperatures for dioctahedral 2:1 layer phyllosilicates (especially smectites and illites) can differ between 150 and 200 °C depending on whether they predominantly consist of *trans*- or *cis*-vacant 2:1 layers. At temperatures above 700 °C, the release of (OH)<sup>-</sup> not only causes significant modifications and structural changes of the clay minerals but also strongly affects their potential of being detected (Cultrone et al., 2001; Moroni and Conti, 2006). Additionally, the modal calcite/

\* Corresponding author. Tel.: +43 1 4277 53318.

E-mail addresses: [cornelius.tschegg@univie.ac.at](mailto:cornelius.tschegg@univie.ac.at) (C. Tschegg), [theodoros.ntaflos@univie.ac.at](mailto:theodoros.ntaflos@univie.ac.at) (T. Ntaflos), [irmgard.hein@univie.ac.at](mailto:irmgard.hein@univie.ac.at) (I. Hein).

clay ratio and the heating rate during the ceramic firing influence the thermally induced reactions of the minerals (Moroni and Conti, 2006). In carbonate rich samples like the Plain White ware, we can observe by far the most conspicuous firing-triggered reactions, which comprise the breakdown and dissociation of  $\text{CaCO}_3$  to  $\text{CaO}$ , the reaction of  $\text{CaO}$  with components of the clay matrix and the triggered growth of new mineral phases. The decomposition of calcite in clay matrices that begins at 600 °C and mainly occurs at temperatures around 650–750 °C (Noll, 1991; Shoval et al., 1993), ends up at 800–900 °C with complete transformation of calcite into Ca-bearing silicates due to the reaction with the phyllosilicatic paste matrix (Maggetti et al., 1984; Noll, 1991; Riccardi et al., 1999; Cultrone et al., 2001 and ref. therein, Rathossi et al., 2004). The progression of the decarbonation process is controlled by the grain size (Núñez et al., 1992), the crystallinity (Shoval et al., 1993) and the chemistry (Shoval,

1988; Cultrone et al., 2001) of the included carbonates. Furthermore, earlier carbonate decomposition can be initiated as the result of clay minerals dehydroxylation (Shoval, 2003 and ref. therein). In Ca-rich ceramics, gehlenite ( $\text{Ca}_2\text{Al}(\text{AlSi})\text{O}_7$ ) appears as the first reaction product at the boundary of carbonate inclusions and clayish matrix (Veniale, 1990; Jordán et al., 1999; Hajjaji and Kacim, 2004). Gehlenite can be initially crystallized at temperatures ranging from 800 to 850 °C. However, it is stable mainly at temperatures around 850–950 °C (Noll, 1991; Riccardi et al., 1999; Moroni and Conti, 2006). In the gehlenite forming reaction, calcium is provided by the decomposing carbonates while silica and aluminum are provided by the breakdown products of clay minerals of the surrounding matrix (Maggetti et al., 1984). The stability field of gehlenite depends on the  $\text{SiO}_2$  saturation of the reaction; i.e. the higher the available Si-contents, the lower the equilibrium temperature at which gehlenite is stable. At temperatures

**Table 1**  
Bulk major and trace element abundances of Cypriot PWW ware samples

|                                | Group I |        |        |        | Group II |        |        |        | Group III |         |        |
|--------------------------------|---------|--------|--------|--------|----------|--------|--------|--------|-----------|---------|--------|
|                                | 2191–15 | 2248–4 | 2248–6 | 2248–9 | 2191–2   | 2191–5 | 2248–1 | 2248–5 | 2191–13   | 2191–14 | 2248–8 |
| <i>XRF analyses [wt.%]</i>     |         |        |        |        |          |        |        |        |           |         |        |
| SiO <sub>2</sub>               | 51.4    | 54.8   | 51.5   | 52.0   | 51.4     | 51.2   | 52.2   | 48.5   | 51.3      | 51.0    | 50.7   |
| TiO <sub>2</sub>               | 0.74    | 0.73   | 0.74   | 0.72   | 0.77     | 0.73   | 0.79   | 0.76   | 0.82      | 0.74    | 0.81   |
| Al <sub>2</sub> O <sub>3</sub> | 13.2    | 13.3   | 14.1   | 13.5   | 14.0     | 13.0   | 14.4   | 13.9   | 12.9      | 13.8    | 14.2   |
| FeO*                           | 6.81    | 6.77   | 7.09   | 6.94   | 7.08     | 6.76   | 7.25   | 7.59   | 7.26      | 7.10    | 7.99   |
| MnO                            | 0.16    | 0.15   | 0.17   | 0.16   | 0.16     | 0.15   | 0.18   | 0.15   | 0.15      | 0.17    | 0.15   |
| MgO                            | 7.01    | 5.13   | 6.10   | 6.68   | 6.32     | 7.73   | 6.41   | 5.62   | 4.54      | 6.74    | 5.51   |
| CaO                            | 15.6    | 14.6   | 15.8   | 14.7   | 16.0     | 15.9   | 15.1   | 19.1   | 17.7      | 16.1    | 16.2   |
| Na <sub>2</sub> O              | 1.82    | 1.50   | 1.35   | 1.48   | 1.47     | 1.68   | 1.54   | 1.44   | 2.69      | 1.55    | 1.59   |
| K <sub>2</sub> O               | 2.22    | 2.89   | 2.95   | 2.72   | 2.34     | 2.13   | 2.04   | 2.24   | 1.73      | 2.41    | 2.29   |
| P <sub>2</sub> O <sub>5</sub>  | 0.24    | 0.21   | 0.23   | 0.31   | 0.23     | 0.21   | 0.23   | 0.28   | 0.24      | 0.30    | 0.20   |
| Total                          | 99.2    | 100.1  | 100.1  | 99.2   | 99.8     | 99.6   | 100.1  | 99.6   | 99.3      | 99.9    | 99.7   |
| LOI <sup>b</sup>               | 10.3    | 12.5   | 11.4   | 12.2   | 7.85     | 8.77   | 7.70   | 7.53   | 4.61      | 4.79    | 5.19   |
| <i>ICP-MS analyses [ppm]</i>   |         |        |        |        |          |        |        |        |           |         |        |
| Li                             | 30.3    | 27.7   | 38.0   | 35.9   | 44.0     | 41.0   | 39.6   | 34.7   | 27.3      | 39.9    | 38.7   |
| Be                             | 1.33    | 1.18   | 1.69   | 1.42   | 1.55     | 1.42   | 1.62   | 1.11   | 0.82      | 1.57    | 1.27   |
| Sc                             | 14.0    | 11.4   | 12.8   | 13.4   | 12.6     | 13.4   | 14.9   | 15.5   | 13.4      | 15.5    | 16.4   |
| V                              | 128     | 130    | 150    | 152    | 129      | 128    | 161    | 188    | 167       | 143     | 185    |
| Cr                             | 274     | 325    | 284    | 385    | 259      | 357    | 305    | 358    | 358       | 317     | 415    |
| Co                             | 29.6    | 28.2   | 33.9   | 34.0   | 29.1     | 30.4   | 37.2   | 32.6   | 25.3      | 34.7    | 34.8   |
| Cu                             | 50.2    | 73.4   | 86.3   | 83.3   | 74.4     | 76.7   | 73.9   | 86.8   | 101       | 112     | 83.2   |
| Zn                             | 84.0    | 95.7   | 85.3   | 153    | 90.5     | 96.4   | 108    | 93.5   | 88.1      | 92.4    | 97.2   |
| As                             | 1.30    | 8.36   | 7.04   | 7.24   | 6.17     | 6.89   | 4.91   | 10.8   | 8.14      | 6.69    | 11.9   |
| Rb                             | 58.5    | 66.3   | 83.5   | 69.2   | 72.7     | 63.8   | 75.4   | 63.9   | 50.8      | 80.1    | 70.7   |
| Sr                             | 445     | 556    | 552    | 562    | 616      | 543    | 489    | 684    | 501       | 674     | 602    |
| Y                              | 21.1    | 19.5   | 23.5   | 22.9   | 21.6     | 22.7   | 26.5   | 24.0   | 21.3      | 24.0    | 24.2   |
| Zr                             | 72.3    | 87.9   | 105    | 87.6   | 78.0     | 109    | 101    | 102    | 72.6      | 97.0    | 99.2   |
| Nb                             | 11.6    | 10.4   | 13.4   | 11.3   | 11.6     | 11.9   | 14.6   | 10.4   | 9.58      | 13.9    | 9.52   |
| Ag                             | 0.07    | 0.03   | 0.04   | 0.14   | 0.02     | 0.02   | 0.07   | 0.08   | 0.03      | 0.03    | 0.03   |
| Cd                             | 0.05    | 0.20   | 0.25   | 0.27   | 0.29     | 0.34   | 0.07   | 0.21   | 0.30      | 0.14    | 0.31   |
| Cs                             | 3.91    | 3.33   | 3.98   | 3.28   | 4.40     | 3.70   | 4.75   | 3.45   | 3.19      | 4.25    | 3.76   |
| Ba                             | 300     | 301    | 356    | 285    | 375      | 363    | 384    | 300    | 240       | 400     | 257    |
| La                             | 19.4    | 18.1   | 21.6   | 19.6   | 22.2     | 21.6   | 24.3   | 17.1   | 15.9      | 22.1    | 16.8   |
| Ce                             | 36.9    | 34.3   | 40.9   | 36.8   | 41.7     | 40.4   | 46.0   | 31.9   | 29.1      | 41.6    | 32.7   |
| Pr                             | 4.89    | 4.44   | 5.43   | 4.98   | 5.58     | 5.43   | 6.11   | 4.39   | 4.08      | 5.55    | 4.31   |
| Nd                             | 19.8    | 17.9   | 21.9   | 20.2   | 22.7     | 22.3   | 24.7   | 18.0   | 16.3      | 22.5    | 17.6   |
| Sm                             | 3.96    | 3.59   | 4.36   | 4.14   | 4.48     | 4.43   | 4.96   | 3.84   | 3.27      | 4.47    | 3.74   |
| Eu                             | 0.91    | 0.92   | 1.01   | 0.98   | 1.06     | 1.07   | 1.16   | 1.00   | 0.92      | 1.07    | 0.98   |
| Gd                             | 3.45    | 3.18   | 3.81   | 3.58   | 3.91     | 3.92   | 4.32   | 3.51   | 3.11      | 3.89    | 3.45   |
| Tb                             | 0.56    | 0.52   | 0.62   | 0.59   | 0.62     | 0.64   | 0.71   | 0.59   | 0.54      | 0.63    | 0.59   |
| Dy                             | 3.41    | 3.17   | 3.77   | 3.65   | 3.78     | 3.89   | 4.29   | 3.72   | 3.49      | 4.05    | 3.79   |
| Ho                             | 0.69    | 0.66   | 0.77   | 0.76   | 0.79     | 0.81   | 0.87   | 0.80   | 0.74      | 0.81    | 0.80   |
| Er                             | 1.81    | 1.69   | 2.02   | 1.96   | 1.98     | 2.04   | 2.28   | 2.09   | 1.89      | 2.06    | 2.08   |
| Tm                             | 0.30    | 0.28   | 0.34   | 0.33   | 0.33     | 0.34   | 0.38   | 0.35   | 0.32      | 0.34    | 0.35   |
| Yb                             | 1.72    | 1.69   | 1.99   | 1.95   | 2.03     | 1.95   | 2.18   | 1.64   | 1.88      | 2.03    | 2.09   |
| Lu                             | 0.24    | 0.24   | 0.29   | 0.28   | 0.27     | 0.28   | 0.31   | 0.30   | 0.26      | 0.29    | 0.30   |
| Hf                             | 1.79    | 1.79   | 2.24   | 1.90   | 1.56     | 2.25   | 2.21   | 2.12   | 1.50      | 1.93    | 2.15   |
| Ta                             | 1.07    | 0.67   | 0.92   | 0.75   | 1.08     | 1.05   | 1.05   | 0.82   | 0.69      | 0.99    | 0.81   |
| Pb                             | 9.24    | 18.6   | 15.9   | 16.9   | 14.6     | 13.9   | 12.8   | 13.0   | 10.6      | 12.6    | 18.9   |
| Th                             | 6.50    | 7.54   | 7.97   | 7.07   | 6.58     | 6.42   | 8.12   | 5.94   | 5.03      | 7.40    | 6.06   |
| U                              | 1.23    | 1.79   | 1.77   | 1.96   | 1.74     | 1.76   | 1.93   | 1.57   | 1.46      | 2.10    | 1.75   |

\*Total iron is shown as FeO.

<sup>b</sup>LOI: Loss on ignition.

Please cite this article as: Tschegg, C., et al., Thermally triggered two-stage reaction of carbonates and clay during ceramic firing – A case study on Bronze Age Cypriot ceramics, Applied Clay Science (2008), doi:10.1016/j.clay.2008.07.029

above 950 °C and in the presence of sufficient silica, gehlenite coexisting with wollastonite ( $\text{CaSiO}_3$ ) will breakdown providing anorthite ( $\text{CaAl}_2\text{Si}_2\text{O}_8$ ) and wollastonite (Rathossi et al., 2004 and ref. therein). If adequate amounts of calcium are available in the reaction, anorthite appears at 1000 °C and forms either consuming the existing gehlenite-phase together with amorphous clay mineral breakdown products or just by reaction of decomposed clay minerals and lime (Hajjaji and Kacim, 2004). Riccardi et al. (1999) found that calcium diffusion from carbonates towards the paste matrix takes place from the very early stage of calcite dissociation until the temperature at which new minerals are formed. The sintering stage in clay–calcite mixtures starts at around 950 °C and is up to calcite amounts of around 10 wt.% mainly controlled by viscous flow (Hajjaji and Kacim, 2004).

Considering all phase reactions that can occur during firing, breakdown and transformation of calcareous inclusions are the most striking and easiest recognizable ones. High-temperature reaction rims evolve around the carbonate grains, enabling fast temperature estimations.

## 2. Methods and samples

### 2.1. Analytical techniques

#### 2.1.1. Bulk geochemistry

Before bulk chemical analyses were carried out, the samples were cleaned and their surface layers were abraded. The specimens were

grounded in an electric agate mill, homogenized, dried at 110 °C and fired at 950 °C. For X-ray fluorescence (XRF) analysis, fused beads were produced, consisting of a 1:5 diluted mixture of fired sample material and flux ( $\text{Li}_2\text{B}_4\text{O}_7$ ). Major element bulk analyses were made with a Philips PW 2400 sequential X-ray spectrometer equipped with a Rh-excitation source (Department of Lithospheric Sciences, University of Vienna). Trace and rare-earth elements analyses were performed with inductively coupled mass-spectrometry (ICP-MS) on a Perkin Elmer ELAN 6100 DRC (Department of Lithospheric Sciences, University of Vienna) following the digestion method and the analytical procedure described in Tschegg et al. (2008).

#### 2.1.2. Petrography, mineralogy, microtextures and phase chemistry

Petrographic investigations and microprobe analyses (EPMA) were carried out on polished and carbon-coated thin sections. A Cameca SX-100 electron microprobe (Department of Lithospheric Sciences, University of Vienna) was used to gain mineral and non-stoichiometric phase chemistries as well as to study micro-scale mineral/phase reactions in detail. All analyses were made against natural standards, using four wavelength-dispersive spectrometers (WDS) with operating conditions of 15 kV acceleration voltage and 20 nA beam current; standard correction procedures were applied. In order to minimize the loss of alkalis, the glassy aluminosilicate reaction rims were measured with a defocused beam current (5  $\mu\text{m}$  diameter). Line scans were performed in 5  $\mu\text{m}$  steps with a 2  $\mu\text{m}$  beam diameter. Very small phases (<3  $\mu\text{m}$ ) were qualitatively defined using the built-in energy-dispersive spectrometer (EDS). The distribution of elements in

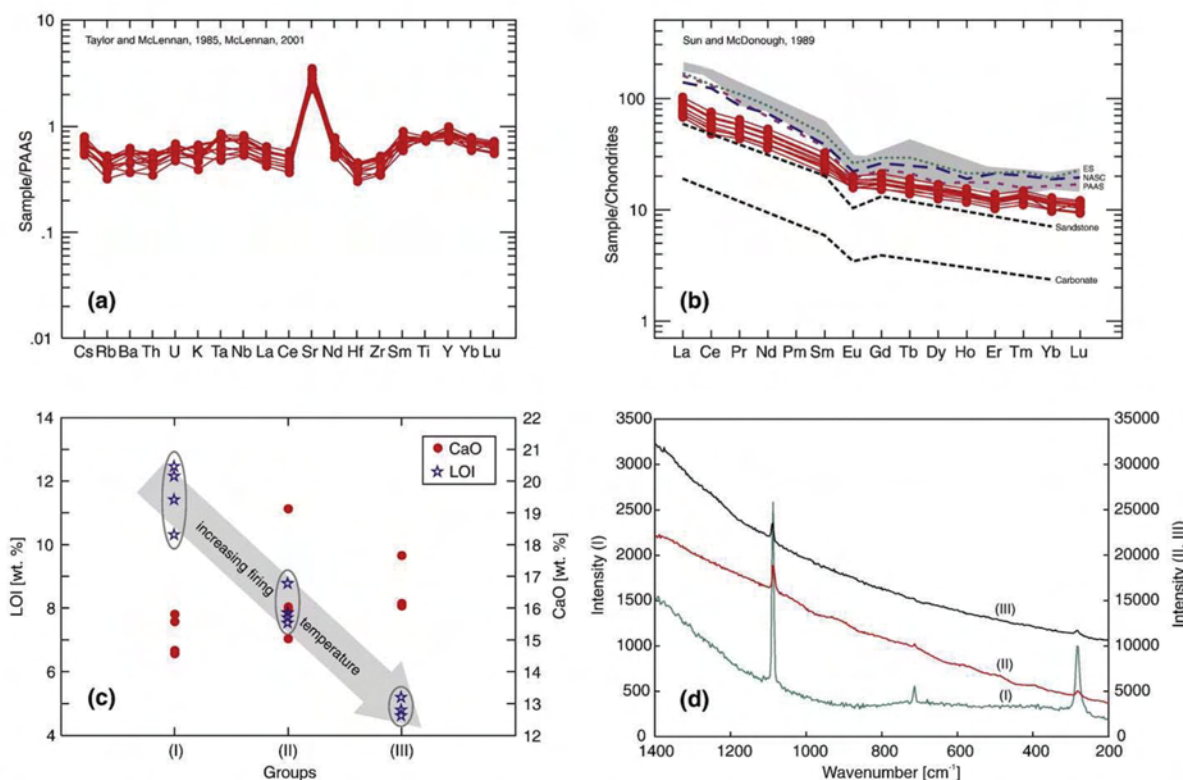


**Fig. 1.** (a) Bulk major- and trace element abundances of Cypriot Plain White Wheelmade ware samples, normalized to the composition of the Post-Archean average Australian shale (PAAS composition after Taylor and McLennan, 1985; McLennan, 2001). (b) Chondrite normalized bulk rare-earth element concentrations of PWW sherds (Sun and McDonough, 1989); ES (European shale composite), NASC (North American shale composite), PAAS (Post-Archean average Australian shale) as well as sandstone and carbonate chemistries after Taylor and McLennan (1985); grey shaded field combines REE compositions of particulate matter from rivers Amazon, Congo, Ganges, Garonne and Mekong (Taylor and McLennan, 1985). (c) Correlation diagram of LOI (loss on ignition) vs. CaO of investigated PWW ware samples – different stages of firing temperatures are indicated on the x-axis, distinct abundances on the y-axis. (d) Representative Raman spectra of calcites from differently fired groups of PWW ceramics.

Please cite this article as: Tschegg, C., et al., Thermally triggered two-stage reaction of carbonates and clay during ceramic firing – A case study on Bronze Age Cypriot ceramics, Applied Clay Science (2008), doi:10.1016/j.clay.2008.07.029

reaction domains was determined with a qualitative high resolution elemental mapping procedure. The size of the measured areas was  $512 \times 512 \mu\text{m}$  with a step size of  $1.0 \mu\text{m}$  at 20 kV acceleration voltage and 20 nA beam current. For supplementary microtextural studies, fresh carbon-coated fracture surfaces were investigated with a JEOL JSM 6400 scanning electron microscope (SEM) equipped with a Link EDX unit, working with an operating voltage of 20 kV (Institute of Mineralogy and Crystallography, University of Vienna). Powder pellets with preferred orientation were prepared for X-ray diffraction (XRD) analysis. The bulk mineralogical assemblages were determined with a Philips PW 1877 X-ray diffractometer (Department for Geodynamics and Sedimentology, University of Vienna) working with Cu-radiation at 45 kV and 35 mA (scanning over the interval of  $2\text{--}70^\circ 2\theta$ ). Raman spectra were obtained with a Renishaw RM-1000 micro-Raman spectrometer with a 20 mW, 488 nm Ar ion laser excitation system and a thermo-electrically cooled CCD detector (Institute of Mineralogy and Crystallography, University of Vienna). The spectra were taken in confocal mode using a Leica DMLM microscope and acquired in the range  $100\text{--}1700 \text{ cm}^{-1}$  with total exposure times of approximately 80 s.

## 2.2. Ceramics

The samples of this study belong to the Late Cypriot Plain White Wheelmade (PWW) ware, a subgroup of the large Plain White (PW) ware family (Aström, 1972). The sherds were found during the excavations of P. Dikaïos from 1948 to 1958 (Dikaïos, 1969–1971) at Enkomi (eastern alluvial Mesaoria Plain, east-coast Cyprus) and compiled by Crewe (2004). The time of production is the Late Cypriot Bronze Age, phases LC I and LC II (approx. 1650–1200 B.C.), whereas the origin of the ware is still enigmatic (Crewe, 2004). Keswani-Schuster (1991) proposed numerous production sites on Cyprus, but preferred the vicinity of Enkomi and Angustina due to the frequent occurrence of the ware in this region. Nevertheless, for the LC II till LC III (down to 1050 B.C.) she suggested also other production centres at the south-eastern Cypriot coast (i.e. Kition and Hala Sultan Tekke).

The PWW ware is of great interest, as it relieves the handmade forms inducing a radical transformation in Cypriot ceramic style and manufacturing techniques. Furthermore, it appears concurrently with the evidence for extensive trade within the island and beyond. Because of its prime position in the centre of the Eastern Mediterranean, the island of Cyprus became an important focus for trade and exchange of cultural goods during the Middle and Late Bronze Age. PWW ware encompasses a

large variety of open and closed vessel forms (Aström, 1972; Keswani-Schuster, 1991; Crewe, 2004). The group reflects not only a domestic serving and storage ware but was moreover used as export goods and travel containers. With the appearance of wheel manufacture, it became obvious that creating PWW pots increased through time; nevertheless the specific manufacturing process so far remained fairly unknown.

## 3. Results

### 3.1. Bulk geochemistry

Bulk major, trace and rare-earth element analyses of the sherds are given in Table 1. Striking is their relatively homogeneous chemical composition. Thus, major elements like  $\text{SiO}_2$ ,  $\text{Al}_2\text{O}_3$ , FeO and MgO marginally vary from 48.5 to 54.8 wt.%, 12.9 to 14.4 wt.%, 6.76 to 7.99 wt.% and 4.54 to 7.73 wt.% respectively. Insignificant amounts of secondary calcite (as only a couple of exiguous calcite crystals have been detected that grew in the porosity after firing) indicate that the high CaO contents (14.6–19.1 wt.%) roughly reflect the modal abundance of Ca-bearing minerals and rock- or fossil-fragments. The loss on ignition (LOI) ranges between 4.61 and 12.5 wt.%, is indeed not to correlate with the CaO concentrations but decreases systematically from group I to group III (Fig. 1c).

In Fig. 1a Post-Archean average Australian shale (PAAS) normalized incompatible elemental abundances of the sherds show patterns that are indistinguishable from each other, consistent with the similarities in composition observed for major elements. In addition, the abundant carbonate inclusions in the sherds can account for the relative to the neighbour elements Ce and Nd pronounced positive Sr anomaly. The sum of measured rare-earth elements (REE) ranges from 81.79 ppm to 122.55 ppm. Chondrite normalized REE abundances are given in Fig. 1b. For comparison together with the REE, abundances of shales, sandstones, carbonates and particulate matter from several rivers are plotted. With respect to average shale compositions (PAAS, NASC and ES) and the similar five selected river particulate matter compositions, a small depletion of all rare earths is noticeable, whereas the LREE indicate the strongest depletion.

### 3.2. Petrography and mineralogy

The fine grained clay-silt fraction is, beside tempered and natural inclusions that appear in the paste, the main factor that controls the

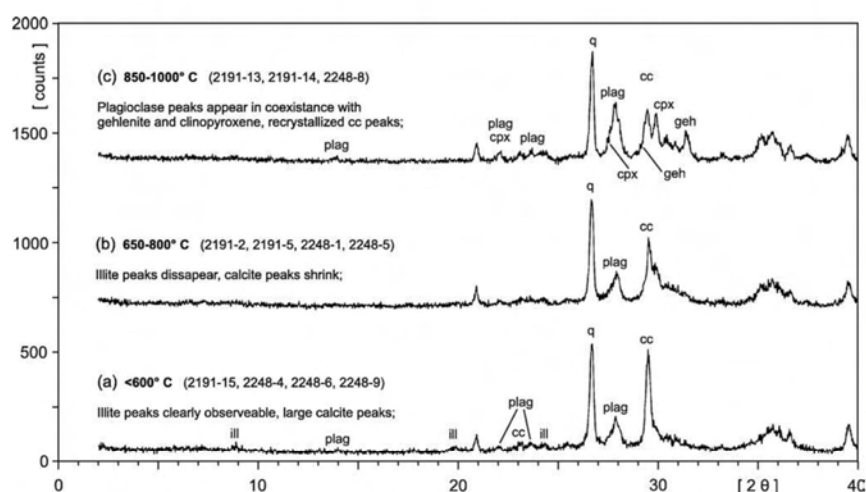


Fig. 2. X-ray diffraction analyses of PWW samples fired at increasing temperatures. (a) Pattern representative for group I, (b) for group II and (c) for group III ceramics (cc – calcite, cpx – clinopyroxene, geh – gehlenite, ill – illite-like phase, plag – plagioclase, q – quartz).

Please cite this article as: Tschegg, C., et al., Thermally triggered two-stage reaction of carbonates and clay during ceramic firing – A case study on Bronze Age Cypriot ceramics, Applied Clay Science (2008), doi:10.1016/j.clay.2008.07.029

composition of the bulk chemistry. Depending on technological differences like raw-material conditioning and firing technique, resulting textural, visual and physical characteristics (e.g. grain size distribution, colour, hardness) may vary in a sample batch like this, while the chemistry is still without major differences.

In all analyzed samples, the grain size of the phyllosilicatic paste matrix ranges from clay to silt size. Smaller than 60  $\mu\text{m}$  sized subangular inclusions of quartz, feldspars (mainly plagioclase) and accessory oxides as well as micas (mainly muscovite) build up the paste matrix. The porosity that can be observed in the sherds is partly due to drying shrinkage and degassing processes during firing, partly due to the breakdown of carbonates in the high fired samples. Just very sporadic, a negligible and inconsequential growth of secondary calcite minerals in pores is present. In all investigated samples, sand-sized (100–500  $\mu\text{m}$ ) quartz-, plagioclase- and mainly carbonate grains are included in the paste, whose amount and size vary. Particularly the conspicuously abundant, large and angular carbonate fragments, which are in all probability tempered artificially, differ in their quantity. The calcareous phases include a wide spectra of fossils

(mainly foraminifera and shell fragments) and bio – and lithosparitic as well as – micritic limestone fragments consisting of calcite. Accessory inclusions that are characteristic for the investigated ware are rock-fragments (from basic source rocks and sandstones), hematites, Ti-magnetites, ilmenites, clay-pellets, Cr-spinels and pyroxenes (mainly diopsides). The fraction of large quartzes, plagioclases and carbonates as well as the mentioned accessory minerals show subangular-angular shapes and therefore indicate that they were shortly transported or even broken up freshly to fabricate the paste-blend.

Controlled by different firing temperatures, three major groups could petrographically be distinguished within the sample set. Group I consists of pottery samples that fired at low temperatures and show completely firing-unaffected carbonate inclusions and non-isotropic paste matrices. Group II sherds (group II) was fired at slightly higher temperatures, which is indicated by partly decomposed carbonates. Their paste matrices however still appear non-isotropic. Group III combines samples that have experienced the highest temperatures, which is reflected by isotropic paste matrices and extensively

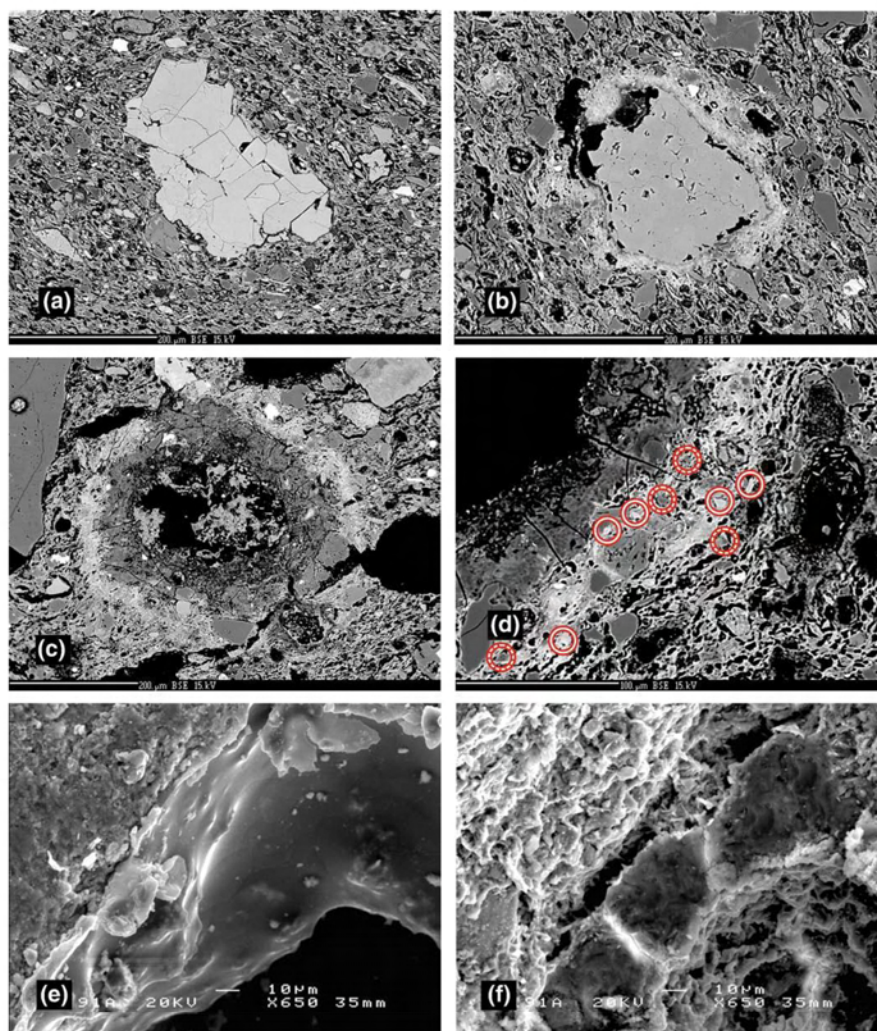


**Fig. 3.** Microprobe BSE images of (a) an unreacted carbonate mineral of a group I sherd, (b) a slightly decomposed carbonate with the first-stage reaction rim of group II, (c) a heavily reacted calcareous inclusion of group III ceramics with well evolved first- and second-stage reaction domains and (d) an enlarged reaction configuration with indicated gehlenites (full line circles) and anorthites (dotted line circles). (e, f) SEM images illustrating the glassy and spherical appearance of the second-stage Al-Si reaction rims.

Please cite this article as: Tschegg, C., et al., Thermally triggered two-stage reaction of carbonates and clay during ceramic firing – A case study on Bronze Age Cypriot ceramics, *Applied Clay Science* (2008), doi:10.1016/j.clay.2008.07.029

decomposed carbonates. The reacted and decomposed calcareous phases are often shrunken and lost their birefringence. At the interface of paste matrix and carbonates an isotropic, glassy, yellowish-brown rim can be observed in plane polarized light.

Fig. 2 divides three X-ray diffraction patterns according to their distinct mineralogical assemblages and different firing temperature estimates. Ceramic samples of group I are characterized by the existence of illite-like clay mineral peaks and high calcite peaks

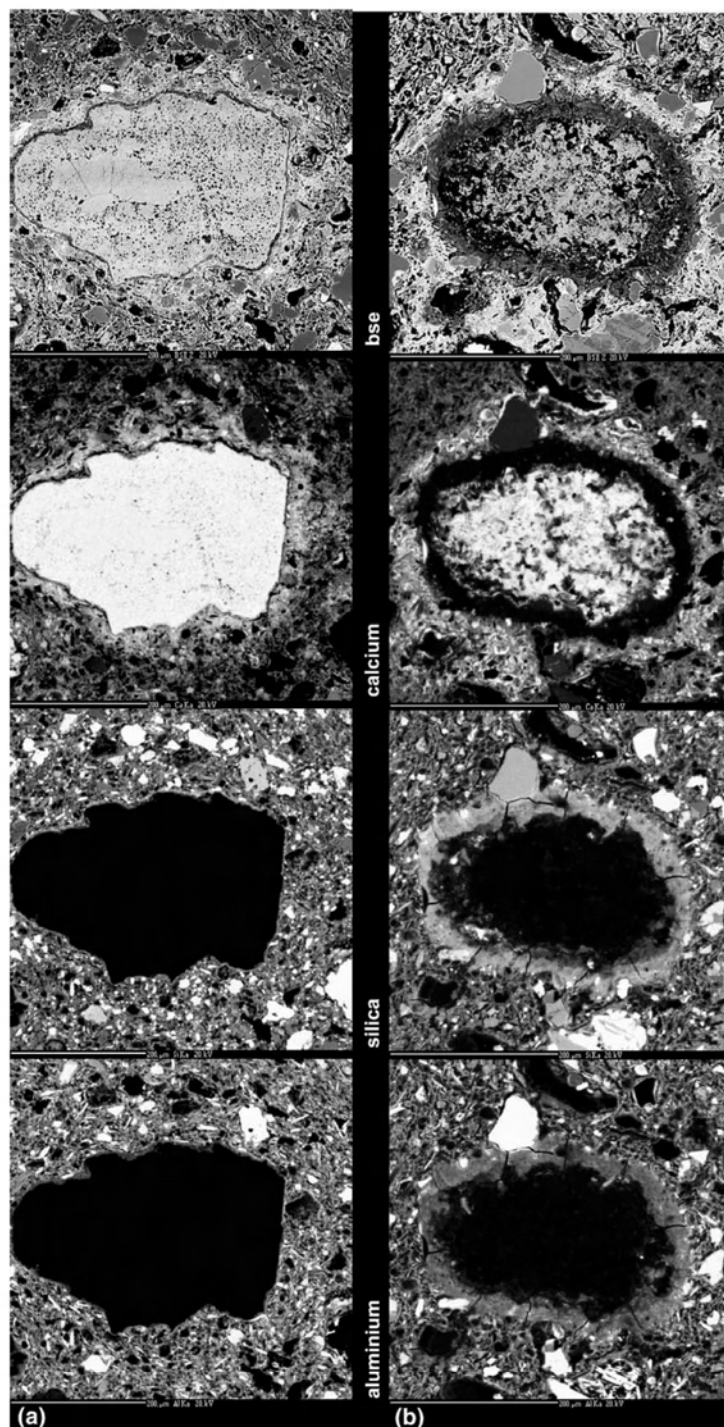


Fig. 4. Element maps of a carbonate reaction stages representative (a) for group II samples and (b) for group III samples.

Please cite this article as: Tschegg, C., et al., Thermally triggered two-stage reaction of carbonates and clay during ceramic firing – A case study on Bronze Age Cypriot ceramics, *Applied Clay Science* (2008), doi:10.1016/j.clay.2008.07.029

(Fig. 2a). The intensities of clay mineral peaks (10 Å and 4.48 Å) are reduced but sufficient to be detected easily; the major high calcite peak (3.035 Å) indicates unreacted carbonates. The pattern representative for ceramics of group II shows the disappearance of the illite-like phase as well as reduction of the calcite reflection consistent with an increase of firing temperatures (Fig. 2b). Despite its minor modal abundance, plagioclase is detectable in group I and II. In the diffraction patterns of group III samples however, unusual high intensities of calcium-silicate phases appear (anorthite, gehlenite and additionally diopside), due to the blastesis of new minerals at high firing temperatures (Fig. 2c). The calcite peak that despite the assumed high temperature is still present can either be accounted to incompletely dissociated large sparitic carbonate inclusions or to recarbonation processes after the firing.

Fig. 1d shows Raman spectra of representative calcite inclusions for each group of sherds. Due to low temperature firing, calcites of group I are nearly unreacted and are therefore characterized by the narrow and large  $1086\text{ cm}^{-1}$  peak together with two low intensity peaks at  $713$  and  $282\text{ cm}^{-1}$  (Fig. 1d–I). Calcites from ceramics of group II already indicate a considerable reduction of peak intensities with simultaneous strong increase of background intensities (Fig. 1d–II). The excitation of a calcareous phase included in a high fired sherd of group III shows the same identifiable bands like in group II, but with higher fluorescence background and even lower peak intensities (Fig. 1d–III). Nevertheless it still can be recognized as a calcite mineral and is not to confuse with dolomite ( $\text{CaMg}(\text{CO}_3)_2$ ), lime ( $\text{CaO}$ ) or portlandite ( $\text{Ca}(\text{OH})_2$ ).

### 3.3. Microtextures

Microtextural studies on the ceramics provide additional evidence for the division into three groups. Group I comprises the pottery fired at lowest temperatures, as no reactions on minerals, mineral-rims or inter-phase contact zones are observable. The temperature-sensitive carbonate inclusions show no alteration or modification compared to unfired calcareous material (see Fig. 3a). In group II, the development

of a reaction domain around carbonate fragments is apparent in the ceramics (Fig. 3b). It is indicated by a 20–30 (up to 50)  $\mu\text{m}$  thick zone enriched in Ca, which appears as a bright halo around the carbonate fragments, as a consequence of calcium transport from the grain into the porous paste matrix. Beside the newly formed reaction domain, the carbonate fragments show variable degrees of mineral dissociation, as sometimes an intact crystal core remains (Fig. 4a). In the enlarged diffusion affected zone, no phase reactions due to the Ca-enrichment can be determined. Group III comprises ceramics that have been fired at highest temperatures as during the firing process variable phase reactions took place. The most noticeable reaction that takes place at this stage of firing is the total decomposition of calcareous inclusions and the simultaneous development of a second temperature triggered reaction zone – a glassy reaction rim at the direct interface of calcareous grains and the clayish paste matrix. These dark and mostly quite homogenous “shells” evolve at the surface of carbonate grains, show “finger-type” geometries at the outside and decouple further grain–matrix interactions (Fig. 3c, d). Depending on the crystallinity of the grain and size, the thickness of the reaction rim ranges from 20 to 50  $\mu\text{m}$ . Cracks in these reaction rims affirm their glassy nature and suggest high cooling rates (see Fig. 3c, d, e, f). In the time these noticeable rims evolve, mineral blastesis takes place in the outer bright Ca-affected zone that is characteristic for the minor fired ceramics of group II (Fig. 3d). Newly formed small gehlenite- and anorthite phases are detectable in the outer first-stage reaction zone that evolved due to reaction of the increased calcium-coated surface area in the porous paste matrix and the breakdown products of the clay (Fig. 3d).

### 3.4. Phase chemistry

Backscattered electron images and element specific X-ray maps (for Ca, Si and Al) of calcites in different temperature regimes are shown in Fig. 4. Fig. 4a displays a calcite mineral representative for a group II sample, whose core-section is, despite thermal influence to some degree, intact, whereas the rest of the phase is already decomposed. The

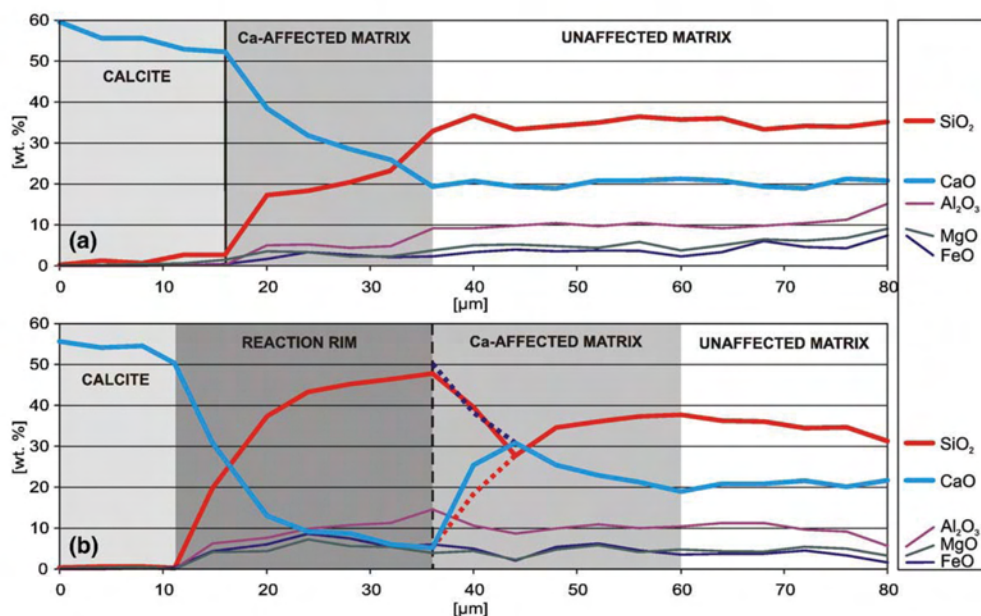


Fig. 5. EPMA line scans from carbonate inclusions to reaction-affected clay paste matrices, representative for phase transformations in samples of (a) group II and (b) group III. See text for more details.

Please cite this article as: Tschegg, C., et al., Thermally triggered two-stage reaction of carbonates and clay during ceramic firing – A case study on Bronze Age Cypriot ceramics, Applied Clay Science (2008), doi:10.1016/j.clay.2008.07.029



**Table 2**  
Representative compositions of second-stage Al–Si reaction rims

|                                | 2191–13 |      | 2191–14 |      | 2248–8 |      |
|--------------------------------|---------|------|---------|------|--------|------|
|                                | Mean    | SD   | Mean    | SD   | Mean   | SD   |
| <i>EPMA analyses [wt.%]</i>    |         |      |         |      |        |      |
| SiO <sub>2</sub>               | 62.8    | 0.45 | 62.2    | 1.01 | 61.9   | 1.35 |
| TiO <sub>2</sub>               | 0.63    | 0.39 | 0.36    | 0.12 | 0.63   | 0.19 |
| Al <sub>2</sub> O <sub>3</sub> | 13.8    | 0.38 | 15.0    | 0.88 | 14.6   | 1.08 |
| FeO*                           | 6.18    | 0.58 | 5.63    | 0.40 | 6.92   | 0.29 |
| MnO                            | 0.21    | 0.14 | 0.06    | 0.02 | 0.02   | 0.01 |
| MgO                            | 7.76    | 0.93 | 8.24    | 0.95 | 6.75   | 0.21 |
| CaO                            | 7.35    | 0.64 | 6.90    | 0.46 | 7.18   | 0.91 |
| Na <sub>2</sub> O              | 0.16    | 0.07 | 0.25    | 0.36 | 0.12   | 0.04 |
| K <sub>2</sub> O               | 0.81    | 0.09 | 1.06    | 0.65 | 0.71   | 0.09 |
| P <sub>2</sub> O <sub>5</sub>  | 0.37    | 0.08 | 0.29    | 0.08 | 1.20   | 0.41 |
| Total                          | 100.0   |      | 100.0   |      | 100.0  |      |

SD – Standard deviation, number of measurements  $n=20$ .

\*Total iron is shown as FeO.

bright Ca enriched halo around the calcite grain is clearly visible in the Ca-specific element map. In this reaction domain, apparently Ca diffuses into the porous grain-surrounding matrix. Si and Al X-ray maps of the same area indicate that these elements remained unaffected around the calcite grain. Fig. 4b illustrates a calcite grain of group III that has heavily reacted due to high firing temperatures. At the carbonate–phyllosilicate boundary, an aluminosilicate rich shell has evolved that is clearly visible in BSE images as well as in element X-ray maps. Within this inner reaction rim, element X-ray maps indicate a depletion of Ca by a simultaneous enrichment of Si and Al. At this stage, the outer Ca-affected domain is chemically isolated through the newly formed reaction-corona, causing considerably reduction of the Ca diffusion rates.

The line scans in Fig. 5 quantify the chemical composition of thermally different influenced calcite minerals and their distinct reaction rims. The profiles characterize the elemental distribution from the outer calcite grains through the thermally triggered reaction rims around the grain into the reaction-unaffected paste matrix. Fig. 5a demonstrates the distribution of five major elements from the calcite mineral to the unaffected matrix in a ceramic of group II. In the Ca-affected reaction domain the Ca concentration decreases continuously from about 55 wt.% close to calcite to 20 wt.% in the paste matrix. Within these 20  $\mu\text{m}$  reaction zone (Fig. 5a), the other analyzed oxides (SiO<sub>2</sub>, Al<sub>2</sub>O<sub>3</sub>, MgO and FeO) are inversely related to CaO distribution. The calcite–phyllosilicate reaction presented in Fig. 5b evolved at considerably higher firing temperatures (group III) and therefore indicates the additional stage in the transformation process. This second stage represents a partial melting or sintering process that takes place at the carbonate–paste matrix interface. The latter reaction is recognisable as a non-stoichiometric rim around the decomposed carbonate grain, in which CaO is decreasing roughly exponentially from 56 wt.% to around 5 wt.% over a distance of 35  $\mu\text{m}$ , with simultaneous negative-exponential increase of SiO<sub>2</sub> from practically zero to about 50 wt.%. Al<sub>2</sub>O<sub>3</sub>, MgO and FeO concentrations increase, like SiO<sub>2</sub>, from zero to concentrations similar to these of the unaffected matrix. Representative average compositions of analyzed second-stage carbonate–clay mineral reaction rims are summarized in Table 2. Adjacent to this reaction rim is the zone of the Ca-affected matrix, indicated by a repeated increase of CaO (up to over 30 wt.%) together with the decreasing, negative correlating SiO<sub>2</sub> (from 50 wt.% to under 30 wt.%) and the following normalisation to paste-matrix dependent values over 25  $\mu\text{m}$ .

#### 4. Discussion

The Plain White Wheelmade ware from Enkomi is due to the range of found vessel types, a multi-purpose ware that was used for liquid and food consumption, serving, trade and storage (Crewe, 2004). Since antiquity, the use of calcareous raw material was a common technique

in pottery production concerning table as well as storage ware, as tempering calcite to the clayey material increases the mechanical behavior of the fired product (Traoré et al., 2000). Furthermore, potters used to know that the addition of temper particles not only reduces the plasticity of the raw-material blend, making vessels easier to shape, but also prevents cracking during drying (Shoval and Beck, 2005). Using e.g. smectitic raw material actually demands tempering, as without the design would destabilize and collapse during manufacturing. A favored firing temperature for such calcareous material would lie around 700–800 °C, as it was sufficient for low temperature sintering and caused the projected consolidation and cementation of the ceramic bodies (Maggetti et al., 1984; Shoval, 2003). Higher temperatures were avoided, as carbonate decomposition could cause defects in the created pots. Material failures were even worse if accompanied calcium hydroxide formation lead to volume expansion and pronounced cracking.

Low variations of bulk geochemical major and trace element concentrations together with distinctive mineralogical assemblages that are observable throughout the PWW ware sherds indicate a common raw-material source and similar raw-material conditioning techniques of the investigated ceramic products. The slight depletion of rare-earth element abundances compared to average shale and river sediment compositions is ascribed to chemical dilution by means of tempering rare earth poor silicate- and carbonate fragments to young terrigenous sediments (Fig. 1b). The characteristic mineralogical assemblage of the investigated ware group reflects the features of regional occurring Holocene to recent alluvial sediments in the area of the eastern Mesaoria Plain (Cyprus) quite nicely (Atalar and Kilic, 2006; Tschegg et al., 2008). Due to varying firing temperatures, three groups of ceramics can be distinguished in this batch of Cypriot Plain White Wheelmade Ware samples. These groupings can be comprehended petrographically and mineralogically but mainly taking microstructural and microchemical changes into account. The most conspicuous reactions – the breakdown of calcareous inclusions, their different stages of decomposition and the associated high-temperature reactions with the clayish paste matrix – have been described above in detail.

With the applied methods, ceramics of group I show no indication for firing temperatures exceeding 600 °C. EPMA and SEM investigations reveal that no phase transformations are present and assure the persistent unaffected nature of included temperature-sensitive carbonate phases. X-ray diffraction patterns confirm the existence of well crystallized carbonates together with intact clay mineral phases and the absence of any high temperature indicating mineral phases (like newly formed Ca-silicates). The perfect state of calcite crystallinity that would not remain at higher temperatures was beside X-ray diffraction emphasized by performed Raman spectroscopy. The detected illite-like structure is due to the peak pattern presumably real illite. Dehydroxylated smectite (meta-smectite) could also be considered, as this group of clay minerals is common in the area of Enkomi (Atalar and Kilic, 2006); the temperatures though are not sufficient for complete dehydroxylation of the crystal structures.

Group II comprises pottery samples fired at temperatures between 650 °C and 800 °C, a temperature range in that endothermic phase transformations (dehydroxylation of clay minerals and CaCO<sub>3</sub> breakdown) are noticeably proceeding. Using XRD, the increase of firing temperature can be assessed by the disappearance of clay mineral peaks and the weakening of the calcite peak, whereas low heating rates can be assumed at these temperatures (Moroni and Conti, 2006). SEM investigations show evidence of small exfoliating muscovites that occur due to (OH)<sup>-</sup> release at temperatures over 700 °C (Cultrone et al., 2001). Calcareous inclusions indicate thermal dissociation to different extents at this state. This is mainly dependent on the size of the chemically active surface area and the crystallinity of the grain (Shoval et al., 1993). Therefore, small micritic limestone fragments would theoretically destabilize at lower temperatures than bigger

Please cite this article as: Tschegg, C., et al., Thermally triggered two-stage reaction of carbonates and clay during ceramic firing – A case study on Bronze Age Cypriot ceramics, Applied Clay Science (2008), doi:10.1016/j.clay.2008.07.029

monocrystalline calcites. Via EPMA it was possible in this study to observe that throughout different kinds of calcareous inclusions, the decarbonation process seems to be controlled by the grain size at a higher degree than by the crystal structure criteria, as in all larger inclusions (>300 µm) intact cores remain at this temperature range. Raman spectra of group II calcites illustrate a major decrease of peak intensities by a simultaneous tenfold increase of background intensities that is ascribed to the ongoing thermal destruction of the crystal lattice. The most conspicuous effect though, is the thermally triggered dispersion of Ca at the interface of carbonate inclusions and clayish paste matrices that leads to spherical calcium enrichment (“Ca-coating”) in the porous matrix around the carbonate grain. BSE images and element X-ray mappings indicate these Ca-affected bright rims around carbonate inclusions most impressively. Detailed line measurements from carbonates into reaction-affected matrices allow to see the “diffusiogenic” decrease of calcium over a distance of 20–30 µm that emerges during firing, whereas the concentrations of Al<sub>2</sub>O<sub>3</sub>, MgO and FeO don't change compared to the chemistry of the unaffected paste matrix (Fig. 5a). Elemental Si and Al X-ray mappings assert this evidence (Fig. 4a). Reaction domains around calcites that evolve due to migration of CaO at increasing temperatures and result in microsites with high Ca activity were also reported by Riccardi et al. (1999). Cultrone et al. (2001) described white rims around carbonates developing at the calcite–phyllosilicate interface at firing temperatures of 800 °C and presumed a wollastonite rim composition. Like Cultrone et al. (2001) reported, no newly formed Ca-silicate phases could be found in this first-stage reaction rim that due to the diffusion-driven enrichment of calcium and the resulting increase of reactive surface areas would favor mineral growth.

In the highest fired sherds that are comprised in group III, further heating causes mineral decomposition, advanced phase transformations and crystal blastesis. The presence of high-temperature-indicative Ca-silicates (gehlenite, anorthite and clinopyroxene) indicated by X-ray diffraction and EPMA as well as the partial melting reactions at the carbonate–matrix interface suggests a temperature range of at least 850–1000 °C for these samples. The first-stage reaction that causes Ca-affected matrix domains around carbonate inclusions is still visible with the difference that a second-stage inner aluminosilicate reaction rim formed additionally. The reaction rates must have been very high in this range of temperatures, so that the initial diffusion transport has changed to a diffusion plus mass transport (Cultrone et al., 2001). Just that way, partial melting at the contact of carbonates and matrix clay minerals could occur in present extents, producing non-stoichiometric reaction products under disequilibrium firing conditions. An enlargement of the reaction front through partial melting at the Ca–Si interface and mass transport into the paste matrix is after what Ortoleva et al. (1987) called “scallop structure” and could be a responsible explanation for the development of the observed fingered geometries of the second-stage reaction rim (Cultrone et al., 2001). The transformation of CaCO<sub>3</sub> to CaO creates contraction space, where matrix constituents (mainly Si and Al) from decomposed clay minerals have space to generate the second-stage reaction domain. The newly formed spherical rim isolates the inner carbonate grain from the paste matrix, thus preventing further element transport. BSE images illustrate and support the concentric build up of the two reaction domains. Element X-ray maps show the Al- and Si-rich interior shell with lacking Ca and the opposed still Ca enriched outer rim. Line scans indicate the diffusion-like decrease of Ca in the dark appearing second-stage reaction rim with a proximate in- and decrease of Ca in the Ca-affected matrix (Fig. 5b). The Ca-curve in the Ca-affected matrix has to be seen as a diffusion-driven gradient – the same as shown in Fig. 5a, which is denoted by the dotted lines – with the difference that it is influenced by the partial melting process at the inner side. Hajjaji and Kacim (2004) made similar observations and stated, that amorphous silica and aluminium coming from the decomposition of clay minerals lead

to formation of calcium-free glassy domains and can trigger significant melting in samples with amounts <10 wt.% of calcite.

Partial melting as described above could also take place at lower temperatures if volatiles/fluxes would have been added as components to the raw material. Such materials like salts and bone meal, rich in alkalis and phosphorous respectively, could reduce the melting point drastically (Slag Atlas, 1995). However they would likely evaporate during firing and therefore would not be detected.

At the same time the partial melting occurs, gehlenite and anorthite crystallize in the outer Ca-affected matrix rim, in that at this stage both reactive lime and breakdown products of clay minerals at sufficient temperatures are available for mineral blastesis. This shows that not partial melting at the carbonate–phyllosilicate contact triggers the Ca-silicate growth, but the first-stage diffusion process, that increases the reactive interface surface area of Ca and therefore enables mineral blastesis when temperatures are high enough. The absence of wollastonite could be ascribed either to the limited direct contacts of lime and quartz grains in the fabric or to insufficient firing temperatures (Hajjaji and Kacim, 2004 and ref. therein). An increasing content of clinopyroxenes is indeed indicated by X-ray diffraction, but is not comprehensible via SEM or EPMA investigations. The Raman spectra of remaining calcites that despite high temperatures still show CO<sub>2</sub> bands, let us assume that no transformation of the hygroscopic lime to portlandite (through interaction with air-moisture or water) has taken place. In case, however that portlandite existed, a reaction with atmospheric CO<sub>2</sub> and slowly retransformation to calcite (Shoval, 2003 and ref. therein) could be responsible for its disappearance. Another possibility is a direct recarbonatation of CaO to CaCO<sub>3</sub> occurred (Deutsch and Heller-Kallai, 1991). Due to crystallization pressure, the transformation to portlandite would generate crack development in the fabric (Cultrone et al., 2001 and ref. therein), a process however that is not to observe in the analyzed sherds. The loss on ignition (LOI) correlates clearly with the firing temperatures and decreases while the latter increase (Fig. 1c). This finally once more affirms three different grades of firing of the assigned groups of PWWV ceramics by similar lost of volatiles. Additionally it explains the CaO abundances that are not to correlate with the LOI, which would be assumable if all sherds were fired at the same temperature.

## 5. Conclusion

The present study deals with a batch of Cypriot Late Bronze-age Plain White Wheelmade ware samples that are assumed to be produced out of the same raw material and indicate common manufacturing techniques. Carbonate temper was added to clayish raw material in order to achieve best mechanical properties for the further usage of this ware group. The volitional firing temperatures for this type of ceramics was around 650–800 °C, as physical features like toughness and strength at this stage reach their optimum and mechanical failures that can develop at higher temperatures, can be avoided. Group II samples exactly reflect ceramics fired at these temperatures, so that we can assume a slight unintentional under- and over-firing for group I and group II samples respectively.

The most conspicuous reactions that take place even at macroscopical extents – the thermally triggered decomposition of carbonates and their reaction with paste matrix clay minerals – in an increasing temperature regime were observed and assigned to distinct temperature ranges. Three groups of ceramics with different but characterizing and temperature-indicating states of mineral transformation could be distinguished. Below 600 °C, no temperature caused phase transformations can be detected referring to included carbonate phases. In the range of 650–800 °C, the first-stage reaction in the form of Ca diffusion from calcareous inclusions into the paste matrix and a resulting increase of the reactive interface surface area around the carbonate phases can be observed. The interplay of carbonates with the matrix clay minerals leads at exceeding temperatures to a

Please cite this article as: Tschegg, C., et al., Thermally triggered two-stage reaction of carbonates and clay during ceramic firing – A case study on Bronze Age Cypriot ceramics, Applied Clay Science (2008), doi:10.1016/j.clay.2008.07.029

decrease of the phyllosilicate fusion-point and induces the second-stage carbonate–phyllosilicate reaction. The shrunken decarbonated grain makes place for an alumo-silicate melt and the Ca-affected matrix favors mineral blastesis simultaneously. The mentioned melt consists of amorphous breakdown products of the clayish matrix and evolves due to viscous mass transport caused by high reaction rates and partial melting. In the Ca-affected matrix – already developed during first-stage reaction – new Ca-silicates grow and indicate temperatures around 850–1000 °C.

#### Acknowledgements

This work has been supported by the Austrian FWF, grant P18908-N19. We are grateful to the Department of Antiquities of Cyprus and to Lindy Crewe (University of Manchester) for making the Cypriot PWW ware samples available. Robert Krickl and Michael Götzinger (Institute of Mineralogy and Crystallography, University of Vienna) have to be thanked for their assistance at the Raman spectrometer and the SEM. We also want to thank Werner Wruss (Vienna University of Technology) and two anonymous reviewers for their constructive comments.

#### References

- Aström, P., 1972. The Middle Cypriote Bronze Age: Architecture and Pottery, vol. 4. The Swedish Cyprus Expedition, Lund, p. 1C.
- Atalar, C., Kilic, R., 2006. Geotechnical properties of Cyprus clays. Engineering Geology for Tomorrow's Cities. The 10th IAEG Congress, Nottingham, paper 419. Geological Society of London.
- Crewe, L., 2004. Social complexity and ceramic technology on Late Bronze age Cyprus: The new evidence from Enkomi. PhD thesis, University of Edinburgh.
- Cultrone, G., Rodríguez-Navarro, C., Sebastian, E., Cazalla, O., De la Torre, M.J., 2001. Carbonate and silicate phase reactions during ceramic firing. *European Journal of Mineralogy* 13, 621–634.
- Deutsch, Y., Heller-Kallai, L., 1991. Decarbonation and recarbonation of calcites heated in CO<sub>2</sub>: Part 1. Effect of the thermal regime. *Thermochimica Acta* 182 (1), 77–89.
- Dikaïos, P., 1969–71. Enkomi, Excavations 1948–1958, vol. I–III. Verlag Philipp von Zabern, Mainz am Rhein.
- Drits, V.A., Besson, G., Muller, F., 1995. An improved model for structural transformations of heat-treated aluminous dioctahedral 2:1 layer silicates. *Clays and Clay Minerals* 43 (6), 718–731.
- Hajjaji, M., Kacim, S., 2004. Clay–calcite mixes: sintering and phase formation. *British Ceramic Transactions* 103 (1), 29–32.
- Jordán, M.M., Boix, A., Sanfeliu, T., de la Fuente, C., 1999. Firing transformations of cretaceous clays used in the manufacturing of ceramic tiles. *Applied Clay Science* 14, 225–234.
- Keswani-Schuster, P., 1991. A preliminary investigation of systems of ceramic production and distribution in Cyprus during the Late Bronze Age. In: Barlow, J.A., Bolger, D.L., Kling, B. (Eds.), *Cypriot Ceramics: Reading the Prehistoric Record*. University Museum Publications, University of Pennsylvania, Philadelphia, pp. 97–118.
- Maggetti, M., 1982. Phase analysis and its significance for technology and origin. In: Olin, J.S., Franklin, A.D. (Eds.), *Archaeological Ceramics*. Smithsonian Institution Press, pp. 121–133.
- Maggetti, M., Westley, H., Olin, J.S., 1984. Provenance and technical studies of Mexican Majolica using elemental and phase analysis. In: Lambert, J.B. (Ed.), *Archaeological Chemistry III*. American Chemical Society, Washington D.C., pp. 151–191.
- McLennan, S.M., 2001. Relationships between the trace element composition of sedimentary rocks and upper continental crust. *Geochemistry, Geophysics, Geosystems* 2 # 2000GC000109.
- Moroni, B., Conti, C., 2006. Technological features of Renaissance pottery from Deruta (Umbria, Italy): an experimental study. *Applied Clay Science* 33 (3–4), 230–246.
- Noll, W., 1991. *Alte Keramiken und ihre Pigmente*. E. Schweizerbart'sche Verlagsbuchhandlung, Stuttgart.
- Núñez, R., Delgado, A., Delgado, R., 1992. The sintering of calcareous illitic ceramics. Application in archaeological research. In: Galindo, A.E. (Ed.), *Electron Microscopy EUREM 92*. University of Granada, Granada, pp. 795–796.
- Ortoleva, P., Chadam, J., Merino, E., Sen, A., 1987. Geochemical self-organization II: the reactive-infiltration instability. *American Journal of Science* 287, 1008–1040.
- Rathossi, C., Tsolis-Katagas, P., Katagas, C.H., 2004. Technology and composition of Roman pottery in northwestern Peloponnese, Greece. *Applied Clay Science* 24, 313–326.
- Riccardi, M.P., Messiga, B., Duminuco, P., 1999. An approach to the dynamics of clay firing. *Applied Clay Science* 15, 393–409.
- Shoval, S., 1988. Mineralogical changes upon heating calcitic and dolomitic marl rocks. *Thermochimica Acta* 135, 243–252.
- Shoval, S., 2003. Using FT-IR spectroscopy for study of calcareous ancient ceramics. *Optical Materials* 24, 117–122.
- Shoval, S., Beck, P., 2005. Thermo-FTIR spectroscopy analysis as a method of characterizing ancient ceramic technology. *Journal of Thermal Analysis and Calorimetry* 82 (3), 609–616.
- Shoval, S., Gaft, M., Beck, P., Kirsh, Y., 1993. Thermal behaviour of limestone and monocrySTALLINE calcite tempers during firing and their use in ancient vessels. *Journal of Thermal Analysis* 40, 263–273.
- Slag Atlas, 2nd ed., 1995. Ed. by Verein Deutscher Eisenhüttenleute, Verlag Stahlisen GmbH, Düsseldorf.
- Sun, S.S., McDonough, W.F., 1989. Chemical and isotopic systematics of oceanic basalts; implications for mantle composition and processes. In: Saunders, A.D., Norry, M.J. (Eds.), *Magmatism in the Ocean Basins*, 42. Geological Society of London, pp. 313–345.
- Taylor, S.R., McLennan, S.M., 1985. *The Continental Crust: Its Composition and Evolution*. Blackwell Scientific Publications, Oxford.
- Traoré, K., Kabré, T.S., Blanchart, P.H., 2000. Low temperature sintering of a pottery from Burkina Faso. *Applied Clay Science* 17, 279–292.
- Tschegg, C., Hein, L., Ntaflou, Th., 2008. State of the art multi-analytical geoscientific approach to identify Cypriot Bichrome Wheelmade Ware reproduction in the Eastern Nile delta (Egypt). *Journal of Archaeological Science* 35, 1134–1147.
- Veniale, F., 1990. Modern techniques of analysis applied to ancient ceramics. In: Veniale, F., Zerra, U. (Eds.), *Proc. ICOMOS-CE Workshop, Advanced Workshop: Analytical Methodologies for the Investigation of Damaged Stones*. Pavia, Italy, pp. 1–45.

## Appendix (D)

---

Tschegg, C., Ntaflos, Th., Hein, I., 2008d. Combined geological, petrological and geochemical method to reveal source material and technology of Late Cypriot Bronze Age Plain White ware ceramics. *Journal of Archaeological Science* (under review).

---

## Combined geological, petrological and geochemical method to reveal source material and technology of Late Cypriot Bronze Age Plain White ware ceramics

Cornelius Tschegg<sup>a</sup>, Theodoros Ntaflos<sup>a</sup>, Irmgard Hein<sup>b</sup>

<sup>a</sup> Department of Lithospheric Research, University of Vienna, Althanstr. 14, 1090 Vienna, Austria

<sup>b</sup> Institute of Egyptology, University of Vienna, Frankgasse 1, 1090 Vienna, Austria

### Abstract

Late Cypriot Bronze Age Plain White Wheelmade ware samples from several Cypriot excavation sites and the northern Canaanite coast were studied to ascertain their production centres as well as their specific pottery manufacturing procedures and post-depositional alterations. The detailed investigation of the ceramics with combined geoscientific analytical techniques (XRF, ICP-MS, XRD and EPMA) allowed distinguishing four groups of pottery that could be outlined due to common raw material sources and/or technological analogies. Sediments that were sampled in East Cyprus (eastern Mesaoria Plain) for comparative reasons provided evidence that most of the investigated ceramics were produced out of raw materials available around the ancient settlement of Enkomi. By reasons of technological variations and discriminative raw material characteristics, different pottery producing workshops could be figured out that distributed their commodities on the island of Cyprus and exported their ceramic products even out of the country.

### 1. Introduction

#### 1.1 Archaeological background

During the Late phase of the Middle Bronze Age (MC III) and the Late Bronze Age (1750-1050 B.C., acc. to Steel, 2002), Cyprus became an important focus for trade and exchange of cultural goods. The prime position of the island in the Eastern Mediterranean as well as the richness in copper and the increase in demand for this metal are considered to be the pivotal reasons for the intensive integration of Cyprus into the Mediterranean trading systems. Together with the distribution of Cu-ores, also cultural goods and pottery started being exchanged inside Cyprus and beyond. Several studies prove the export of pottery from Cyprus to ancient Eastern and Southern Mediterranean markets (e.g. Knapp and Cherry, 1994 and ref. therein, Maguire, 1995, Gomez et al, 2002 and ref. therein, Tschegg et al., 2008). Trade networks within the island of Cyprus are less understood and assignments of ceramic artefacts to distinct Cypriot localities are rarer and did not always turn out satisfactory (Gomez et al., 2002 and ref. therein).

In this study, we present a direct correlation of Late Cypriot Bronze Age ceramics (to a large extent Plain White Wheelmade PWW ware samples excavated in Enkomi with comparison material from other Cypriot localities and the Canaanite coast) and their source material. Enkomi is a Late Cypriot Bronze Age settlement

that lies 1 km to the east of the modern village Enkomi, about 3.5 km away from the eastern Cypriot coast (see Fig. 1). It is the most extensively excavated LC site in Cyprus and considered to be the first established “state-like” settlement on the island (Crewe, 2004, 2007). Beside a well developed copper smelting site, Enkomi furthermore occupied the main Cypriot harbor for trade to the Eastern Mediterranean and therefore stands out as a centre for exports and imports of multifaceted products (Knapp and Cherry, 1994).

The Cypriot PWW ware on that the study focuses is one of the subgroups of the large Plain White ware family, a ware group that first appeared as handmade forms in small numbers in MC III (1750-1600 B.C.) and continued throughout the LC phases (1600-1050 B.C.), expanding to include wheel-made versions (Aström, 1972). A broad variety of vessel types and styles can be recognized within these PWW samples (the majority are closed vessels though), all of them however are still categorizable as utilitarian table-, household- and storage pottery. The ware represents a radical transformation in Cypriot ceramic style and manufacturing techniques, appearing concurrently with the first evidence for extensive trade contacts of Cyprus to other Mediterranean regions. Although the PWW ware wasn't initially thought to be a regular export ware, it was also distributed outside Cyprus, as was demonstrated by sherds found on the northern Canaanite coastal region (Tell Abu Hawam; Artzy, M., 2006) and in the Egyptian Nile Delta (Tell el-Dab'a; Hein and Jánosi, 2004). Centralized pottery productions are assumed to increase during Protohistoric Bronze Age on Cyprus, there is evidence though that local, sometimes specialized manufacturing took place simultaneously (Knapp and Cherry, 1994). Typological studies indicate a high likelihood of several manufacturing centers and regional ceramic exchange throughout the island. Provenancing pottery via identification of the original source material facilitates pinpointing definite production centers/manufacturing workshops as well as specific trading contacts on the island.

## 1.2 Geological Setting

The coastal LC site of Enkomi is located near the locality Ayios Iakovos in the most eastern part of the Mesaoria Plain just off the Famagusta gulf (see Fig. 1). The Mesaoria Plain extends from the Morphou Bay in the west to the Famagusta Bay in the east of the island of Cyprus and is bounded to the north by the Kyrenia Range that comprises Carboniferous to Cretaceous limestones overlain by Late Palaeogene to Neogene flysch deposits and up to recent alluvial/colluvial sediments. In the south, the basin adjoins to the Upper Cretaceous rocks of the Troodos ophiolite sequence and its Upper Cretaceous to recent sedimentary successions. Morphologically, the Mesaoria Plain lying beneath 300 m.a.s.l. is framed by the northern Kyrenia range with elevations up to 910 and the southern Troodos with heights of up to 1940 m.a.s.l. (Neal, 2002).

The geological formations cropping out in the eastern Mesaoria Basin are sediments of the Pliocene Nicosia Formation and the Pleistocene Athalassa Formation that are stratigraphically overlain by Pliocene-Pleistocene Fanglomerates and terrace deposits as well as Holocene alluviums (McCallum and Robertson, 1995, Robertson et al., 1995). The Nicosia Formation consists of limestones, marls, sandstones, conglomerates, gravels and silts (Calon et al., 2005, GSD, 1995). This cycle of marine sedimentation is followed by the conformably deposited, shallow marine calcarenites, sandstones, marls and conglomerates of the upper Pliocene to Pleistocene Athalassa Formation (GSD, 1995, Robertson and Woodcock, 1986). The overlying extensive deposition of fluvial and alluvial material during Quaternary is related to erosion resulted from the uplift of the

Troodos-massif. It consists of an unconformably deposited undifferentiated lower marine sequence and an upper terrigenous sequence of conglomerates, breccias, gravels, sands, silts and lacustrine muds, summarized as the Pleistocene Fanglomerate (Calon et al., 2005, GSD, 1995). The Holocene alluvium, represented by spacious floodplains, alluvial channels and fan deposits comprises sands, silts, clays and gravel (GSD, 1995, Newell et al., 2004).

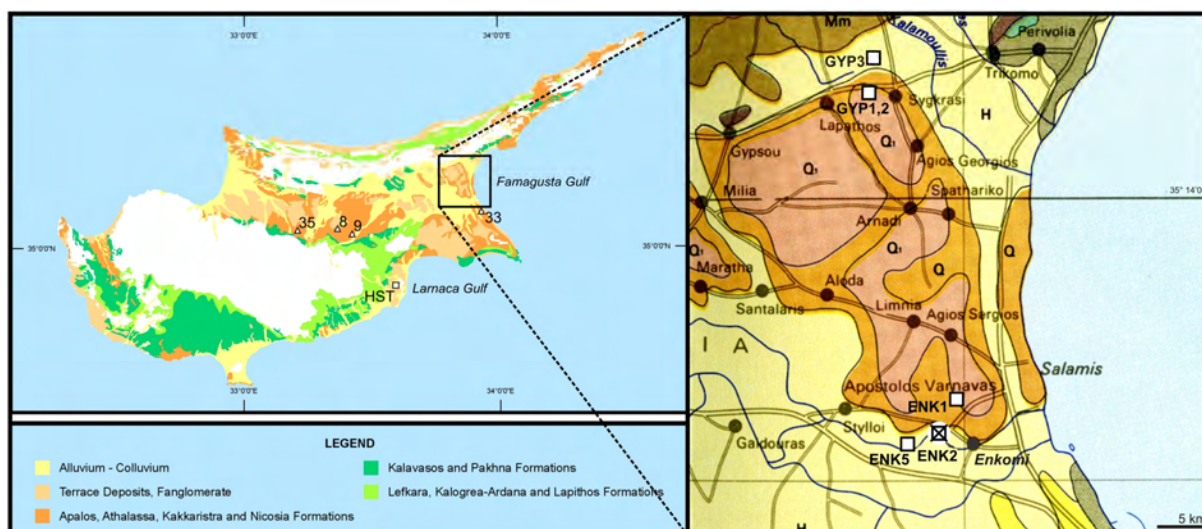


Fig.1: Map of the circum-Troodos sedimentary successions (modified; provided by the Geological Survey Department, Nicosia, Cyprus) and detail from the geological map of Cyprus (modified; GSD, 1995). Squares indicate sediment sample points from this study; triangles, sample points from Vaughan (1987). The cross locates the Enkomi excavation site. (Q – Pleistocene Athalassa Fm., Q1 – Pleistocene Fanglomerate Fm., H – Holocene alluviums and colluviums)

## 2. Raw material sampling and ceramic collection

Sample identification numbers, specific ware types and excavation-sites of all analysed ceramic specimens and raw materials of this study are summarized in Table 1. Raw materials suitable for pottery production were collected from typically outcropping geological formations in the vicinity of the Enkomi excavation site to compare their chemical and mineralogical composition to ceramic samples that are supposed to be locally produced in ancient Enkomi. Three samples were collected from Pleistocene Fanglomerate terraces, one (ENK1) close to the Enkomi excavation site, two (GYP1, GYP2) at road outcrops between Lapathos and Sygkrasi (see Fig. 1). These loose silty clays (USDA classification; Soil Survey Division Staff, 1993) consist mainly of siliceous and calcareous constituents, the clay mineral fraction is composed of smectite-, illite-, chlorite group minerals at  $\pm$  same proportions and few kaolinite (see Fig. 5b-d). All three Pleistocene samples contain few sand sized calcareous shell fragments. ENK2 was taken from a near-surface horizon directly in the excavation area whereas GYP3 samples a floodplain more northern. Both samples represent Holocene silty loams (USDA classification; Soil Survey Division Staff, 1993) from different alluvial environments. ENK5 reflects the silty fraction of a fluviually deposited Holocene sequence in the west of the excavation. Beside considerable amounts of dolomite, the Holocene samples indicate a similar bulk mineralogy as the Pleistocene ones, their clay mineral fraction however is less and consists mainly of smectite group minerals (see Fig. 5a). An

additional sample was taken near Larnaca at Hala Sultan Tekke. As the other Holocene samples it is also dolomite bearing and moreover shows substantial amounts of halite. Comparative marl clays from the Pliocene Nicosia Formation collected by Vaughan (1987) in the vicinity of Famagusta but also in the southern Mesaoria Plain (see Fig. 1) were added to the geochemical considerations of this study. With respect to clay mineralogy, the marl clays mainly contain smectite and chlorite group minerals (Vaughan, 1987).

Concerning the ceramic samples, the predominant part of Plain White Wheelmade (PWW) ware samples investigated in this study harkens back to excavations at Enkomi in the late 1940-50's (Dikaïos, 1969-1971) and was reworked by Lindy Crewe (Crewe, 2004, 2007). The Cypriot PWW ware is an appropriate ware group for provenance investigations as it's a mass-produced "workaday-ware" that is quite simple made, without applying intensive raw-material conditioning or complex surface treatments. Therefore it reflects the used raw material relatively pristine what considerably eases the quest for provenance.

Additional PWW samples, excavated in Cyprus and the northern Canaanite coast were added to the study for comparison (see Table 1). Two sherds were found in Galinopourni (Cyprus), one in Halefga (Cyprus). F1 and F1/1 represent sherds from a well at Hala Sultan Tekke (Cyprus, early 14<sup>th</sup> century B.C.), F6002/1 and F6008 from a LC IIIA1 layer at Hala Sultan Tekke (Åström and Åström, 1972, Öbrink, U., 1979, 1983). The sample LCII was found in a disturbed LC layer (assumed to be LC II) at Kalopsidha (Cyprus). Four comparative PWW specimens were found during a salvage excavation in 2001 in Tell Abu Hawam, a site in the vicinity of modern Haifa (Israel) where a large percentage of found ceramic material is assumed to be imported from Cyprus. The pottery samples can mainly be assigned from the 14<sup>th</sup> to the first half 13<sup>th</sup> century B.C. (Artzy, M., 2006). Finally, four Red on Black (RoB) samples, also from Enkomi (Dikaïos' excavations) were additionally analysed to see differences and analogies of unequal ware groups from the same excavation and the same assumed provenance.

**Table 1: List of ceramic samples and sediments with their associated findsites**

| <b>Plain White Wheelmade ware</b>                              |  |                        |
|--|--|------------------------|
| Enkomi   | 2191/2, 2191/5, 2191/13, 2191/14, 2191/15, 2248/1, 2248/4, 2248/5, 2248/6, 2248/8, 2248/9, 4527/17, 2300a, 2300b, 2300/4, 2300/7, 2300/12, 2300/13 |                        |
| Galínopourni   | Sherd1, Sherd6   |                        |
| Halefga  | T2   |                        |
| Hala Sultan Tekke  | F1, F1/1, F6002/1, F6008   | } Comparative material |
| Kalavassos   | LCII   |                        |
| Tell Abu Hawam   | 5014/6, 5046/36, 5064/69, 5103/7   |                        |
|  |  |                        |
| <b>Red on Black ware</b>                                       |  |                        |
| Enkomi   | 2191/6, 2192/10, 2267/1, 2267/2  |                        |
| <b>Sediments (see also Fig. 1)</b>                             |  |                        |
| Eastern Mesaoria Plain ENK1, ENK2, ENK5, GYP1, GYP2, GYP3, HST |  |                        |

### 3. Analytical techniques

Bulk major element compositions of pottery specimens and collected raw materials were analyzed with the sequential wavelength dispersive X-ray spectrometer (XRF) Philips PW 2400, trace- and rare earth element compositions were gained using the inductively coupled mass spectrometer (ICP-MS) Perkin Elmer Elan 6100



DRC (both from the Department of Lithospheric Research, University of Vienna). Sample preparation and measuring techniques followed the procedure described in Tschegg et al. (2008a). Loss on ignition was determined firing the specimens for 3 h at 950 °C.

For qualitative bulk mineralogical analyses, all samples were prepared with preferred orientation and measured with the X-ray diffraction (XRD) Philips PW 1820 (Department of Geodynamics and Sedimentology). On the <2 µm fractions of the raw material samples (obtained by sedimentation), the clay mineral groups were determined. Before, the sediments were disaggregated and homogenized with a 400 W ultrasonic probe; organic matter was removed by treatment with diluted H<sub>2</sub>O<sub>2</sub>. Ethylene-glycol saturated, oriented XRD mounts of the <2 µm fractions were additionally prepared to define expandable clay mineral groups.

Mineral assemblages and textural features of the ceramics were studied on polished thin sections with an optical microscope. Microtextural relationships and mineral chemistries were analyzed on carbon-coated thin sections with the Cameca SX 100 electron-microprobe (EPMA) equipped with four wavelength-dispersive (WDS) and one energy-dispersive (EDS) spectrometers (Department of Lithospheric Research, University of Vienna). Operating conditions were 15 kV and 20 nA, all measurements were made against natural standards and standard correction procedures were applied. For the microchemical and micromorphological characterization of the collected raw material samples and the comparison of ceramic-included minerals/microfossils with minerals/microfossils in the raw materials, grains of the raw material fraction >63 µm were embedded in resin and analyzed with the EPMA. On selected areas, line-scans with a defocused beam technique (5 µm) were applied on some ceramic specimens with a slip to compare ceramic body and slip geochemistry. The distribution of elements in slip and body was also determined with a high resolution qualitative WDS elemental mapping procedure (20 kV, 20 nA). Image analyses with Scion Image for Windows (© Scion Corporation) were performed to determine the percentage of porosity. SPSS 15.0 for Windows (© SPSS Inc.) was used to perform statistical data reduction treatments.

## 4. Results

### 4.1 Bulk geochemistry – major elements

Bulk geochemical compositions of ceramics and sediments are reported in Table 2 and illustrated in Figs. 2 and 3. Four groups of ceramics can be discriminated on the basis of their bulk major and trace element chemistry. Group A comprises the largest part of PWW ware samples excavated in Enkomi, but also sherds from Galinopourni, Halefga, Hala Sultan Tekke, Kalavassos and Tell Abu Hawam. Their amount of SiO<sub>2</sub> ranges from 47.5 to 55.3 wt. %, Al<sub>2</sub>O<sub>3</sub> from 12.1-14.4 wt. %, CaO varies from 11.4-23.6 wt. % and K<sub>2</sub>O from 1.7 to 3.3 wt. %. Group B includes three PWW and four RoB sherds from Enkomi and one PWW sample from Hala Sultan Tekke. Compared to group A, the specimens of this group have lesser variations in chemical composition what is shown by higher concentrations of SiO<sub>2</sub> (56.3-58.3 wt. %), Al<sub>2</sub>O<sub>3</sub> (15.6-16.5 wt. %) and K<sub>2</sub>O (3.2-3.5 wt. %) and lower amounts of CaO (7.5-10.5 wt. %). Group C comprises two PWW ware samples from Tell Abu Hawam with SiO<sub>2</sub>, Al<sub>2</sub>O<sub>3</sub>, CaO and K<sub>2</sub>O contents varying between 47.7-51.2 wt. %, 10.7-11.9 wt. %, 17.0-23.7 wt. % and 1.4-1.8 wt. % respectively and therefore shows a similar bulk major element composition as group A.





Group D includes one sample from Tell Abu Hawam and one from Hala Sultan Tekke and is characterized by comparatively low amounts of  $\text{SiO}_2$  and  $\text{K}_2\text{O}$  (44.8-46.6 wt. % and 0.7-1.1 wt. %) at very high concentrations of  $\text{CaO}$  (28.7-31.6 wt. %).

The Pleistocene sediments have  $\text{SiO}_2$ ,  $\text{Al}_2\text{O}_3$ ,  $\text{CaO}$  and  $\text{K}_2\text{O}$  concentrations that range from 48.2-56.5 wt. %, 11.4-14.0 wt. %, 18.7-20.6 wt. % and from 1.8 to 2.4 wt. % respectively - therefore they plot in the same range as the group A samples. The Holocene raw material specimens have low  $\text{SiO}_2$  and  $\text{Al}_2\text{O}_3$  contents (36.2-44.6 wt. % and 8.8-10.1 wt. %) at very high  $\text{CaO}$  contents (28.2-36.3 wt. %).

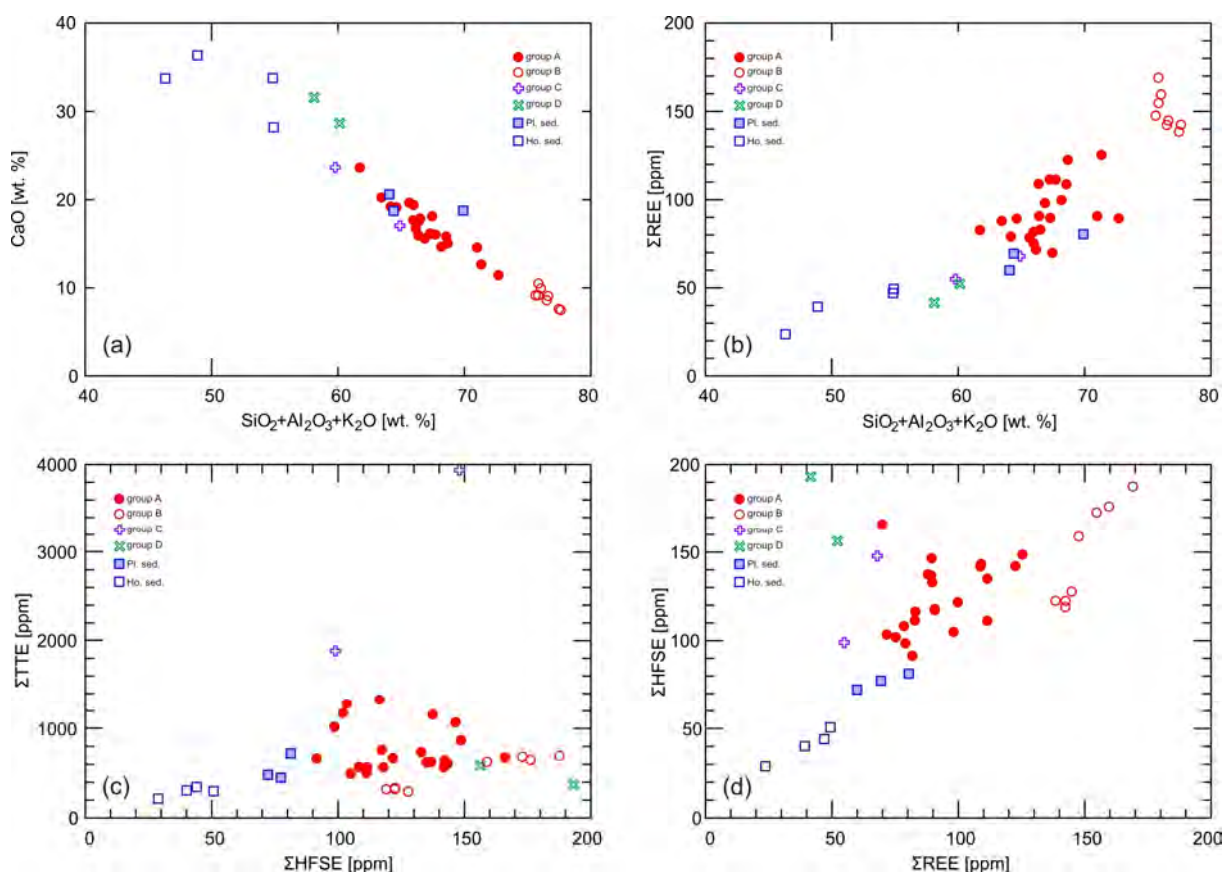


Fig. 2: Co-variation diagrams for major and trace elements of the analysed ceramic and sediment samples. (a) Clay constituents ( $\text{SiO}_2 + \text{Al}_2\text{O}_3 + \text{K}_2\text{O}$ ) against  $\text{CaO}$ , (b) clay constituents against total REE concentrations, (c) total HFSE (high field strength elements) concentrations against total TTE (transition trace elements) concentrations, (d) REE total against HFSE total. (Pl. sed. – Pleistocene sediments, Ho. sed. – Holocene sediments)

#### 4.2 Bulk geochemistry – trace elements

To simplify the large set of trace elements, it was appropriate to categorize it into four groups of geochemical related elements: LILE (large ion lithophile elements: Rb, Sr, Ba, Th, U), HFSE (high field strength elements: Y, Zr, Nb), TTE (transition trace elements: Sc, V, Cr, Co, Cu, Zn) and REE (rare earth elements: La-Lu). Co-variation diagrams of REE, HFSE and TTE are presented in Fig. 2b, c and d. The total LILE concentrations ( $\Sigma\text{LILE}$ ) in group A range from 604 to 1397 ppm, the summarized HFSE ( $\Sigma\text{HFSE}$ ) vary from 99-166 ppm, total TTE ( $\Sigma\text{TTE}$ ) from 580-1411 ppm and the sum of REE ( $\Sigma\text{REE}$ ) range from 70 to 125 ppm.

Group B has  $\Sigma$ LILE concentrations from 658-1445 ppm,  $\Sigma$ HFSE from 119-188 ppm,  $\Sigma$ TTE from 370-814 ppm and  $\Sigma$ REE concentrations that range from 139 to 169 ppm. In group C the total amount of LILE varies between 783-1084 ppm, of HFSE between 99-148 ppm, concerning TTE it ranges from 1943-4033 ppm and the  $\Sigma$ REE vary from 55-68 ppm. Summarized concentrations of LILE, HFSE, TTE and REE in group D range from 958-1648 ppm, 156-193 ppm, 480-687 ppm and 41-52 ppm respectively.

La and Lu concentrations of group B as well as the whole REE patterns correspond closest to the composition of the UCC (Upper Continental Crust, Taylor and McLennan, 1985, McLennan, 2001), all other samples have lower amounts of these elements (see Fig. 3). Compared to the UCC composition, group A is depleted by a factor of 1.7 and 1.1 concerning the average amounts of La and Lu, whereas groups C and D are depleted by a factor of 2.7 and 1.3 as well as 3 and 2.5. The average composition of the Pleistocene sediments is 2.1 and 1.7 times lower concerning La and Lu, the Holocene sediments are 3.8 and 2.7 times lower. The mean La/Sm ratio is with 5.5 the highest in group B indicating an almost flat pattern of light REE (LREE) in contrast to the lowest in group C (3.8) that shows the strongest depletion in LREE. All samples have relatively flat heavy REE (HREE) patterns, average Gd/Yb ratios vary from 1.6 in group C and 2.1 in group B. Due to increased modal amounts of feldspars in all analysed samples, REE patterns show positive Eu anomalies. In general it can be observed that CaO concerning major element compositions has the largest variations within the analysed dataset and correlates negatively with the major clay constituents  $\text{SiO}_2$ ,  $\text{Al}_2\text{O}_3$ ,  $\text{K}_2\text{O}$  as well as HFSE and REE (see Fig. 2a, b and d).

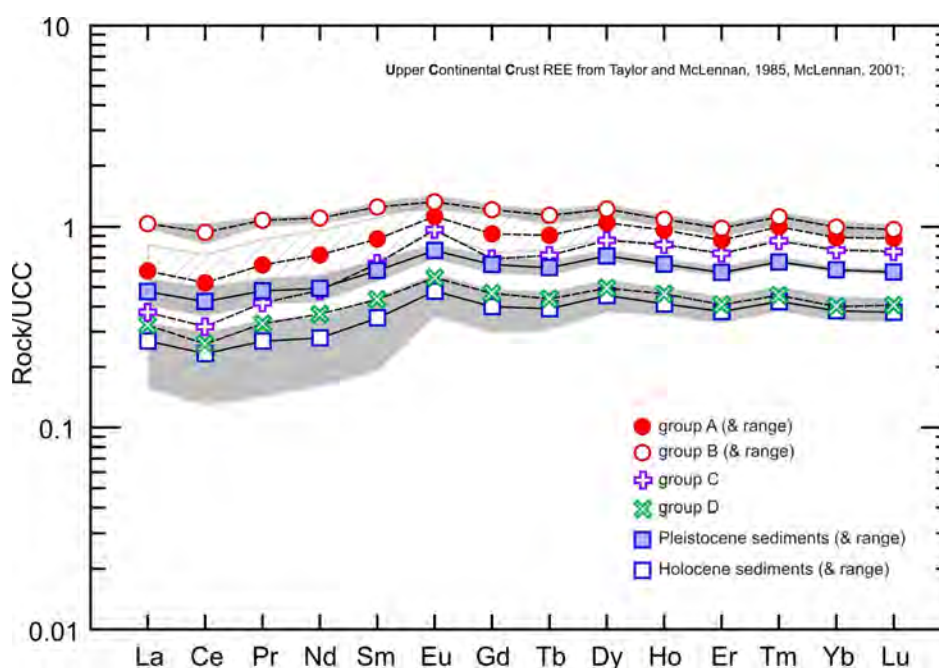


Fig. 3: Upper Continental Crust (Taylor and McLennan, 1985, McLennan, 2001) normalized REE patterns showing average sample-group compositions and ranges (minima-maxima) of element concentrations.

The statistical processing of the present dataset via principal component analysis summarizes and nicely illustrates the main geochemical variations of all studied ceramics and sediments. Group A comprehends the largest cluster of ceramics to which the Pleistocene sediments from the vicinity of Enkomi and four Pliocene sediments from Vaughan (1987) conform. The main group-determining elements are illustrated in Fig. 4. High

concentrations of REE and the positively correlating amounts of  $\text{Al}_2\text{O}_3$  and  $\text{K}_2\text{O}$  as well as comparatively low amounts of  $\text{CaO}$  account for the separation of samples in group B. High TTE concentrations separate samples of group C from all other samples, whereas group D is characterized by low REE as well as high  $\text{CaO}$  and HFSE amounts. The collected Holocene sediments have the by far highest amounts of  $\text{CaO}$  what effects a dilution of the minor and trace element content.

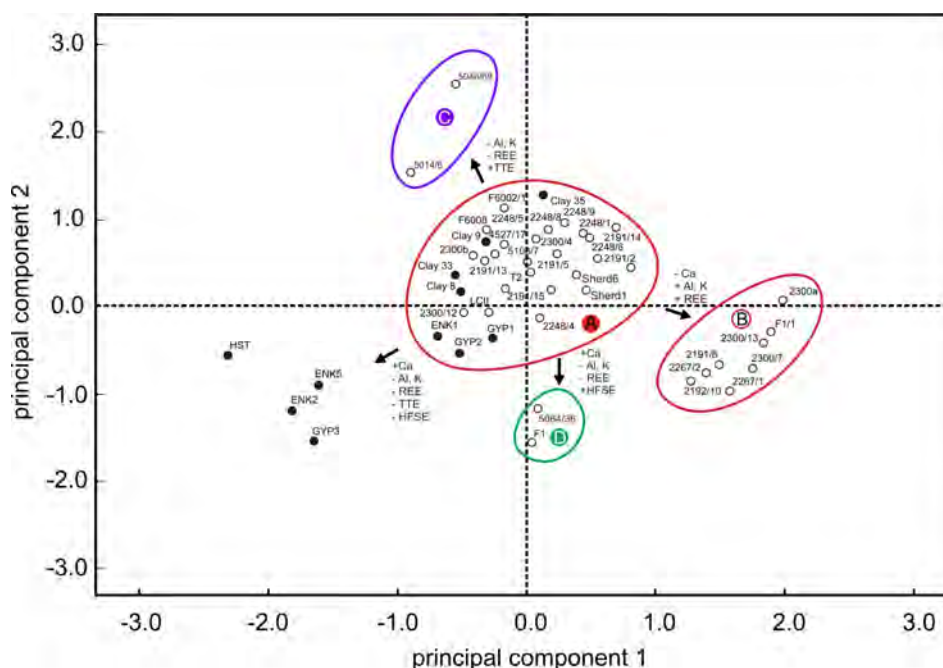


Fig. 4: Score plot of a principal component analysis based on 22 major and trace elements ( $\text{TiO}_2$ ,  $\text{Al}_2\text{O}_3$ ,  $\text{FeO}$ ,  $\text{MgO}$ ,  $\text{MnO}$ ,  $\text{CaO}$ ,  $\text{Na}_2\text{O}$ ,  $\text{K}_2\text{O}$ ,  $\text{Li}$ ,  $\text{Sc}$ ,  $\text{V}$ ,  $\text{Cr}$ ,  $\text{Co}$ ,  $\text{Cu}$ ,  $\text{Zn}$ ,  $\text{Sr}$ ,  $\text{Y}$ ,  $\text{Zr}$ ,  $\text{Nb}$ ,  $\text{Ba}$ ,  $\text{La}$ ,  $\text{Ce}$ ) restricted by availability of data in the literature. PC1 (46.2 %) and PC2 (21.4 %) explain 67.5 % of the total variance of a dataset that includes all ceramic samples and sediments of this study together with four sediment-analyses from Vaughan (1987). Ceramic specimens are indicated by open circles, sediments by full circles. Main group determining elements as well as group-combining fields are also given.

### 4.3 Petrography and Mineralogy

Despite variations of paste textures (sorting, size and morphology of inclusions) and differences concerning the temperature of firing (already described in Tschegg et al., 2008b), the whole set of ceramics can due to their specific assemblage of included components (minerals, rock and ceramic fragments, fossils) be divided into four groups:

*Group A:* The phyllosilicate paste matrix covers grain dimensions ranging from clay to mainly silt size. Within the matrix clay minerals, 80  $\mu\text{m}$  sized or smaller sub-angular inclusions of quartz, feldspars, and accessory Fe- and Ti-oxides as well as micas are present. In varying modal amounts and shapes (sub-rounded to angular) quartz, plagioclase and calcareous grains of sand size are included in the paste. The calcareous phases include mainly micritic and sparitic rock fragments and a conspicuous assemblage of foraminifera together with scarce larger shell fragments. Few inclusions of gabbro and sandstone fragments are characteristic just like accessory single pyroxene phases.

*Group B:* Typical for this group is the fine-grained silty clay sized paste matrix that despite smaller amounts of quartz, feldspar or oxide inclusions is very similar to the one of group A. The paste textures vary from scarce small inclusions of quartz and sandstone fragments to up to 2 mm large, angular also sporadically embedded grains of the same mineral and same type of rock. Occasionally grog inclusions as well as fossils can be found.

*Group C:* The paste matrix is more or less similar to this of group A. Noticeable in these sherds are the high amounts of diopside, olivine and Fe-, Cr- and Ti-rich oxides like magnetite, Cr-spinel and Ti-magnetite as well as numerous gabbroic rock-fragments. Furthermore grog-tempering with clasts up to 500  $\mu\text{m}$  and considerable amounts of carbonate fragments as well as calcareous microfossils are observable.

*Group D:* A highly calcareous silty paste-matrix with included micritic carbonate fragments (up to 400  $\mu\text{m}$ ), few quartz and anorthite grains as well as some large gabbroic rock-fragments (300-400  $\mu\text{m}$ ) build up the paste. Grog inclusions (up to 700  $\mu\text{m}$ ) and sparse fossils are additional distinctive features.

X-ray diffraction was firstly applied to get a comparable overview of the main minerals that assemble the investigated ceramics and secondly to define the bulk as well as clay mineral fraction of the collected sediments. The gained diffraction patterns of ceramics and their potential raw materials were finally compared and assessed. Fig. 5 shows a lineup of the two collected groups of sediments and two low-temperature fired (Tschegg et al., 2008b) ceramic samples, one representative for group A, the other for group D. The diffraction patterns of sediment ENK1 (Fig. 5b) and sample 2248/9 (Fig. 5e) show the same proportions concerning their main quartz (3.343  $\text{\AA}$ ), calcite (3.035  $\text{\AA}$ ) and feldspar peaks. The  $<2 \mu\text{m}$  fraction of ENK1 (Fig. 5c) points up the clay mineralogy and indicates the existence of smectite and illite group minerals (15  $\text{\AA}$  and 10  $\text{\AA}$ ) as well as chlorite and lesser amount of kaolinite group minerals. As the main peak of smectite widens up from 15  $\text{\AA}$  to 17  $\text{\AA}$  when treated with Ethylene-glycol (Fig. 5c, d), its existence as well as its expandable character are confirmed (Moore and Reynolds, 1997). The chlorite group minerals are indicated by the 7.17  $\text{\AA}$  and 3.541  $\text{\AA}$  peaks as shown in Fig. 5c, the kaolinite group by the common peak at 7.17  $\text{\AA}$  and the 3.579  $\text{\AA}$  peak. The diffraction pattern in Fig. 5a represents the analyzed Holocene raw materials, sediments with higher amounts of feldspars and calcite as well as additional dolomite (2.88  $\text{\AA}$ ). Their  $<2 \mu\text{m}$  fraction shows generally much lower clay mineral contents with no illite and hardly detectable amounts of chlorite and kaolinite group minerals. Dominant calcite and dolomite peaks are also characteristic features of samples from group D. Fig. 5f shows this diffraction pattern and illustrates the parallels to the bulk mineralogy of the Holocene sediments from Fig. 5a.

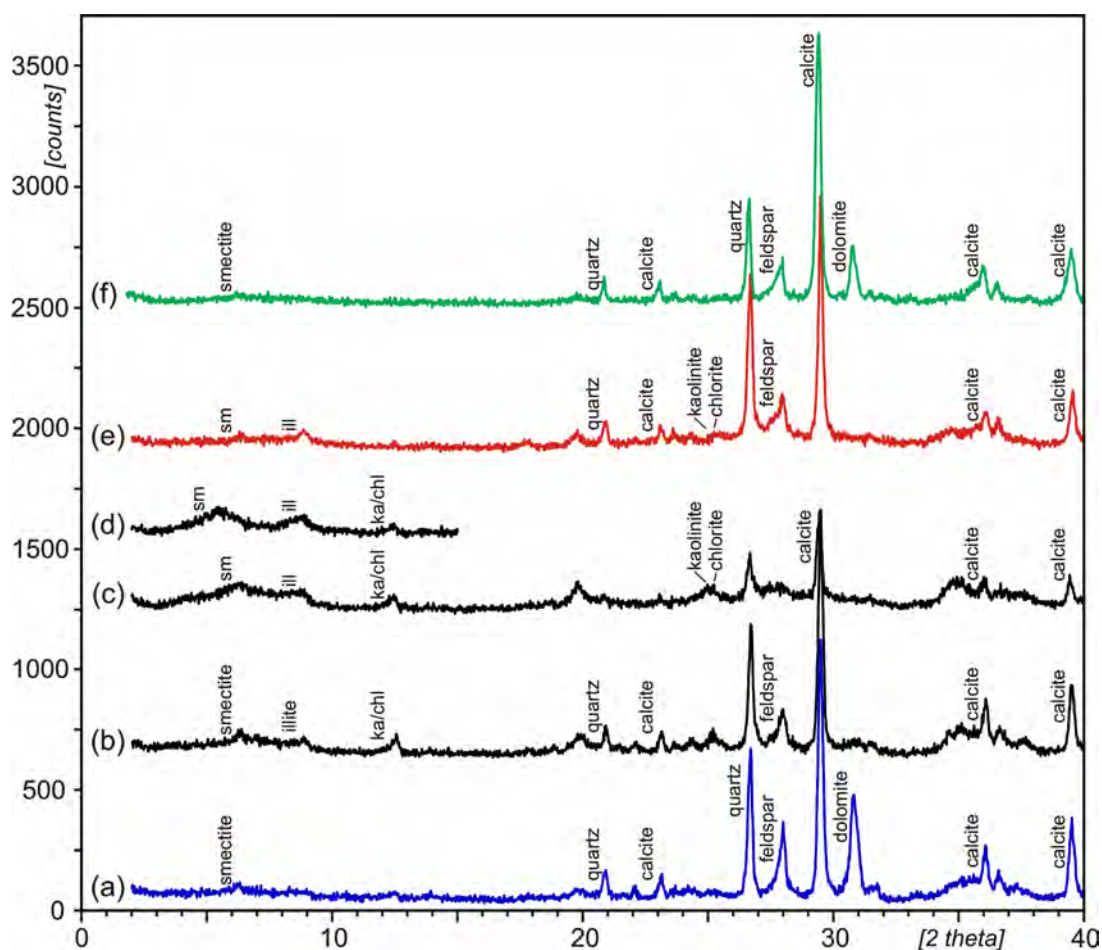


Fig. 5: X-ray diffraction patterns of (a) ENK2 - representative for Holocene sediments, (b) ENK1 - representative for Pleistocene sediments, (c) <math><2\ \mu\text{m}</math> fraction of ENK1, (d) <math><2\ \mu\text{m}</math> fraction of ENK1 saturated with Ethylene-glycol, (e) 2248/9 - representative for group A samples and (f) 5064/36 representative for group D. Relevant peaks are labelled, some with abbreviations: chl - chlorite group, ill - illite group, ka - kaolinite group, sm - smectite group minerals;

#### 4.4 Microtextural observations

As the investigated ceramics, especially from group A and C contain a lot of characteristic calcareous microfossils, also the collected raw material samples were examined in consideration of their fossil content. The >63  $\mu\text{m}$  fraction of the Pleistocene sediment ENK1 has a fossil composition that comprises benthonic and planktonic foraminifera, holothurian sclerites and scaphopod dentalia. The complete compilation of these microfossils can also be found in the sherds of group A and C, partly in group B and D. Fig. 6 shows a lineup of the fossil assemblage that can be found in both the sediment and the investigated PWW samples.

During the study it turned out that textural features (geometric and morphological characteristics of the paste and its inclusions) are within the present set of sherds inappropriate for pottery discriminating aspects. Different techniques of raw material conditioning and firing can change the texture of the pastes though the same sediment was initially used (Tschegg et al., 2008b).



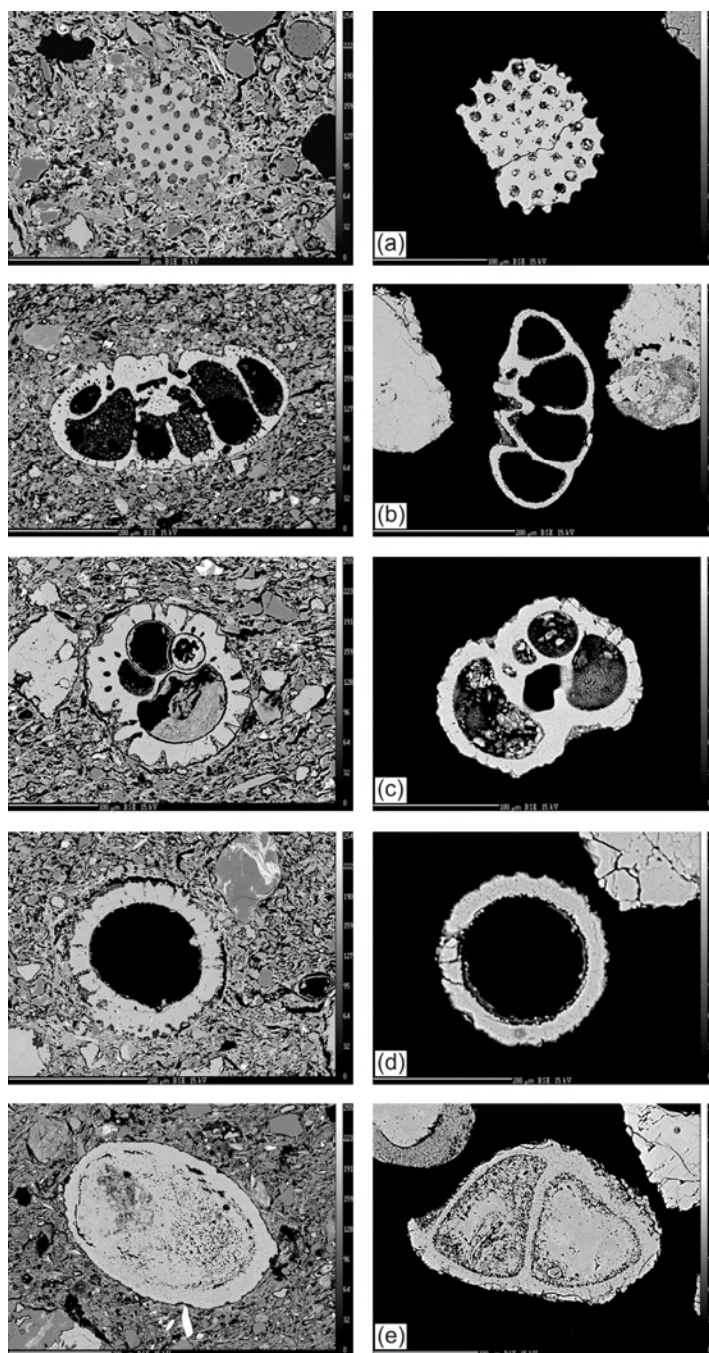


Fig. 6: BSE images of the microfossil assemblage found in ceramics of group A (left side) opposing the same kind of fossils found in the fraction  $>63 \mu\text{m}$  of the Pleistocene sediment ENK1 (right side). (a) Holothurian sclerite, (b and e) benthonic foraminifera, (c) planktonic foraminifera, (d) scaphopod dentalium;

An interesting observation concerning texture though is that macroscopically few PWW ware sherds seem to have an intentionally manufactured slip or at least some kind of “self-slip” that formed as a result of the final reshaping of vessels with a lot of water. The close investigation of this pretended slip revealed that not refining of the clay paste at the surface of the vessels but a strong increase in porosity makes the surface appearing brighter. The backscattered-electron image of Fig. 7 illustrates the  $200 \mu\text{m}$  wide surface layer in which

the average porosity is increased by 25 % compared to the body of the sherd. Three element-indicative WDS mappings (Fig. 7a-c) show the distribution of Ca in 150x112  $\mu\text{m}$  large areas in the ceramic body, the surface layer and their transition zone. As indicated by these calcium distribution maps as well as line scans that were carried out from the ceramic body into the surface layer, the calcium content at the surface is reduced to more than half compared to the body. Unlike an abrupt intersection between ceramic body and surface that would be typical for slips, the interfaces here show a gradual transition.

## 5. Discussion

Combining bulk geochemical, petrographical and mineralogical features, the investigated Cypriot PWW ware samples together with the comparative material from Cyprus and the northern Canaanite coast can be divided into four groups. Raw/source material assignments can largely be made.

Group A combines most of the samples that were excavated directly in Enkomi but also additional sherds found at other Cypriot locations. Taking the gained data and observations into account, the ceramic samples of group A indicate according to their mineralogical and palaeozoological assemblage as well as their bulk geochemical and petrographic characteristics a common raw material source. Due to different modal amounts of included calcareous phases, their bulk CaO content is variable and shows a relative range of 12 wt. % (12.2-23.6 wt. %). With increasing concentrations of CaO, the percentage of clay constituents  $\text{SiO}_2$ ,  $\text{Al}_2\text{O}_3$  and  $\text{K}_2\text{O}$  decrease, so do also most of the trace elements (see Fig. 2a, b). This trend is observable in all analysed samples of this study and clearly indicates the dilutive function of carbonates (and calcareous inclusions in general) containing low amounts of e.g. REE (Taylor and McLennan, 1985). Systematic variations of major and trace element concentrations can therefore in this case to a large extent be assigned to variable modal amounts of calcareous inclusions.

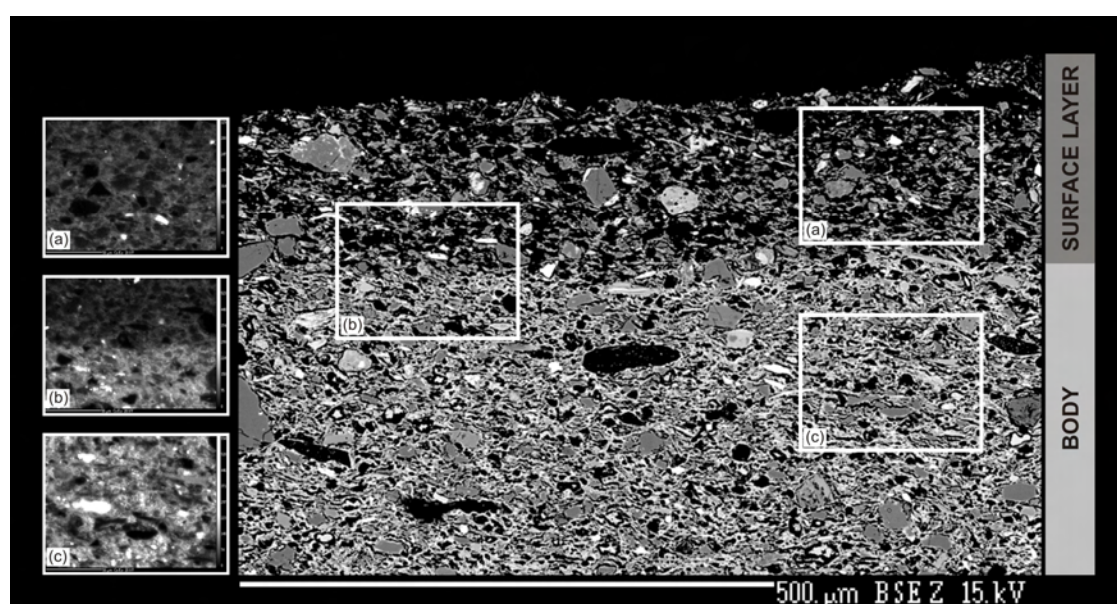


Fig. 7: Backscattered electron image showing the surface area of sherd 2191/2 (group A). Calcium indicative WDS-mappings illustrate the distribution of Ca in the ceramic body (Fig. 7c), its surface layer (Fig. 7a) and the transition zone (Fig. 7b). Ca maps exactly cover the areas where they are indicated.

The Pleistocene sediment samples that were collected in the closer surrounding of the Enkomi excavation site fulfil the qualifications of being a potential raw material for the production of group A ceramics. Comparing the bulk composition (Fig. 2, 3, 4), mineralogy (Fig. 5) as well as microfossil content (Fig. 6) of the sediments with the sherds of group A, they show a strong similarity. The slight lower amounts of trace elements in the sediments correlate with larger shell-fragments that are sporadically included in the sediment and weren't removed for bulk analysis. Comparing average REE concentrations of group A sherds to the mean REE contents of 38 Corinthian-style roof tiles that after Gomez et al. (2002) are related to Mesaoria sediments around Enkomi, a surprising correlation turns out. The La concentration in the roof tiles reaches 17.79 ppm (std. dev.: 1.07), Eu 0.93 (std. dev.: 0.06) and Lu 0.29 (std. dev.: 0.03), whereas in the PWW ceramics of group A, La reaches 18.07 ppm (std. dev.: 3.30), Eu 0.99 ppm (std. dev.: 0.09) and Lu 0.28 ppm (std. dev.: 0.02). Beyond a common source material, as inferred from micro- and macro-textural details, this ware group suggests fabrication with a similar manufacturing technique. During the conditioning of the Pleistocene material for pottery production, coarse shell fragments were presumably separated out; in all other respects the suggested source material could have been directly used for the manufacturing procedure.

The geochemically homogeneous sample-set of group B seems to have a similar raw material source as group A but indicate a different way of preparing it for pottery manufacturing. The source material, as suggested from the observed refinement of the fabric, was levigated. Consequently the lack of larger calcareous inclusions increases the bulk budget of trace elements (Fig. 2, 3). The flat LREE patterns as well as the high REE abundances in general, confirm the features of a chemically non-diluted material whose composition is quite close to the UCC (Taylor and McLennan, 1985, McLennan, 2001). Larger angular inclusions of sandstone and related quartz grains as well as grog may possibly indicate intentional tempering of these phases.

The microtextural investigations, mainly concerning the paste matrix, indicate that group C has the same characteristics as group A. However, a difference consists in that the sand sized mineralogical assemblage in the paste of samples belonging to this group shows stronger affinity to rocks from the Troodos ophiolite massif (McCallum and Robertson, 1995, Poole and Robertson, 1998). Although still microfossils are present that are also to find in the Pleistocene sediments around Enkomi (in the Pleistocene formations of the eastern Mesaoria Plain respectively), the increased modal abundance of Fe-Cr-Ti bearing ores, pyroxenes and olivines reveal a raw material source that is closer to the Troodos and that is therefore enriched in Troodos-derived material (Garzanti et al., 2000). The high transition trace element abundances (high TTE, Fig. 2c) in group C confirm the affinity to mafic-ultramafic rocks and therefore suggest a source material from Troodos-closer erosional sedimentary successions, most likely from the area between the gulf of Famagusta and Larnaca.

The highly calcareous paste matrix in sherds of group D precludes any correlation with the Pleistocene eastern Mesaoria sediments. Their XRD patterns indicate an origin from younger, more heterogeneous sedimentary successions with a much higher Ca content and dolomite in their fine-fraction (see Fig. 5).

Detailed investigations of Pleisto- and Holocene sediments from the eastern Mesaoria Plain show that the clay mineral content in the <2  $\mu\text{m}$  fraction is much higher in the Pleistocene than in the younger materials. The higher amounts especially of expandable clay minerals (smectite group minerals) and their mixture with illite and chlorite as well as the naturally included calcareous phases made the Pleistocene silty clays a preferred, well workable raw material that when fired to the accurate temperature provides high-quality physical and mechanical properties (Tschegg et al., 2008b). From bulk geochemical and mineralogical aspects, the Pleistocene sediments from the area around Enkomi are probable and potential source materials for the

fabrication of ceramics of group A, B and C, with variations that result from different raw material conditioning techniques and regional inhomogeneities. The analogy of the microfossil assemblage that is traceable in both the sediments and their ceramic products respectively confirms the close relation of the mentioned material groups. Sherds of group D are not associated to the Pleistocene raw materials and presumably are related to young alluvial sediments of the area.

The supposed white slip that some samples show is on closer inspection a corroded surface, resulting from post-depositional alteration. During burial, mainly Ca leaches out at the surface-near layers and causes an increase in porosity involving an enlargement of the specific surface area. Ca in the form of calcite tends to be easily affected by post-depositional processes (Schwedt et al, 2004) like e.g. soil invading and percolating fluids that affect surface-near extraction/dissolution of sherd constituents (Maggetti, 1982). The resulting high-porous, whitish appearing surface layer is an analogue effect to the “espresso-crema” that gets its bright colour by reasons of reflection, refraction and scattering of light at increased gas-solid/gas-liquid interfaces (Durian et al., 1991, Vera et al., 2001). Moreover, just like the espresso crema, the sherd-surface beyond the physical alteration additionally changes its chemical composition versus the base material.

## 6. Conclusion

In this study, we were able to assign Late Cypriot Bronze Age Plain White Wheelmade ware samples excavated in Cyprus and the Canaanite coast to sediment sources on the island of Cyprus. Supported by petrographic, mineralogical, palaeozoological, petrological and geochemical evidence, four groups of ceramics could be distinguished and related to specific sediments that are available in eastern Cyprus. Sherds of groups A and B are manufactured out of Pleistocene sediments that can be found in the eastern Mesaoria Plain around Enkomi. Mirroring the same raw material source, they reflect varying conditioning techniques though. This implies that the potters from ancient Enkomi indeed used the Pleistocene silty clays as base material but moreover it signifies that diverse workshops existed that had differing recipes for manufacturing pottery. As the raw material that was used for the production of group C is very similar to the one from group A and B, with the difference that it is noticeably influenced by Troodos derived components, we assume a raw material source for this group that is still in the Mesaoria Plain but geographically closer to the Troodos massif. The origin of group D samples can not be located exactly; nevertheless they show consistency to younger Holocene sediments that are also available in the Famagusta gulf.

The assignment of ceramic commodities from several Cypriot excavation sites and from the Canaanite coast to regional scattered Cypriot pottery workshops proves trade networks within the island and beyond during the Late Bronze Age, also for utilitarian ceramics such as the PWW ware.

The paper furthermore demonstrates the necessity in pottery analyzing studies to use integrated methods that provide sufficient information for accurate statements concerning affiliations, provenance and technology of ancient ceramics.

## Acknowledgements

This work has been supported by Austrian Science Fund FWF (grant P18908-N19). We are grateful to the Department of Antiquities of Cyprus and to Lindy Crewe (University of Manchester, Great Britain) for providing the PWW samples from Cyprus, to Prof. Paul Åström (University of Gothenburg, Sweden) and Prof. Michal Artzy (University of Haifa, Israel) for additional samples from Cyprus and Tell Abu Hawam and their site-specific information. Shalom Yanklevitz, Ragna Stidsing and Yossi Salmon (University of Haifa, Israel) have to be thanked for fruitful discussions and information. Thanks also to Prof. Johann Hohenegger (Department of Paleontology, University of Vienna) for the identification of microfossils.

## References

- Artzy, M., 2006. The Carmel Coast during the Second Part of the Late Bronze Age: A Center for Eastern Mediterranean Transshipping. *Bulletin of the American Schools of Oriental Research* 343, 45-64.
- Åström L., Åström P., 1972. The Late Cypriote Bronze Age. The Swedish Cyprus Expedition IV: 1D, Lund.
- Åström, P., 1972. The Late Cypriot Bronze Age. The Swedish Cyprus Expedition, Volume IV, Part 1C. Lund.
- Calon, T.J., Aksu, A.E., Hall, J., 2005. The Neogene evolution of the Outer Latakia Basin and its extension into the Eastern Mesaoria Basin (Cyprus), Eastern Mediterranean. *Marine Geology* 221, 49-73.
- Crewe, L., 2004. Social complexity and ceramic technology on Late Bronze age Cyprus: The new evidence from Enkomi. Unpublished PhD thesis, University of Edinburgh.
- Crewe, L. 2007. Early Enkomi. Regionalism, trade and society at the beginning of the Late Bronze Age on Cyprus. *Archaeopress, British Archaeological Reports*, Oxford.
- Dikaios, P., 1969-71. Enkomi, Excavations 1948-1958. Volumes I-III B. Verlag Philipp von Zabern, Mainz am Rhein.
- Durian, D.J., Weitz, D.A., Pine, D.J., 1991. Multiple Light-Scattering Probes of Foam Structure and Dynamics. *Science* 252, 686-688.
- Garzanti, E., Andò, S., Scutellà, M., 2000. Actualistic Ophiolite Provenance: The Cyprus Case. *Journal of Geology* 108, 199-218.
- Gomez, B., Neff, H., Rautman, M.L., Vaughan, S.J., Glascock, M.D., 2002. The source provenance of Bronze Age and Roman pottery from Cyprus. *Archaeometry* 44, 1, 23-36.
- Geological Survey Department, Cyprus, 1995. Geological map of Cyprus, 1:25000. Ministry of agriculture, natural resources and environment, Nicosia.
- Hein, I., Jánosi, P., 2004: Tell el-Dab<sup>c</sup>a XI. Areal A/V, Siedlungsrelikte der Späten Hyksoszeit. *Denkschriften*. Verlag Österreichischen Akademie der Wissenschaften, UZK XXI, Wien.

- Knapp, A.B., Cherry, J.F., 1994. Provenance studies and Bronze Age Cyprus. Monographs in World Archaeology No. 21, Prehistory Press, Madison.
- Maguire, L.C., 1995. Tell el-Dab<sup>c</sup>a, The Cypriot connection in: Davies, W.V. and Schofield, L. (Eds.), Egypt, the Aegean and the Levant, British Museum Press, London, 54–65.
- Maggetti, M., 1982. Phase Analysis and Its Significance for Technology and Origin in: Olin, J.S., Franklin, A.D. (Eds.), Archaeological Ceramics. Smithsonian Institution Press, 121-133.
- McCallum, J.E., Robertson, A.H.F., 1995. Sedimentology of two fan-delta systems in the Pliocene-Pleistocene of the Mesaoria Basin, Cyprus. *Sedimentary Geology* 98, 215-244.
- McLennan, S.M., 2001. Relationships between the trace element composition of sedimentary rocks and upper continental crust. *Geochemistry, Geophysics, Geosystems* 2, No. 2000GC000109.
- Moore, D.M., Reynolds, R.C., 1997. X-ray Diffraction and the Identification and Analysis of Clay Minerals (2<sup>nd</sup> Ed.). Oxford University Press, Oxford.
- Neal, C., 2002. The mineralogy and chemistry of fine-grained sediments, Morphou Bay, Cyprus. *Hydrology and Earth System Sciences* 6, 819-831.
- Newell, W.L., Stone, B., Harrison, R., 2004. Holocene alluvium around Lefkosia (Nicosia), Cyprus: an archive of land-use, tectonic processes, and climate change in: Martin-Duque, J.F., Brebbia, C.A., Godfrey, A.E., Diaz de Teran, J.R. (Eds.), *Geo-Environment*. WITPress.
- Öbrink, U., 1979. Excavations in the Area 22, 1971-1973 and 1975-1979, Hala Sultan Tekke 5. *Studies in Mediterranean Archaeology XLV: 5*, Göteborg.
- Öbrink, U., 1983. A Well in the early 14<sup>th</sup> Century B.C. in: Åström, P. et al. (Eds.), Excavations 1971-1979, Hala Sultan Tekke 8. *Studies in Mediterranean Archaeology XLV: 8*, Göteborg, 16-58.
- Poole, A., Robertson, A.H.F., 1998. Pleistocene fanglomerate deposition related to uplift of the Troodos ophiolite, Cyprus in Robertson, A.H.F., Emeis, K.C., Richter, C., Camerlenghi, A. (Eds.), *Proceedings of the Ocean Drilling Program, Scientific Results* 160, 545-566.
- Robertson, A.H.F., Eaton, S., Follows, E.J., Payne, A.S., 1995. Depositional processes and basin analysis of Messinian evaporates in Cyprus. *Terra Nova* 7, 2, 233-253.
- Robertson, A.H.F., Woodcock, N.H., 1986. The role of Kyrenia Range lineament, Cyprus, in the geological evolution of the eastern Mediterranean area. *Philosophical Transactions of the Royal Society of London A* 317, 141–177.
- Schwedt, A., Mommsen, H., Zacharias, N., 2004. Post-depositional elemental alterations in pottery: Neutron activation analyses of surface and core samples. *Archaeometry* 46, 1, 85-101.
- Soil Survey Division Staff, 1993. Soil survey manual. U.S. Department of Agriculture Handbook, No. 18.
- Steel, L., 2002. Cyprus before History. From Earliest Settlers to the End of the Bronze Age. Duckworth Publishing, London.

Taylor, St.R., McLennan, S.M., 1985. *The Continental Crust: its Composition and Evolution*. Geoscience texts, Blackwell Scientific Publications, Oxford.

Tschegg, C., Hein, I., Ntaflos, Th., 2008a. State of the art multi-analytical geoscientific approach to identify Cypriot Bichrome Wheelmade Ware reproduction in the Eastern Nile delta (Egypt). *Journal of Archaeological Science* 35, 1134-1147.

Tschegg, C., Ntaflos, Th., Hein, I., 2008b. Thermally triggered two-stage reaction of carbonates and clay during ceramic firing - a case study on Bronze Age Cypriot ceramics. *Applied Clay Science* (accepted).

Vaughan, S.J., 1987. *Fabric analysis of Late Cypriot Base Ring Ware: Studies in ceramic technology, petrology, geochemistry and mineralogy*. Unpublished PhD thesis, University College London.

Vera, M.U., Saint-Jalmes, A., Durian, D.J., 2001. Scattering optics of foam. *Applied Optics* 40, 24, 4210-4214.

---

# CURRICULUM VITAE



---

*cornelius.tschegg@univie.ac.at*

Name: Cornelius Tschegg  
Date of birth: 11. 04. 1980  
Place of birth: Feldkirch, Austria  
Nationality: Austrian

## EDUCATION

---

1998 Finished High School (Feldkirch, Austria)  
2005 Master in Geology at the Institute of Geological Sciences –  
University of Vienna  
2008 PhD in Geology at the Department of Lithospheric Research – University of  
Vienna

## JOBS

---

2000 – 2005 Dr. R. Bernasconi, Consultant for Geology and Hydrogeology, CH - Sargans  
2004 – 2005 SCIEM 2000, Synchronization of civilizations in the eastern Mediterranean  
in the 2<sup>nd</sup> millennium BC. Special research: Ceramics, Vienna  
2005 – 2006 Institute of Geological Sciences – Department of Environmental  
Geosciences, Vienna  
Since 2006 PhD position at the Department of Lithospheric Research – University of  
Vienna



---

## PUBLICATIONS - selected

---

- Ntaflos, Th., **Tschegg, C.**, Coltorti, M. and Akinin, S., Kosler, 2008. Asthenospheric signature in fertile spinel lherzolites from the Viliga Volcanic Field in NE Russia, in Coltorti, M., Gregoire, M. (Eds.): *Metasomatism in Oceanic and Continental Lithospheric Mantle*. Geological Society, London, Special Publications, 293, 57–83.
- **Tschegg, C.**, Hein, I., Ntaflos, Th., 2008. State of the art multi-analytical geoscientific approach to identify Cypriot Bichrome Wheelmade Ware reproduction in the Eastern Nile delta (Egypt). *Journal of Archaeological Science* 35, 1134-1147.
- **Tschegg, C.**, 2008. A geoscientific, methodologically integrated realisation to reconsider Egyptian pottery of the 18<sup>th</sup> Dynasty in Hein, I. (Ed.): *The Manual of Bichrome Wheelmade Ware of the Eastern Mediterranean*. Verlag der Österreichischen Akademie der Wissenschaften, Wien (accepted).
- **Tschegg, C.**, Ntaflos, Th., Hein, I., 2008. Thermally triggered two-stage reaction of carbonates and clay during ceramic firing - a case study on Bronze Age Cypriot ceramics. *Applied Clay Science* (in press).
- **Tschegg, C.**, Ntaflos, Th., Hein, I., 2008. Combined geological, petrological and geochemical method to reveal source material and technology of Late Cypriot Bronze Age Plain White ware ceramics. *Journal of Archaeological Science* (under review).

---

## ABSTRACTS - selected

---

- **Tschegg, C.**, Ntaflos, Th., Coltorti, M., Akinin, S., 2004. Mantle xenoliths from the Viliga Volcanic Field, NE - Siberia: Evidence for a fertile subcontinental lithosphere. 32<sup>nd</sup> International Geological Congress, Florence, Italy.
- Berger, A., Gier, S., **Tschegg, C.**, 2005. Porosity-preserving chlorite cementation in volcanoclastic sandstones, Sawan (Pakistan). *Geophysical Research Abstracts*, Vol. 7 - EGU - General Assembly 2005, Vienna, Austria.
- Ntaflos, Th., Krumpel, G., Harangi, S., **Tschegg, C.**, 2007. The origin of the alkaline and high-K calc-alkaline magmas along the SE margin of the styrian basin, Austria. *Petrological evolution of the European Lithospheric mantle: from Archean to present day*. EMAW 07, Ferrara.

- **Tschegg, C.**, Hein, I., Ntaflos, Th., 2007. Bichrome Wheelmade Ware: Origin and Reproduction. EMAC 07, Budapest.
- **Tschegg, C.**, Grasemann, B., 2008. Quantitatively estimated mass transfer, volume change and quantitative kinematics investigations in ductile low-angle shear zones (Serifos, Greece). Geophysical Research Abstracts, Vol. 10 - EGU - General Assembly 2008, Vienna, Austria.
- Lein, R., **Tschegg, C.**, 2008. Herkunftsanalyse prähistorischer Keramik der Höhensiedlung Malleiten bei Bad Fischau (N.Ö.). Pangeo 2008, Vienna, Austria.